Analysis of FOXC1 Regulation of Exocytosis

by

Alexandra Rasnitsyn

A thesis submitted in partial fulfillment of the requirements for the degree of

Master of Science

Medical Sciences - Medical Genetics
University of Alberta

Abstract

Glaucoma is a neurodegenerative disease which is among the leading causes of blindness in the world. Glaucoma is characterized by progressive visual field loss, caused by retinal ganglion cell (RGC) death. Both surgical glaucoma treatments and medications are available; however, they only halt glaucoma progression and are unable to reverse damage. Furthermore, many patients do not respond well to treatments, illustrating the importance for better understanding of glaucoma pathogenesis.

Patients with Axenfeld-Rieger syndrome (ARS) offer important insight into glaucoma progression. ARS patients are at 50% risk of developing early onset glaucoma and respond poorly to treatments, even when surgical treatments are combined with medications. Mutations in the transcription factor FOXC1 were shown to cause ARS. Alterations in FOXC1 levels were previously shown to cause ocular malformation and disrupt stress response in ocular tissues, thereby contributing to glaucoma progression.

In the present work I have shown that FOXC1 regulates the expression of RAB3GAP1, RAB3GAP2 and SNAP25, three genes with central roles in both exocytosis and endocytosis, responsible for extracellular trafficking. I have shown that FOXC1 positively regulates RNA and protein levels of RAB3GAP1 and RAB3GAP2 in HeLa cells, and that FOXC1 regulation of SNAP25 in HeLa cells follows a bimodular model with either increase or decrease in FOXC1 beyond its normal range resulting in SNAP25 decrease. In immortalized human trabecular meshwork (TM1) cells FOXC1 positively regulates RAB3GAP1 and RAB3GAP2 at the RNA level, but only RAB3GAP1 at the protein level,

while SNAP25 is negatively regulated by FOXC1 in TM1 cells, specifically isoform SNAP25a.

FOXC1 regulation of RAB3GAP1, RAB3GAP2 and SNAP25 has physiological consequences, and in HeLa cells affects secretion of exogenous Myocilin (MYOC), a protein associated with juvenile onset glaucoma and steroid induced glaucoma. Knockdown of either FOXC1 or combined knockdown of all three of its targets, RAB3GAP1, RAB3GAP2 and SNAP25, resulted in decrease in both intracellular and extracellular MYOC. In turn, knockdown of either RAB3FAP1 or SNAP25 led to decrease in intracellular MYOC and increase in extracellular MYOC indicating increased MYOC secretion while RAB3GAP2 knockdown had the same effect on MYOC as FOXC1 knockdown. FOXC1 regulation of exogenous MYOC secretion is therefore complicated and mediated through its targets, RAB3GAP1, RAB3GAP2 and SNAP25.

My research reveals that FOXC1 is an important regulator of exocytosis and established a new link between FOXC1 and MYOC-associated glaucoma.

Preface

This thesis is an original work by Alexandra Rasnitsyn. No part of this thesis has been previously published.

Acknowledgments

I would like to express my gratitude to my supervisor, Dr. Michael Walter, for his expertise, understanding, and guidance. His knowledge and support made my graduate experience exciting and rewarding, encouraged me to explore beyond my area of study and helped me focus when I spread myself too thin. I would like to thank the other members of my committee, Dr. David Eisenstat, and Dr. William Allison for their advice and guidance throughout my graduate studies, which helped me focus and move my project forward, and my external examiner Dr. Joseph Casey. I would also like to thank Dr. Vincent Raymond for his support and assistance with MYOC experiments, and immense helpfulness every time I contacted him for advice.

A very special thanks goes out to Tim Footz for his endless patience, guidance and expertise, and helping me troubleshoot countless experiments. May Yu's invaluable help with tissue culture and other experiments helped me move my research forward, while her moral support and friendship carried me through many challenges. I'd also like to thank Dr. Georgina MacIntyre for many enlightening science themed conversations, her guidance helped me critically assess and improve my work, and her friendship greatly enhanced my graduate experience. I would also like to thank my lab mates Morteza Seifi and Dr. Lance Doucette for their support and valuable suggestions throughout my studies.

I'd like to thank my graduate advisor Dr. Sarah Hughes for her help and encouragement as well as her guidance during Journal Club to critically examine my own work and the work of my peers. I would also like to thank Shari Barham for her kindness and helpfulness which greatly assisted me in navigating the administrative labyrinth of applications and scholarships. I also recognize that this research would not have been possible without the financial assistance of CIHR, the Department of Medical Generics and the Faculty of Medicine and Dentistry in the University of Alberta.

I would also like to thank my family for the support and encouragement they provided me throughout my studies. This accomplishment would not have been possible without them.

Alexandra Rasnitsyn

Table of Contents

List of Tables

List of Figures

Abbreviations in Order of Appearance

RGC - Retinal ganglion cells

ARS - Axenfeld-Rieger syndrome

FOXC1- Forkhead box C1

RAB3GAP1- Rab3 GTPase-activating protein catalytic subunit

RAB3GAP2 - Rab3 GTPase-activating protein non-catalytic subunit

SNAP25 - Synaptosomal-Associated Protein, 25kDa

TM1- Human immortalized trabecular meshwork cell line

HeLa – Immortalized cervical cancer cell line, taken from Henrietta Lacks

MYOC - Myocilin, trabecular meshwork inducible glucocorticoid response

POAG - Primary Open-Angle Glaucoma

CYP1B1- Cytochrome P450 1B1

JOAG – Juvenile open angle glaucoma

OPTN- Optineurin

ASD – Anterior segment dysgenesis

PAX6 - Paired box protein 6

PITX2 - Paired-Like Homeodomain 2

IOP – Intraocular pressure

TM – Trabecular meshwork

DEX - Dexamethasone

NMDA - N-methyl-D-aspartate

NPCE – Non pigmented ciliary epithelial cells

FOXO1 - Forkhead box protein O1

TGF-β1 - Transforming growth factor beta 1

HSPA6 - Heat Shock Protein 6

CLOCK - Circadian Locomotor Output Cycles Kaput

MEIS2 - Meis Homeobox 2

STXBP6 - Syntaxin Binding Protein 6 (Amisyn)

SNAP23 - Synaptosomal-associated protein 23

SYN2 - Synapsin II

RAB – Ras associated in the brain

GTPase - Hydrolase enzymes binding and hydrolyzing guanosine triphosphate (GTP)

Ras - reticular activating system

SNARE - SNAP (Soluble NSF Attachment Protein) REceptor

IL-1- Interleukin-1

NF- kappaB - Nuclear factor kappa-light-chain-enhancer of activated B cells

ATP - Adenosine triphosphate

GDP - Guanosine triphosphate

RAB3GEP – RAB3 guanine nucleotide exchange factor

CNS – Central nervous system

VAMP - Vesicle-associated membrane protein

BoNT - Botulinum toxin

BS – Binding site

ChIP - Chromatin immunoprecipitation

DMEM - Dulbecco's Modified Eagle Medium

PBS - Phosphate-buffered saline

PMSF - Phenylmethane sulfonyl fluoride

PIPES - Piperazine-N,N′-bis(2-ethanesulfonic acid)

PIC – Protease inhibitor cocktail

EDTA - Ethylenediaminetetraacetic acid

PCR - Polymerase chain reaction

IP - Immunoprecipitation

IgG - Immunoglobulin G

H3K4ME3 - Histone H3 tri methyl K4

ssDNA - Single-stranded DNA

WT – Wild type

pGL3.TK - pGL3 Luciferase vector with a thymidine kinase promoter

pRLTK - Renilla luciferase vector with a thymidine kinase promoter

FBS - Fetal bovine serum

pCMV-β-gal – Cytomegalovirus β- galactosidase

LAR I - Luciferase assay reagent I

OptiMEM - Minimal essential medium

siRNA - Small interfering RNA

cDNA - Complementary DNA

M-MLV - Moloney Murine Leukemia Virus

HPRT1- Hypoxanthine Phosphoribosyltransferase 1

RQ – Relative quantification

SDS - Sodium dodecyl sulfate

PAGE - Polyacrylamide gel electrophoresis

DTT - Dithiothreitol

HRP - Horseradish peroxidase

TFIID - Transcription factor II D

ABCA8 - ATP-Binding Cassette, Sub-Family A (ABC1), Member 8

SLC12A6 - Solute Carrier Family 12 (Potassium/Chloride Transporter), Member 6

qRT-PCR – Quantitative real-time polymerase chain reaction

kDa - kiloDalton

miR - microRNA

TSS – Transcription start site

RIM1- Regulating synaptic membrane exocytosis protein 1

ATP - Adenosine triphosphate

TBC1D17 - TBC1 Domain Family, Member 17

RGC-5 - Immortalized rat retinal ganglion cell line

FEZ1- Fasciculation and elongation protein zeta-1

mRNA – Messenger RNA

$p21^{CDKN1A}$ - Cyclin-dependent kinase inhibitor

GABA - gamma-Aminobutyric acid

NGF - Nerve growth factor

PC12 – Immortalized cells derived from the pheochromocytoma of the rat adrenal medulla

1. Introduction

1.1 - Glaucoma overview

Glaucoma is among the leading causes of blindness is the world, affecting over 60 million people worldwide and is estimated to impact over 110 million people by 2040[1]. Glaucoma often affects both eyes; however the damage tends to be asymmetric, affecting one of the eyes to a greater extent than the other[2].

Glaucoma is characterized by progressive visual field loss, caused by retinal ganglion cell (RGC) death[3]. Vision loss in glaucoma which progresses from loss of mid-peripheral visual field to a loss of central visual field [3]. Glaucomatous vision loss is caused by retinal ganglion cell (RGC) death, instigated by stress transfer from the sclera and cornea to the RGC axons [3,4]. RGC nerve fibers, part of the optic nerve head (Fig. 1A), pass through the optic disc, creating a cup shape[3]. The ratio of the cup to the overall disc area increases as more RGC are damaged during the progress of glaucoma[3]. Damage at the optic nerve head results in axonal injury and disruption of anterograde and retrograde axonal transport[3,5]. In turn, damaged axonal transport decreases delivery of trophic molecules important for RGC growth and survival and as a result RGC apoptosis is initiated[3,6]. RGC death creates a toxic environment for its neighboring RGC and increases the stress exerted on them[3].

When glaucoma develops as a complication of another disease, such as chronic uvetis, it is referred to as secondary, otherwise it is known as primary[7]. Glaucoma is also characterized by the formation of the angle between the iris and the cornea, as either angle-closure glaucoma or open angle glaucoma[3]. In angle closure glaucoma the displaced iris blocks the trabecular meshwork and prevents most of the aqueous humor outflow[3]. The most common

form of glaucoma is primary open angle glaucoma (POAG), and it has the highest prevalence in Africa where it affects 4.20% of the population between 40-80 years of age[1].

Glaucoma is also characterized by the age of onset. When POAG presents at birth or within two years it is called congenital or infantile[8,9]. Mutations in *CYP1B1* are often associated with congenital/infantile glaucoma, with 92% of Saudi Arabian and 20% of Japanese patients having pathogenic *CYP1B1* mutations[8,10,11]. POAG diagnosed in patients between 2 and 40 years of age is designated as juvenile onset POAG, shortened to JOAG[8,12]. *MYOC* mutations were described in 36% of JOAG patients[13]. POAG prevalence greatly increases with age in all ethnic groups, with a risk increase of at least 1.5 per decade[14]. Optineurin (*OPTN*) mutations are mainly associated with late onset POAG without ocular hypertension, also known as normal tension glaucoma[15]. Mutations in Myocilin (*MYOC*) are present in around 3% of late onset POAG patients[16].

An additional POAG subgroup, developmental glaucoma, describes POAG associated with anterior ocular segment dysgenesis (ASD) disorders, referring to conditions with cornea, iris, and lens developmental abnormalities[17]. Mutations in the transcription factors *PAX6*, *PITX2* and *FOXC1* are associated with developmental glaucoma[18]. Glaucoma subtypes are summarized in Table 1.

Present treatments which include both surgical interventions, such as trabeculectomy, and medications, among them the prostaglandin Latanoprost, aim to halt glaucoma progression by lowering intraocular pressure (IOP), the buildup of aqueous flow resistance which contributes to RGC damage, but are unable to reverse damage[19,20]. In many cases despite interventions glaucomatous damage worsens with time, as ~ 27% of patients with open

angle glaucoma may still face blindness in one eye, and 7% in both eyes after years of treatment[21].

1.2 - Glaucoma pathogenesis

Both environmental and genetic factors are involved in pathogenic mechanisms implicated in RGC death (Fig. 1C), among these mechanisms are ocular hypertension, oxidative stress and glutamate excitotoxicity.

Ocular Hypertension

Aqueous humor is produced in the ciliary body then circulated through the ciliary epithelium into the anterior chamber and drains into the episcleral venous system mainly through the trabecular meshwork and Schlemm's canal, in the trabecular/conventional outflow pathway (Fig. 1B)[22,23]. The aqueous humor also drains to a lesser degree through the anterior ciliary body, in the unconventional/ uveoscleral outflow pathway (Fig. 1B) [22,23]. Intraocular pressure (IOP) represents a buildup of aqueous humor flow resistance, which in turn facilitates aqueous humor outflow through the trabecular meshwork (TM)[23]. At normal IOP aqueous humor production is balanced by aqueous humor drainage through the TM[23]. When aqueous humor outflow is disrupted, it results is high intraocular pressure (IOP), also known as ocular hypertension[3]. Ocular hypertension is neither necessary nor sufficient for glaucoma development[3,24]. However, ocular hypertension increases the risk of developing glaucoma and its progression, as it creates mechanical stress which is transmitted to optic nerve cells[3,25].

Several environmental factors have been examined for involvement in glaucoma pathogenesis, generally considered to act by causing IOP increase and contributing to RGC

death[26]. Smoking has been investigated since the 1970s as an IOP elevating factor; however, results are contradictory[27]. In a recent study in Chinese patients with juvenile and adult onset POAG, no significant correlation between smoking and POAG onset or increase in IOP was found[28]. However there was association between smoking and central corneal thickness in patients with adult onset POAG indicating that smoking might contribute to glaucoma pathogenesis[28]. Another recent study in Japanese patients found a significant correlation between smoking and increased IOP, but only in men[29].

Corticosteroid use is also considered to contribute to glaucoma pathogenesis through IOP increase, following reports of patients developing glaucoma after use of topical corticosteroids[32]. Around 18-36% of patients undergo a mild increase in IOP following topical corticosteroid use[30–33]. Topical glucocorticoid use has a more severe effect with 5% of the general population and 46-92% of POAG patients experiencing and a sharp and damaging increase in IOP following use[32–38]. Treatment of TM cells *in vitro* with the glucocorticoid Dexamethasone (DEX) results in MYOC over-expression[39,40]. MYOC is also associated with juvenile onset glaucoma, and disrupted MYOC secretion was shown to damage TM cells and increase IOP [13,41]

Glutamate excitotoxicity

Another mechanism contributing to glaucoma pathogenesis is glutamate excitotoxicity. Glutamate excitotoxicity is generated by disrupted glutamate transport resulting in abnormally high glutamate levels in the synapse, leading to neurotoxicity through NMDA receptor activation, which causes influx of Ca^{2+} into the cell and activates apoptotic pathways[42,43]. In hypertension animal models of glaucoma abnormally high levels of

glutamate were detected in the retina, as well as in glaucoma patients and RGC were shown to be highly sensitive to NMDA activation[44,45].

Oxidative stress

One of the central mechanisms implicated in early onset forms of glaucoma is oxidative stress which occurs when the level of oxidants exceed that of antioxidants, resulting in macromolecular damage[46]. Oxidative stress plays an important role in congenital POAG, primary associated with *CYP1B1* mutations[5]. Retinal epithelial cells of *CYP1B1* knockout mice have reduced capillary morphogenesis, migration and had difficulty to adhere to matrix protein, and the phenotype was reversed by lowering oxygen levels[47]. *CYP1B1* knockout mice also have low levels of endothelial nitric oxide-synthase and heightened oxidative stress in retinal epithelial cells that can be reduced with administration of endothelial nitric oxide synthase, suggesting these proteins act together as regulators of oxidative state in retinal epithelial cells[48].

1.3 - Axenfeld-Rieger Syndrome and FOXC1

Developmental POAG is associated with developmental abnormalities in the anterior segment of the eye[49]. Schlemm's canal and the trabecular meshwork, the tissues involved in conventional aqueous humor outflow, are adjacent to the iris and cornea can be impacted by anterior segment abnormalities[49]. Axenfeld Rieger syndrome (ARS) is part of the anterior segment dysgenesis spectrum of disorders[49]. Ocular abnormalities in ARS patients include iris thinning and pupil displacement[50]. In most patients the cornea is also malformed with displaced Schwalbe's line and iris strands attaching to the trabecular meshwork and at times to the Schwalbe's line[50]. The ocular malformations in ARS patients

contribute to obstruction of aqueous humor outflow leading to increased IOP[51]. Patients with ARS are at 50% or greater risk of developing POAG, and in the majority of cases glaucoma develops between infancy and early adulthood[51,52].

Moreover, glaucoma in ARS patients is difficult to treat as both IOP lowering surgeries and medications have limited effect in halting glaucoma; only 18% of ARS patients respond to treatments, even when surgery and medication are combined[53].

In addition to ocular malformations, ARS patients also have craniofacial and dental abnormalities and in some cases growth retardation and pituitary abnormalities[50]. Developmental malformations in ARS occur in tissues derived from neural crest cells, which are neuroectodermal cells migrating from the neural tube crest during development, and are important for formation of the anterior segment of the eye, bone, teeth and skull cartilage[50]. Some ARS patients also have systemic abnormalities which include congenital heart defects such as aortic and pulmonic valve stenosis, atrio-septal defect and mitral valve abnormalities[54–57].

ARS has an autosomal dominant inheritance and mutations in two developmental transcription factors, *PITX2* and *FOXC1*, are associated with ARS[58,59]. PITX2 regulates transcription of downstream genes by binding to upstream regions through its homeodomain and is involved in development of anterior segment tissues during embryogenesis[50]. FOXC1 and PITX2 are co-expressed in the mouse periocular mesenchyme and PITX2 interacts through its homeodomain with FOXC1[60].

FOXC1 is a member of the Forkhead box (FOX) family of transcription factors which, contain a conserved 110 amino acid Forkhead domain, through which they bind upstream

of genes and promote activation[50]. The DNA binding Forkhead domain shared by FOX helices, three β-strands and two loops near its C-terminal region[61]. FOX proteins interact transcription factors has a 'winged helix' shape which is composed of three N-terminal α- with specific DNA sequences through one of the helixes in the Forkhead domain, called the 'recognition helix'[62]. The Forkhead domain also contains nuclear localization sequences allowing FOX proteins to enter the nucleus and affect transcription of their target genes[61]. FOX proteins have central roles in both embryonic development and adult function[61].

Pathogenic *FOXC1* mutations include missense mutations inside the Forkhead domain and nonsense and frame shift mutations in the upstream *FOXC1* region that result in a truncated protein[63,64]. Interestingly, some ARS patients have chromosomal duplications of *FOXC1*[63,65,66]. However, it is still unknown whether FOXC1 duplications result in increased FOXC1 expression [65]. FOXC1 mutations disrupt the protein's ability to activate downstream targets, by binding to its consensus binding sequence, 5′-GTAAATAAA-3′ [64,67]. The FOXC1 missense mutation S131L, results in reduced ability of FOXC1 to bind and transactivate a TK-Luciferase reporter through the consensus FOXC1 binding site[64].

FOXC1 mutations were also found in patients with Dandy-Walker malformation, characterized with abnormal cerebellar development[68]. Patients with the S131L FOXC1 mutation showed mild cerebellar vermis hypoplasia in brain scans[68]. Mice with a protein-destabilizing point mutation have also exhibited cerebellar vermis hypoplasia as well as ataxia[68]. FOXC1 is expressed in the posterior fossa mesenchyme adjacent to the cerebellum and is hypothesized to regulate cerebellar development through mesenchymal signaling[68].

The role of FOXC1 in development is exerted through the downstream genes it regulates. Several microarrays have been carried out to find downstream FOXC1 targets. Berry et al. (2008) carried out a microarray in non-pigmented ciliary epithelium cells (NPCE) that identified genes whose expression changed following FOXC1 induction[69]. Among the candidate downstream targets found in the microarray was FOXO1, a transcription factor noted for its role in oxidative stress resistance[69]. FOXC1 was shown to bind and activate the *FOXO1* promoter in NPCE cells and following morpholino FOXC1 knocked down in zebrafish, RNA levels of *FOXO1* decreased in ocular tissues while ocular cell death increased[69]. When FOXC1 was knocked down in human trabecular meshwork (TM1) cells, FOXO1 protein levels decreased and following addition of H_2O_2, cell viability of FOXC1 knockdown cells dropped sharply relative to controls[69]. FOXO1 was also shown to promote wound healing through keratinocyte migration and TGF-β1 activation along with oxidative stress resistance, suggesting that *FOXC1* mutations, which lower levels of FOXO1 might impair tissue regeneration following injury in ocular tissue and promote glaucoma pathogenesis[70].

FOXC1 was also shown to regulate the molecular chaperone, Heat-shock protein A6 (*HSPA6*), also discovered as a potential target in the microarray performed by Berry et al. (2008) [69,71]. FOXC1 was shown to bind to and up regulate RNA levels of *HSPA6* and add another mechanism of action in FOXC1 role in modulating the stress response pathway[71].

Another microarray by Paylakhi et al. (2013) in human trabecular meshwork cells, looked at genes that changed RNA levels following FOXC1 knockdown[72]. Among the target genes identified by the microarray was *CLOCK*, a gene involved in circadian rhythm

regulation which was shown to regulate IOP levels and *MEIS2* a homeobox transcription factor important for lens and retina development[73,74].

The microarray screen performed by Berry at al. (2008) detected several exocytic proteins providing a potential link to exocytosis, responsible for extracellular trafficking. Interestingly, exocytosis has an important role in glutamate excitotoxicity and other mechanisms involved in glaucoma[42,43,69]. Among the predicted FOXC1 exocytic targets were *RAB3GAP1*, *SNAP25* and *STXBP6*[68]. In a microarray conducted by Paylakhi et al. (2013) additional exocytic FOXC1 targets were found, including *SNAP23* and *SYN2*[74].

The focus of this thesis will be on investigating the role of FOXC1 regulation of RAB3GAP1, RAB3GAP2 which form the RAB3GAP, complex with RAB3GAP1. In addition, FOXC1 regulation of SNAP25, a member of the SNARE complex will be investigated as well as the impact of FOXC1 on exocytosis.

1.4 - Exocytosis and its role in glaucoma

Exocytosis overview

Exocytosis is responsible for release of secretory molecules by both neuronal and non-neuronal cells[75]. During exocytosis a secretory vesicle is recruited to the plasma membrane and prepared for docking, then it is tethered to the plasma membrane and primed for fusion, and finally the vesicle fuses with the plasma membrane and its contents are released outside the cell[76]. Following exocytosis the vesicle membrane that fused with the plasma membrane is recycled through endocytosis[75]. Endocytosis is also important for maintenance of the plasma membrane through lipid and protein sorting[75]. In neuronal

chemical synapses the combination of exocytosis and endocytosis is termed the synaptic vesicle cycle[75].

The vesicle docking and tethering stage of exocytosis is mediated through RAB (Ras-related in brain) proteins, which are small GTPases belonging to the Ras protein superfamily[76–78]. RABs cycle between an active GTP bound state, when localized to the membrane, and an inactive GDP bound state, when localized to the cytosol[79]. GTP bound RABs deliver vesicles to the membrane and interact with downstream effectors which tether the vesicle to the plasma membrane[79]. Once the vesicle is ready for fusion active RABs need to undergo GTP hydrolysis to be recaptured and returned to the cytosol[79]. In switching between an active and inactive state RABs regulate exocytosis spatially and temporally[80].

Following RAB mediated docking to the plasma membrane, vesicles proceed to fuse with the plasma membrane with the help of SNARE proteins[76]. Majority of SNAREs are membrane proteins partly exposed in the cytoplasm while some SNAREs contain a lipid anchor[76]. SNAREs are classified as either v-SNAREs, when they are attached to the vesicle membrane or as t-SNAREs when they are attached to the transmembrane[76]. During membrane and vesicle fusion a v-SNARE forms a complex with a t-SNARE, bringing the two membranes together[76].

MYOC secretion and other glaucomatous mechanisms associated with exocytosis

Exocytosis is indirectly linked to several pathogenic pathways in glaucoma. MYOC secretion presents a potential link between exocytosis and glaucoma in the trabecular meshwork. MYOC is associated with JOAG and most MYOC mutant proteins found in

glaucoma patients were shown to aggregate in the endoplasmic reticulum of TM cells instead of being secreted outside the cell, inducing stress and disrupting cell morphology as well as cell proliferation, thereby interfering with normal TM function[41].

Pathogenic MYOC mutations were also shown to activate the IL-1/NF- kappaB inflammatory stress response pathway that acts to protect against oxidative stress and promote aqueous humor outflow[81]. In turn, wild type MYOC was shown to inhibit the IL-1/NF-kappaB pathway[81]. IL-1/NF-kappaB activation induced endogenous MYOC expression, supporting a role for MOYC as an inhibitor of the IL-1/NF-kappaB through a negative feedback loop[81]. MYOC was also linked to corticosteroid induced glaucoma after treatment of TM cells *in vitro* with the glucocorticoid Dexamethasone (DEX) resulted in MYOC over expression[39,40]. However, while abnormal MYOC secretion was shown to contribute to glaucoma pathogenesis, the mechanism of MYOC secretion in TM cells is not fully understood but it was suggested to associate with exosome like vesicles[82].

In addition, exocytosis is important for cyclic mechanical stress induced ATP release in the trabecular meshwork[83]. Extracellular ATP signaling triggers arachidonic acid mobilization from the plasma membrane and prostaglandin secretion, which in turn acts to lower IOP[83]. Furthermore, exocytosis is involved in glutamate release thereby connecting to glutamate excitotoxicity, associated with RGC apoptosis in glaucoma[84].

As endocytosis and exocytosis act to balance cell trafficking, exocytosis also impacts endocytotic function which in turn is associated with glaucoma through *OPTN* mutations in adult onset glaucoma patients[15]. The interaction of OPTN with RAB proteins has an important role in Transferrin receptor transport and degradation[85,86].

1.5 – Predicted exocytic targets of FOXC1

RAB3GAP

The heterodimeric complex RAB3GAP accelerates RAB3 GTP hydrolysis and promotes RAB3's return to an inactive, GDP bound, state together with RAB3GEP, through interaction with its switch region[87]. RAB3 is important in secretory vesicle tethering and docking to the plasma membrane during exocytosis[76,77]. RAB3GAP is a made of a catalytic subunit, RAB3GAP1, and non-catalytic subunit, RAB3GAP2[88].

RAB3GAP1 mutations are associated with Warburg-Micro syndrome[89]. Warburg-Micro syndrome is an autosomal recessive disorder characterized with ocular defects among microphthalmia, microcornea, congenital cataracts, and optic atrophy, neurodevelopmental malformations such as microcephaly, cortical gyral abnormalities and spastic cerebral palsy and hypogenitalism[90–94] . *RAB3GAP1* is also associated with keratoconus, a condition causing corneal thinning, which is among the leading causes for corneal transplants[95]. Mutations in the non-catalytic RAB3GAP subunit, *RAB3GAP2*, cause Martsolf syndrome. Martsolf syndrome is similar to Warburg-Micro syndrome but with a milder phenotype, characterized with congenital cataracts, microphthalmia, hypogonadism, and mild mental retardation[96].

RAB3GAP1 was shown to have a ubiquitous expression during zebra fish development while RAB3GAP2 is expressed in the central nervous system and only once larval development started, suggesting the complex RAB3GAP1 and RAB3GAP2 act as a complex in the central nervous system (CNS) during development[96]. In ocular tissues RAB3GAP1 has the highest expression in the inner nuclear layer (INL) and to lesser

degree in photoreceptors while RAB3GAP2 is mainly expressed in the proliferative zone of the retina, representing the remnants of the ciliary margin[96].

SNAP25

SNAP25 is a member of the SNARE complex responsible for fusion of vesicles with the plasma membrane during exocytosis[76]. SNAP25 is a t-SNARE protein, meaning that it is attached to the plasma membrane unlike v-SNARE proteins which are attached to vesicles[97]. During vesicle fusion with the plasma membrane, SNAP25 along with another t-SNARE protein Syntaxin, which is integrated in the plasma membrane, forms a complex with the v-SNARE protein VAMP[97]. The SNARE complex formation "zips" the plasma membrane with the vesicle membrane and leads to release of the vesicle contents outside the cell[76].

SNAP25 is mainly associated with synaptic vesicle exocytosis in neurons[97]. It is essential in neuronal exocytosis as application of botulinum neurotoxins (BoNT) A and E serotypes, which cleave SNAP25, results in blocking of exocytosis in both isolated axons and synapses[98]. SNAP25 also plays a role in endocytosis as SNAP25 cleavage with BoNT inhibits endocytosis in synapses[99]. SNAP25 is hypothesized to be involved in endocytosis initiation along with other members of the SNARE complex and underlie the mutual dependence of exocytosis and endocytosis[99].

SNAP25 has two alternatively spliced isoforms, *SNAP25a* and *SNAP25b*, differing in nine amino acids encoded by the exon 5 sequence [100]. Both *SNAP25* isoforms are mainly expressed in neuronal cells[100]. *SNAP25b* is considered the more evolutionary-ancient isoform as it shares greater similarity with the non-neuronal *SNAP25* homolog *SNAP23*[101].

SNAP25 polymorphisms were found to associate with several neuropsychiatric disorders, among them Antisocial Personality Disorder, Attention-Deficit Hyperactivity Disorder and Schizophrenia[102–106].

Other Exocytic FOXC1 Targets

Additional exocytic genes detected as potential FOXC1 targets in microarrays are *SNAP23*, *SYN2* and *STXBP6*[69,72]. *SNAP23* shares 60% similarity with *SNAP25* and has a ubiquitous expression[107]. SNAP23 is considered a non-neuronal homolog of SNAP25 with a similar role in exocytosis by forming the SNARE complex and directing secretory vesicle and plasma membrane fusion[107].

The second exocytic FOXC1 target, SYN2 is involved in neurotransmission and synaptic remodeling and is expressed mainly in central and peripheral nervous systems and at lower levels in some non-neuronal cells[108]. *SYN2* expression is initiated during progenitor differentiation and reaches its peak during synaptogenesis[108–110].

The third exocytic FOXC1 target, STXBP6 also known as Amisyn binds to the SNARE complex member Syntaxin1 thereby assembling into the SNARE complex during vesicle and plasma membrane fusion[111]. STXBP6, was shown to regulate the stability of the fusion pore during exocytosis through binding to Syntaxin1, and also act independently of Syntaxin1 as an exocytosis inhibitor[111].

1.6 – Glaucoma pathogenesis and FOXC1 function in exocytosis

Glaucoma is among the leading causes of blindness in the world; however present treatments cannot reverse vision loss and are have low effectively in many patients[1,53]. It is therefore important to better understand glaucoma pathogenesis in order to develop more efficient treatments.

ARS presents an important model for glaucoma pathogenesis due to the high risk of patients to develop glaucoma and their poor response to treatments[53,112]. FOXC1 mutations, associated with developmental glaucoma in ARS patients, were previously shown to disrupt ocular development and response to oxidative stress through misregulation of FOXC1 target genes[69,71,74]. FOXC1 has hundreds of predicted target genes and few of them were investigated in detail[69]. Investigating the function of FOXC1 in exocytosis through potential regulation of the RAB3GAP complex, composed of RAB3GAP1 and RAB3GAP2 and SNAP25, could uncover an additional mechanism through which FOXC1 promotes glaucoma in ARS patients. Exocytosis in glaucoma was previously linked to glutamate excitotoxicity in RGC and ATP release in the TM[83,113]. Another pathogenic pathway which could be affected by exocytosis in glaucoma is MYOC secretion. Abnormal MYOC secretion has been linked both to genetic JOAG and steroid-induced glaucoma[16,114]. Exploring the role of FOXC1 in exocytosis and the impact of abnormal FOXC1 levels would improve our understanding of the glaucoma pathogenesis in ARS patients and shed light on the interaction of two proteins associated with early-onset glaucoma, FOXC1 and MYOC.

1.7 - Aims and hypothesis

As discussed above, microarray analyses identified the exocytic genes *RAB3GAP1* and *SNAP25* as potential FOXC1 targets[69]. FOXC1 knockdown was also shown to decrease the RNA levels of *RAB3GAP1* in both NPCE cells and in ocular tissues of zebrafish[69]. My studies investigated the role of FOXC1 in the regulation of exocytosis in human cervical cancer (HeLa) and human trabecular meshwork cells. Specifically, I to sought to validate RAB3GAP1 as a positive target gene of FOXC1, look at potential FOXC1 regulation of RAB3GAP2, a protein which forms a heterodimeric complex with RAB3GAP1, and at potential negative regulation of SNAP25 by FOXC1 and the physiological impact of such regulation. Experiments were conducted in two cell lines, HeLa and TM1. HeLa cells were used as they are a resilient human cell line which transfects well. TM1 cells, in turn, are a human cell line physiologically relevant to glaucoma due to the role of the trabecular meshwork in aqueous humor drainage.

My Hypothesis - FOXC1 modulates exocytosis through positive regulation of the exocytic proteins RAB3GAP1, RAB3GAP2 and negative regulation of SNAP25. Abnormal FOXC1 levels results in irregular expression of RAB3GAP1, RAB3GAP2 and SNAP25, which in turn disrupt MYOC secretion (Fig. 2). To test this hypothesis, I had two aims:

Aim 1- Investigate the ability of FOXC1 to bind and activate expression of RAB3GAP1, RAB3GAP2 and SNAP25. Analyze the effect of FOXC1 knockdown on RNA and protein levels of RAB3GAP1, RAB3GAP2 and SNAP25.

Aim 2- Analyze the impact of FOXC1 on exocytosis of MYOC, a protein secreted from the trabecular meshwork and associated with glaucoma pathogenesis[13,41].

2. Methods

2.1 - FOXC1 Binding Sites and Primers

FOXC1 binding sites (BS) located within 10,000 bp upstream of transcription start sites of target genes were detected with the Possum software (http://zlab.bu.edu/~mfrith/possum/) using a FOXC1 binding matrix determined by Pierrou et al. (1994)[67]. Primers corresponding to the binding sites were designed using Primer3 (http://bioinfo.ut.ee/primer3-0.4.0/). Primers surrounding the RAB3GAP1 FOXC1 binding site were designed by Tim Footz. Primers surrounding FOXC1 binding sites upstream of RAB3GAP1, RAB3GAP2 and SNAP25 are described in Table 2.a.

2.2 - Chromatin Immunoprecipitation (ChIP)

Eight plates of HeLa cells (seeded at 10^7 per 100 mm plate) were grown to confluency for 2 days in 10 ml DMEM (1x Gibco Thermo Fisher Scientific Waltham Massachusetts, USA)(10% FBS, 1%Antimycotic). On the third day, formaldehyde was added to each plate to a final concentration of 1% and plates were incubated for 10 minutes in room temperature for cross-linking. To stop the reaction 1.25 mM of glycine was added per plate and incubated for 5 minutes at room temperature with gentle shaking. Media were aspirated and cells washed two times with cold PBS (Na_2PO_4 9.1 mM, NaH_2PO_4 1.7 mM, NaCl 150 mM), then scraped with 1 ml cold PBS mixed with 1 mM PMSF. The lysates were combined and spun at 1500 rpm in 4°C for 5 minutes and the supernatant was aspirated. The pellet was lysed with 5 ml ChIP cell lysis buffer (PIPES pH 8.0 5 mM, KCl 85 mM, IGEPAL CA-630 0.5%) with 1 mM PMSF and 0.05% final concentration of Protease Inhibitor Cocktail (PIC) (Sigma-Aldrich, St. Louis, Missouri, United States) and incubated for 10 minutes on

ice. The lysate was transferred to a Dounce homogenizer (B pestle) and homogenized 6 times then spun at 3000 rpm in 4°C for 5 minutes.

The supernatant was aspirated and pellet re-suspended with 1 ml ChIP Nuclear lysis buffer (Tris pH 8.0 50 mM, EDTA 10 mM, SDS 1%) with 0.05% PIC and 1 mM PMSF transferred to a 1.5 ml tube and incubated on ice for 10 minutes. The nuclear lysate was sonicated with 3x 15 seconds pulses (5-7 W) using a Sonic dismembrator 60 (Thermo Fisher Scientific, Waltham, Massachusetts, United States) on ice, with 15 seconds of rest between each pulse. The lysate was spun at 15,000 xg at 4°C for 10 minutes. Supernatant was transferred to a new tube and 80 µl of well-suspended Protein A/G PLUS-Agarose (Santa Cruz Biotechnology, Dallas, Texas, United States) were placed into the supernatant. The lysate was rotated at 4°C for an hour then spun at 6,000 xg at 4°C for 1 minute. Twenty five µl of supernatant were set aside and used for an "Input" PCR template sample (10% of each IP reaction) and kept at -20°C. The remaining supernatant was divided into 250 µl aliquots and moved to new tubes, 750 µl of ChIP Dilution Buffer (Tris pH8.0 16.7 mM, EDTA 1.2 mM, NaCl 167 mM, SDS 0.01%, Triton X-100 1.1%, PIC 0.05%, 1 mM PMSF) was added per tube.

To each tube, 3 µg of either Rabbit anti-IgG (CALTAG Laboratories Buckingham UK), a negative control, Rabbit anti-H3K4ME3 (a generous gift from Dr. David Eisenstat), a positive control for transcriptionally active chromatin, or Goat anti-FOXC1(OriGene, Rockville, Maryland, United States) were added and tubes were rotated at 4 °C overnight. The next day 40 µl of well-suspended Protein A/G PLUS-Agarose (Santa Cruz) and 2 µl of 10 mg/ml sonicated salmon sperm ssDNA (Invitrogen, Carlsbad, California, United States) were added to each tube, rotated at 4°C for 1 hour and spun at 6,000 xg at 4°C for 1

minute. Supernatant was aspirated and the beads were washed with 1 ml ChIP Wash Buffer (Tris 20 mM, EDTA 2 mM, SDS 0.1%, Triton X-100 1%) by rotating at 4°C for 5 minutes and spinning at 6,000 xg at 4°C for 1 minute. Next, the beads were washed with 1 ml ChIP Final Wash Buffer (Tris pH 8.0, EDTA 2 mM, NaCl 500 mM, SDS 0.1%, Triton X-100 1%) for 30 minutes, then with 1 ml LiCl wash buffer (0.25 M LiCl, 1% deoxycholate, 1 mM EDTA, 10 mM Tris-HCl (pH 8.1), 1% NP-40) for 30 minutes and finally two times with TE buffer pH8.0 (2x) with spinning and buffer aspiration after each wash. The DNA was eluted by adding 125 µl of ChIP Elution Buffer (Sodium Bicarbonate 100 mM, SDS 1%) to the beads followed by 15 minutes of rotation and spinning down. The supernatants were transferred to new tubes and the elution was repeated with another 125 µl of ChIP Elution Buffer, incubation at 95°C for 1 minute, and rotation at room temperature for 15 minutes. The tubes were centrifuge and the supernatant was added to the elution buffer used before. The "Input" sample preciously stored at -20 °C was thawed and combined with 225 µl of ChIP Elution Buffer. Next, five µl of Proteinase K (20 mg/ml) (Invitrogen) was added to each tube, including "Input" and the tubes were incubated at 65 °C overnight. The next day DNA from each sample was purified with a QIAGEN quick PCR Purification kit (Qiagen, Hilden, Germany) according to the manufacturer's protocol. One µl of purified DNA was used as a template for PCR runs with ChIP primers for RAB3GAP1, RAB3GAP2 and SNAP25 described in Table 2.a.

2.3 - Plasmids

Xpress plasmid constructs

Xpress-Empty vector was purchased from Invitrogen. pcDNA4:Xpress-FOXC1(WT) was created by Ramsey A. Saleem as described previously[64].

An Xpress-FOXC1 (S131L) construct, containing a patient mutation resulting in reduced binding of FOXC1 to its target genes, was created by Ramsey A. Saleem as described previously[64].

pGL3 and pGL3.TK plasmid constructs

To clone upstream target gene regions containing predicted binding sites into pGL3 and pGL3.TK, SacI and BglII binding sites were added to the RAB3GAP1, RAB3GAP2, SNAP25 ChIP primers as described in Table 2.b, the primers were amplified by PCR with a 2% dilution of genomic DNA and cloned with the use of pGMT-Easy cloning system (Promega Madison, Wisconsin, United States) into pGL3 (Promega) to generate the plasmid constructs pGL3.RAB3GAP1, pGL3.RAB3GAP2 and pGL3.SNAP25.

Additionally, upstream RAB3GAP2 and SNAP25 regions were cloned into the pGL3.TK reporter to generate pGL3.TK.RAB3GAP2 and pGL3.TK.SNAP25 constructs. The pGL3.TK reporter was constructed by Ramsey A. Saleem as described previously[64], briefly, a herpes simplex–virus thymidine kinase (TK) promoter, from pRLTK (Promega) was cloned into the BglII-HindIII sites of pGL3. The pGL3.TK reporter contains a promoter, and the FOXC1 binding sites in those genes were more than 4000 bp away from

the transcription start site. Thus are more likely to act as enhancers than proximal promoter elements.

Additional constructs were generated with the 16 bp containing the predicted binding sites deleted (while the rest of the upstream region remained) to assess the importance of the predicted binding site for transcriptional regulation of the target gene by FOXC1. The RAB3GAP1 upstream region contained three potential binding sites and each was deleted separately to generate three constructs; pGL3.RAB3GAP1.del1, pGL3.RAB3GAP1.del2, and pGL3.RAB3GAP1.del3. In each of the RAB3GAP2 and SNAP25 upstream regions, one predicted FOXC1 binding site was deleted to generate: pGL3.RAB3GAP2.del, pGL3.TK.RAB3GAP2.del, pGL3.SNAP25.del, and pGL3.TK.SNAP25.del. The deletions were made using site directed mutagenesis performed on intermediate pGMT vector constructs using the QuickChange Lightning Kit (Agilent technologies Santa Clara, California, United States) with primers described in Table 2.c. Following mutagenesis, target upstream regions with the binding sites deleted were cloned into pGL3 and pGL3.TK.

The pGL3.FOXO1 plasmid, acting as a positive control for Luciferase transactivation by FOXC1 in constructs with the pGL3 reporter, was constructed by Fred B. Berry as described previously[69]. Briefly, a region 580 bp upstream and 250 bp downstream of the transcription start site was cloned by PCR and inserted into pGL3 (Promega) vector[69].

The pGL3.TK.6xFBS plasmid, a positive control in Luciferase transactivation with the pGL3.TK reporter, was constructed by Ramsey A. Saleem by cloning six copies of the FOXC1-binding site into the *Eco*RI- *Nhe*I sites on the TK promoter[64].

2.4 - Luciferase Transactivation Assay

40,000 HeLa cells were seeded per well on 24 well plates and grown over night in DMEM. Transfections were performed using Lipofectamine2000® reagent (Invitrogen Carlsbad California, United States), per the manufacturer's instructions diluted in OptiMEM. Cells within wells were transfected in triplicate with 30 ng pRL-CMVβ (Promega) as a transfection efficiency control and either 500 ng Xpress-FOXC1 (WT) or Xpress-FOXC1 (S131L), to compare the ability of WT versus mutant FOXC1 to activate the Luciferase reporter. Additionally each well triplicate was transfected with 100 ng of either of pGL3, pGL3.FOXO1 (positive control), and the constructs with target gene upstream regions described in Table 2.b and c, with the predicted binding site present or deleted for example either pGL3.RAB3GAP1 or pGL3.RAB3GAP1.del1. Alternatively, 100 ng of either of pGL3.TK, pGL3.TK.6xFBS (positive control) were used in transfections. Each condition was transfected in triplicate. Each experiment was repeated at least three times.

Three days after transfection, Luciferase transactivation assays were performed using the Promega Dual –Luciferase reporter assay system per the manufacturer's protocol. Briefly, following two washes with PBS cells were lysed with 1x Reporter Lysis Buffer (Promega), frozen for 15 minutes at -80°C, then thawed on a shaker for 15 minutes at room temperature. Lysates were collected into 1.5 ml tubes and centrifuged at max speed for 1 minute at 4°C. Fifty µl of lysate were combined with 50 µl of 2x Assay Buffer (Promega), mixed and incubated for 30 minutes at 37°C, the reaction was then stopped with addition of 900µl of 1 M Sodium Carbonate and β-galactosidase (transfection efficiency control) values were measured at $O.D._{420}$ on a spectrometer. While the β-galactosidase control was incubating at 37°C, Luciferase activation was measured on the TD-20/20 luminometer

(Turner Design Sunnyvale, CA, United States) by adding 10 µl of lysate to 100 ul LAR I (Promega), vortexing the mix for 2 seconds and measuring Luciferase activation. Luciferase values were normalized to β -galactosidase values to control for transfection efficiency, then scaled to the activation level of the empty Luciferase reporter when treated with Xpress-FOXC1(WT) to compare changes in activation.

2.5 - Transfections for qRT-PCR and Western Analysis

10^6 HeLa or Human Trabecular Meshwork (TM1) cells were seeded in 100 mm plates and grown overnight in 10 ml DMEM. The following day transfections were performed with 12.5 µl Lipofectamine2000® reagent, diluted in 400 µl OptiMEM I(1x)(Gibco) and incubated for 5 minutes in room temperature before being added to a plasmid or siRNA premixed with 400 µl OptiMEM.

For FOXC1 knockdown experiments, 500 ng of Silencer negative control siRNA #1 (Ambion, Thermo Fisher Scientific) or FOXC1 siGENOME #4 (Dharmacon Lafayette, Colorado, United States) were used. For FOXC1 over-expression experiments 12500 ng of either Xpress-Empty or Xpress- FOXC1 (WT) were used. The mix was incubated for 20 minutes then added drop wise into the plate. The transfected cells were grown for three nights in 37°C and 5% CO_2 prior to collection.

2.6 - qRT-PCR

Cells were washed twice with PBS, and then treated with 1ml Trizol (Ambion) to isolate total RNA. Two µg of RNA were used for cDNA preparations with M-MLV Reverse Transcriptase (Invitrogen) according to the manufacturer's protocol and treatment with DNnase I (Invitrogen).

Primers for *FOXC1* and *HPRT1* (a housekeeping gene, used as a reference gene for normalization) were designed by Tim Footz. Primers for *RAB3GAP1*, *RAB3GAP2* and *SNAP25* (detecting both isoforms) were designed using the Primer3 software. Primers were designed to separately detect the *SNAP25a* and *SNAP25b* isoforms as described in He´raud et al. (2008)[115]. The primer sets are described in Table 2.d.

qRT-PCR assays were performed with a QuantiTect SYBR Green PCR kit (Applied Biosystems Foster City, California, United States) on a 9700HT Thermal Cycler (Applied Biosystems) at least three times with each reaction in triplicate. Dissociation curves were performed with each qRT-PCR to confirm the homogeneity of the PCR product and primer specificity. RNA levels were normalized to *HPRT1* through the ΔΔCt method and changes in RNA levels were described in relative quantification (RQ).

2.7 - Western Blot Analysis

Cells were washed twice with PBS, scraped with 1 ml PBS and centrifuged at 1000 xg for 5 minutes. Next, PBS was aspirated and the pellet was lysed with 100 µl IP lysis buffer (IGEPAL ® CA-680, Tris pH 8.0 0.05 M, NaCl 0.15 M, PMSF 1 mM, Protease Inhibitor Cocktail 0.05%). Lysates were mixed with 6x SDS-PAGE Loading Buffer (Stacking Gel Buffer -0.06 M Tris 0.05% SDS, Glycerol 10%, SDS 0.02%, DTT 1%, Bromophenol Blue 0.05%) and denatured for 10 minutes at 65°C. The denatured proteins were then size separated on 8% SDS-PAGE gel at 150 V for 55-120 minutes on a Protean 3 minigel system (Bio-Rad Hercules, California, United States) in an Electrophoresis running buffer (25 mM Tris, 200 mM glycine, 0.2% SDS). PageRuler (Thermo Scientific), a prestained marker was used to measure protein sizes. The proteins were then transferred into a

nitrocellulose membrane (Bio-Rad) on a Protean 3 semidry transfer apparatus (Bio-Rad) at 100 V for 1 hour, then blocked for 1 hour with a 5% skim milk in TBST (10 mM Tris-HCl pH7.5, 75 mM NaCl, 0.05% Tween 20). Blots were incubated overnight at 4°C with either of the following primary antibodies: Rabbit anti-FOXC1 (Cell Signaling, Danvers, Massachusetts, United States) 1:5000, Rabbit anti-RAB3GAP1 (AssayBioTech Sunnyvale, California, United States) 1:5000, Rabbit anti-RAB3GAP2 (AssayBioTech) 1:5000, Rabbit anti-SNAP25 (Abcam, Cambridge, United Kingdom) 1:1000 in 5% skim milk in TBST. The following day blots were rinsed twice with TBST then washed three times with 5 ml TBST for 10 minutes and incubated for 1 hour at room temperature with secondary HRP-conjugated antibodies diluted 1:5000 in 5% skim milk in TBST. Blots were also incubated with Mouse anti- α-Tubulin (Santa Cruz), as loading control, for 1 hour in room temperature 1:5000 in 5% skim milk in TBST and a secondary HRP-conjugated antibody diluted 1:5000 in 5% skim milk in TBST for 1 hour. After incubation with secondary antibody, blots were washed again three times in TBST for 10 minutes, and the secondary antibody signal was exposed by SuperSignal™ West Femto Maximum Sensitivity Substrate substrate (Thermo Scientific). Images were taken on Imagestation4000 with 10 minute exposure. Net intensity of bands was normalized to the net intensity of α-Tubulin then scaled to the control for each treatment. Experiments were repeated at least in triplicate.

2.8 - Analysis of Myocilin Secretion Following FOXC1 Knockdown

HeLa cells seeded at 10^6 on 100 mm plates the day before were transfected using Lipofectamine2000® with 12.5 µg of pRc-Myocilin-Myc[116] a generous gift of Dr. Vincent Raymond (University of Laval, PQ) and either 500 ng of Silencer negative control

siRNA#1 or FOXC1 siGENOME #4 (siRNA FOXC1). After 3 days a 1 ml sample of the cell media was collected and cells were lysed with IP Lysis buffer as described previously. Protein lysates and media were centrifuged at max rpm for 12 minutes at 4°C. Next, 100 ng of protein lysates and 20 µL of media were denatured with 6x SDS-PAGE Loading Buffer at 65°C for 10 minutes then size separated on a 10 well 8% SDS gel at 150 V for 55 minutes. Proteins were transferred to a nitrocellulose membrane for 1 hour at 100 V. The blots were blocked with 5% skim milk in TBST for 1 hour. To look at intracellular and media MYOC levels, the blots were incubated for 1 hour with Goat anti-MYOC (Santa Cruz Biotechnology) diluted in 5% skim milk in TBST at 0.75:5000 at room temperature, blots were washed with TBST then incubated for 1 hour with a secondary HRP-conjugated antibody diluted 1:5000 in 5% skim milk in TBST for 1 hour. The MYOC band net intensity was normalized to Ponceau Red stain (total protein control) net intensity in media bands. Whole cell lysates were normalized to the loading control, TFIID, after incubation for 1 hour in room temperature with 1:5000 Rabbit anti-TFIID (Santa Cruz Biotechnology) diluted in 5% skim milk and it's secondary HRP-conjugated antibody diluted 1:5000 in 5% skim milk. Blots were also incubated with Rabbit anti-FOXC1 overnight at 1:5000 dilution in 5% skim milk then the following day for 1 hour at room temperature it's secondary HRP-conjugated antibody diluted 1:5000 in 5% skim milk. Then, net intensity of intracellular FOXC1 was normalized to TFIID. After normalizations protein levels were scaled to the treatment control. Experiments were repeated in triplicate.

2.9 - Analysis of Myocilin Secretion Following RAB3GAP1, RAB3GAP2 and SNAP25 Knockdown

HeLa cells seeded at 10^6 cells per 100 mm plate the day before were transfected using Lipofectamine2000® with 12.5 µg of pRc-Myocilin-Myc and either 250 ng of Silencer negative control siRNA #1, siRNA RAB3GAP1(5′-UCAGUACACUCACUUAUCA-3′), siRNA RAB3GAP2 (5′-UGACUUGGCUCUGUUACUA-3′), both custom ordered from Dharmacon and designed after Spang et al. 2014[117] , combination of siRNA RAB3GAP1 and siRNA RAB3GAP 2, SNAP25 Silencer® Select S13188 (Ambion, Thermo Fisher), and a combination of RAB3GAP1, siRNA RAB3GAP2 and SNAP25 Silencer® Select. After three days media was collected and cells were lysed as previously described. Next, 10µl of cell media and 50 ng of protein lysate were denatured with 6x SDS-PAGE Loading Buffer at 65°C for 10 minutes then size separated on a 15 well 8% SDS gel at 150 V for 55 minutes the transferred to a nitrocellulose membrane for 1 hour at 100 V. Intracellular and media MYOC protein levels were measured as described previously. Blots were then incubated with either Rabbit anti-RAB3GAP1 (1:5000), Rabbit anti-RAB3GAP2 (1:5000) or Rabbit anti-SNAP25(1:1000) overnight in 4 °C and for an hour the following day with their secondary HRP-conjugated antibody diluted 1:5000 in 5% skim milk. Protein net intensity was normalized to TFIID and scaled to the treatment control. Experiments were repeated in triplicate.

2.10 - Statistical Analysis

Statistical significance was evaluated using the Mann-Whitney U test, a non-parametric test for independent samples. P-values were calculated using AI-Therapy Statistics software (https://www.ai-therapy.com/psychology-statistics/hypothesis-testing/two-samples). One-tailed analysis was carried out to confirm FOXC1, RAB3GAP1, RAB3GAP2 and SNAP25 knockdown with siRNAs and FOXC1 over-expression with Xpress-FOXC1 (WT). For all other tests two-tailed analysis was used. Correlation of increase in RAB3GAP2 protein levels with increase in FOXC1 protein levels was evaluated using the non-parametric Spearman's-Rho test with the Social Sciences Statistics software (http://www.socscistatistics.com/tests/spearman/Default2.aspx).

2.11 - miRNA Predictions

To look for potential miRNA candidates targeting SNAP25, I used two miRNA programs microRNA.org and miRWalk2.0 (http://zmf.umm.uni-heidelberg.de/apps/zmf/mirwalk2/) to predict miRNA that could target SNAP25 and other negatively regulated FOXC1 targets detected by Berry et al. (2008), among them *ABCA8*, *RAB1A*, *SLC12A6*[69]. The miRNA candidates were initially sorted by two criteria. The first criterion was if they targeted at least one target gene, predicted to be negatively regulated by FOXC1, in addition to SNAP25, which would increase the likelihood of them being in turn regulated by FOXC1. The second criterion was if they were predicted to target SNAP25 by both programs, increasing the accuracy of the prediction.

3. Results

3.1 - Enrichment of FOXC1 at upstream regions of *RAB3GAP1*, *RAB3GAP2* and *SNAP25*

The microarray performed by Berry et al. (2008) in NPCE cells predicted several genes involved in exocytosis targets for FOXC1, among them *RAB3GAP1*, the catalytic subunit of RAB3GAP, and *SNAP25*[69]. *RAB3GAP1* RNA levels were also shown to decrease following morpholino FOXC1 knockdown in ocular tissues of zebrafish embryos and Northern Analysis of NPCE cells[69]. To further explore FOXC1 regulation of RAB3GAP1, as well as the potential regulation of the non-catalytic subunit of RAB3GAP, RAB3GAP2, and SNAP25, potential FOXC1 binding sites upstream of those genes were explored. FOXC1 binding sites were found up to 10,000 bp upstream of *RAB3GAP1*, *RAB3GAP2* and *SNAP25* with Possum software using a FOXC1 binding matrix[67]. Next, using Primer3 software, primers surrounding the binding sites were designed (Table 2.a). Potential FOXC1 binding sites (BS1) were found 191 bp upstream of *RAB3GAP1* (Fig.3A), 9265 bp upstream of *RAB3GAP2*, and 4933 bp upstream of *SNAP25* (Fig. 3A).

Next, to see if FOXC1 could interact with upstream regions of *RAB3GAP1*, *RAB3GAP2* and *SNAP25*, a chromatin immunprecipitation (ChIP) assay was performed with HeLa and human trabecular meshwork (TM1) cell lines. During ChIP, HeLa and TM1 DNA was cross linked and immunoprecipitated with antibodies, either anti-IgG (acting as negative control), anti-H3K4ME3 (a marker of transcriptionally active chromatin and thus a positive control), or anti-FOXC1. The DNA was then used for PCR with primers (Table 2.a)

surrounding the upstream regions of *RAB3GAP1*, *RAB3GAP2* and *SNAP25* illustrated in Fig. 3A containing FOXC1 binding sites.

The FOXC1 band in *RAB3GAP1* ChIP (Fig.3B) was darker then the negative control IgG in both HeLa and TM1 cells indicating strong enrichment of FOXC1 at the upstream region. Similarly, the FOXC1 band in the *RAB3GAP2* upstream region (Fig. 3B) was also enriched in both HeLa and TM1 cells. The FOXC1 band in the *SNAP25* ChIP (Fig. 3B) however, showed strong enrichment in HeLa cells but weak in TM1 cells indicating stronger interaction between FOXC1 and *SNAP25* in HeLa cells than in TM1. ChIP results are summarized in Table. 3.

3.2 - Luciferase transactivation by FOXC1 through upstream regions of *RAB3GAP1*, *RAB3GAP2* and *SNAP25*

To determine if FOXC1 could alter gene activation through the upstream regions of *RAB3GAP1*, *RAB3GAP2* and *SNAP25* used for ChIP, the upstream regions were cloned independently into pGL3 reporter plasmids. The pGL3 Luciferase reporter has no promoter; therefore any sequences cloned into the reporter must have basic promoter elements needed for Luciferase expression.

Two versions of the upstream region and Luciferase constructs of each gene were created; one construct had the upstream gene region used for ChIP cloned upstream the Luciferase reporter and one with the 16 bp containing the Possum predicted FOXC1 binding site (BS) deleted (designated with .del) while the rest of the upstream region remained. The empty pGL3 reporter was used to control for basal activation level while pGL3.FOXO1[69], a previously tested, FOXC1- responsive construct containing a FOXO1 upstream region,

was used as a positive control. HeLa cells were used for transactivation experiments since in the ChIP experiment upstream regions of *RAB3GAP1*, *RAB3GAP2* and *SNAP25* showed strong enrichment of FOXC1 in these cells (Fig. 3B).

During the assay, HeLa cells were co-transfected with a pGL3 construct, pCMV-β-gal (used as tranfection efficiency control), and either Xpress FOXC1 (WT) or Xpress FOXC1 (S131L), containing a pathogenic patient mutation leading to reduced activation due to lesser binding ability[118]. Luciferase activity for pGL3 constructs was normalized to β-galactosidase and then scaled to normalized pGL3 reporter activity when co-transfected with Xpress FOXC1 (WT).

When HeLa cells were transfected with pGL3.R3G1, Luciferase activation significantly increased 2.8 fold compared to an empty pGL3 reporter (Fig. 4A), indicating that the cloned 225 bp *RAB3GAP1* region contains regulatory elements through which FOXC1 regulates gene activation. Additionally, when the pGL3.R3G1 construct was co-transfected with Xpress FOXC1 (WT), Luciferase activity significantly increased 2.5 fold compared to co-transfection with Xpress FOXC1 (S131L), indicating that majority of the Luciferase activation was through FOXC1 binding to the upstream region. Removal of the predicted binding sites (BS1), however, did not decrease activation (Fig. 4A). To see if another site was present through which FOXC1 acted, the sequence was examined again with Possum and two additional, lower scoring sites were found (BS2 and BS3) (Fig. 3A). Two additional pGL3 construct were then created with the new sites deleted one at a time; pGL3.R3G1.del2 and pGL2.R3G1.del3. However, removal of the sites (one at a time) did not reduce activation (Fig. 4B). It appears that the presence of any of the three sites is sufficient for FOXC1 to interact with the upstream region of *RAB3GAP1*.

When HeLa cells were transfected with pGL3.R3G2 Luciferase activation significantly decreased to 0.7 fold, while removal of the binding site (pGL3.R3G2.del) decreased activation further to 0.4 fold (Fig. 5A). However, as the sequence is located nearly 10 kb away from the transcription start site (Fig. 3A) it is likely that the FOXC1 binding site is located in an enhancer region rather than a promoter element. To test this possibility the *RAB3GAP2* upstream region and the upstream region with the predicted binding site deleted were cloned into a pGL3.TK reporter upstream of a TK promoter. Transfections were performed as described before, and an empty pGL3.TK reporter was used to control for basal levels of activation and pGL3.TK.6xFBS construct, tested previously[64] containing the consensus FOXC1 binding site was used as a positive control. Luciferase activity significantly increased 1.5 fold when pGL3.R3G2 was co-transfected with Xpress FOXC1 (WT) compared to pGL3.TK (Fig. 5B). Furthermore, when pGL3.R3G2.del was co-transfected with Xpress FOXC1 (WT), Luciferase activation decreased and there was no significant difference in activation compared to pGL3.TK (Fig. 5B). Therefore, FOXC1 is able to enhance activation through the upstream region of *RAB3GAP2* and acts through the Possum predicted binding site (Fig. 1A). In addition, there was a significant 2.5 fold increase in activation when pGL3.R3G2 was co-transfected with Xpress FOXC1 (WT) compared to co-transfection with Xpress FOXC1 (S131L) indicating the need for functional FOXC1 binding at the upstream region to promote activation.

When pGL3.SNAP25 was co-transfected with Xpress FOXC1 (WT), Luciferase activation significantly decreased to 0.5 fold compared to the empty reporter, while removal of the binding site significantly decreased activation to 0.7 fold compared to pGL3 (Fig. 6A). However, as the binding site is located 5 kb upstream of the transcription start site of

SNAP25 it is likely than the region would be located within an enhancer like *RAB3GAP2* rather than promoter elements. To test if FOXC1 could act as an enhancer through the upstream region both the complete 151 bp upstream region and the upstream region with the 16 bp predicted binding site removed (Fig. 1A) were cloned into a pGL3.TK promoter. As described previously, pGL3.TK was used to estimate basal transactivation and pGL3.TK.6xFBS was used as a positive control. When pGL3.TK.SNAP25 was co-transfected with Xpress FOXC1 (WT), Luciferase activation significantly increased 1.5 fold compared to pGL3.TK (Fig. 6B) showing that FOXC1 can promote transcription through the SNAP25 upstream region which acts as an enhancer. Additionally, Luciferase activation through pGL3.SNAP25 was significantly higher, 2.8 fold, when co-transfected with Xpress FOXC1 (WT) compared to co-transfection with Xpress FOXC1 (S131L), indicating the importance of FOXC1 binding to the region for activation. However, removal of the binding site did not decrease Luciferase activation as there was no significant difference between Luciferase activation when pGL3.TK.SNAP25 was co-transfected with Xpress FOXC1 (WT) compared to pGL3.TK.SNAP25.del. Re-examination of the 151 bp upstream sequence revealed possible additional FOXC1 binding sites. However, no additional constructs with alternate FOXC1 binding sites deleted were created; while at least one binding site is still present so FOXC1 would likely still affect activation as was observed with *RAB3GAP1*. Luciferase transactivation results are summarized in Table. 3.

FOXC1 was shown to promote Luciferase activation through the *RAB3GAP1* upstream region and enhance activation through the *RAB3GAP2* and the *SNAP25* upstream regions in HeLa cells.

3.3 - *FOXC1* knockdown changes RNA levels of *RAB3GAP1*, *RAB3GAP2* and *SNAP25*

ChIP and Luciferase transactivation results showed that FOXC1 can interact with and activate gene expression through the upstream regions of *RAB3GAP1*, *RAB3GAP2* and *SNAP25*. Next, I used qRT-PCR to determine if reducing FOXC1 levels would affect the RNA levels of its target genes. HeLa and TM1 cells were transfected with either siRNA Control or siRNA FOXC1. RNA was isolated from the cells on the third day after transfection and reverse transcribed into cDNA. qRT-PCR was performed next with primers designed for *RAB3GAP1*, *RAB3GAP2* , both *SNAP25* isoforms (*SNAP25ab*) or each of the isoforms separately *(SNAP25a* and *SNAP25b*), and *HPRT1* (used as housekeeping control) (Table 2.c). qRT-PCR results were analyzed using the ΔΔCt method, with normalization to *HPRT1* and scaling the siRNA FOXC1 treatment to the siRNA Control treatment.

When *FOXC1* was significantly knocked down to 0.5 fold in HeLa cells, levels of both *RAB3GAP1* and *RAB3GAP2* significantly decreased to 0.6 fold and 0.7 fold respectively (Fig.7A). In TM1 cells significant knockdown of *FOXC1* to 0.4 fold lead to significant decrease in *RAB3GAP1* and *RAB3GAP2* levels to 0.6 fold and 0.7 fold respectively (Fig.7B). The qRT-PCR results show positive regulation of *RAB3GAP1* and *RAB3GAP2* RNA levels in by FOXC1 in both HeLa and TM1 cells.

With *SNAP25* a more complicated relationship was observed. In HeLa cells significant knockdown of *FOXC1* to 0.5 fold significantly reduced levels of *SNAP25ab* to 0.4 fold (Fig.8A), *SNAP25a* to 0.3 fold and *SNAP25b* to 0.5 fold (Fig.8B), supporting a positive regulation of both *SNAP25* isoforms by FOXC1. In TM1 cells however, significant

knockdown of FOXC1 to 0.5 fold resulted in a significant1.2 fold increase in *SNAP25ab* (Fig.9A), and a significant1.6 fold increase in *SNAP25a* but had no effect on *SNAP25b* (Fig.9B), indicating negative regulation of *SNAP25a* in TM1 cells, as was predicted by the microarray experiment performed by Berry et al. (2008)[69]. qRT-PCR results are summarized in Table.3.

The differential regulation of *SNAP25* by FOXC1 depending on the cell line indicates that additional players are involved in the SNAP25-FOXC1 regulatory network, and potential candidates include miRNAs, depending on which are present in the cell FOXC1 regulation of *SNAP25* could be positive, as was observed for HeLa cells, or negative as was observed in TM1 cells and predicted in a microarray performed in NPCE cells[69].

3.4 - FOXC1 knockdown changes protein levels of RAB3GAP1 and RAB3GAP2

I next used western blot analysis to see if the effect of FOXC1 knockdown on its target genes RNA levels would be also observed at the protein level. HeLa and TM1 cells were transfected with either siRNA Control or siRNA FOXC1. Cells were lysed three nights after transfection and proteins extracts were used for western blot analysis. Western blots were probed with antibodies against RAB3GAP1, RAB3GAP2, SNAP25, FOXC1 and α-tubulin (loading control). Images of the blots were taken with Imagestation4000 and band intensity was first normalized to α-tubullin, then the siRNA FOXC1 treatment was scaled to siRNA Control treatment.

When FOXC1 was significantly knocked down in HeLa cells to 0.3 fold, a significant decrease in levels of both RAB3GAP1 and RAB3GAP2 was observed to 0.7 fold, supporting positive regulation of RAB3GAP1 and RAB3GAP2 by FOXC1 at the protein

level (Fig. 10A). In TM1 cells, significant FOXC1 knockdown to 0.4 fold resulted in a significant RAB3GAP1 decrease to 0.7 fold but had no significant effect on RAB3GAP2 (Fig. 11A), even though its RNA levels were decreased (Fig. 7B). Therefore, FOXC1 positively regulates both RAB3GAP1 and RAB3GAP2 protein levels in HeLa cells but affects only RAB3GAP1 in TM1 cells.

Changes in SNAP25 protein levels following FOXC1 knockdown mirrored the changes observed at the RNA level (Fig. 9, Fig. 10). In HeLa cells when FOXC1 was significantly knocked down to 0.4 fold, SNAP25 levels significantly decreased to 0.6 fold supporting positive regulation by FOXC1 (Fig. 12A). However, in TM1 cells significant FOXC1 knockdown to 0.5 fold resulted in a significant 2.7 fold increase in SNAP25 (Fig. 12C) consistent with negative regulation by FOXC1. Results are summarized in Table. 3.

3.5 - FOXC1 over-expression changes protein levels of RAB3GAP1, RAB3GAP2 and SNAP25

Since knockdown of FOXC1 was shown to change protein levels of RAB3GAP1, RAB3GAP2 and SNAP25, I next tested if FOXC1 over-expression would also affect protein levels. HeLa cells were transfected with either Xpress Empty or Xpress FOXC1 (WT). HeLa cells were lysed three days after transfection and protein extracts were used for western blot analysis. Western blots were probed with antibodies against RAB3GAP1, RAB3GAP2, SNAP25, FOXC1 and α- tubulin (loading control). Images of the blots were taken with Imagestation4000 and band intensity was first normalized to α-tubulin, then the Xpress FOXC1 (WT) treatment was scaled to Xpress Empty treatment.

When FOXC1 was significantly over-expressed 22.8 fold, protein levels of RAB3GAP1 significantly increased 1.7 fold (Fig. 13A) further supporting positive regulation on RAB3GAP1 by FOXC1 in HeLa cells.

Changes in RAB3GAP2 protein levels following FOXC1 over-expression showed a more complicated pattern. RAB3GAP2 protein levels increased only when FOXC1 protein was over expressed more than 13 fold. To examine the relationship between FOXC1 over-expression and RAB3GAP2 protein levels, a Spearman's rank correlation test was performed. I found a correlation coefficient of 0.72 (Fig. 14A), indicating positive correlation between FOXC1 and RAB3GAP2 in HeLa cells.

When FOXC1 protein was significantly over-expressed 13.3 fold, SNAP25 protein levels significantly decreased to 0.7 fold (Fig. 15A). Western Analysis results are summarized in Table.3.

Negative regulation of SNAP25 by FOXC1 in HeLa cells contrasts with the FOXC1 knockdown experiments where both RNA (Fig. 8) and protein (Fig. 12A) levels of SNAP25 decreased following FOXC1 knockdown. Two possibilities present themselves. The first possibility is that FOXC1 was not sufficiently over-expressed in my experiments to see SNAP25 levels increase, and FOXC1 and SNAP25 have a positive correlation that appears only after a certain over-expression threshold is reached, as was observed with RAB3GAP2 (Fig. 14A). The second possibility is that SNAP25 experiences bimodal regulation by FOXC1, where either decrease or increase of FOXC1 levels beyond a narrow range result in reduced SNAP25 protein levels.

3.6 - Knockdown of FOXC1 and FOXC1's exocytotic protein targets RAB3GAP1, RAB3GAP2 and SNAP25 affects secretion of exogenous MYOC

In previous experiments FOXC1 was shown to interact and regulate transactivation through upstream regions of SNAP25, RAB3GAP1 and RAB3GAP2, as well as regulate their protein and RNA levels. All three genes are linked to exocytosis; therefore, the next question was if FOXC1 could affect secretion through its regulation of RAB3GAP1, RAB3GAP2 and SNAP25. I tested the functional consequences of this regulation through analyses of MYOC secretion. MYOC is secreted in trabecular meshwork cells and has an important role in glaucoma, but it is present at very low levels in HeLa cells unless its expression is induced[41]. To ensure that any effects on MYOC would be through exocytotic FOXC1 target genes and not through potential contribution of FOXC1 to transcriptional regulation of MYOC, I looked at exogenous MYOC secretion. To induce exogenous MYOC production in HeLa cells I used the plasmid pRcMYOC previously used by Gobeil et al. (2004) to study secretion of Wild Type MYOC[116]. Three days following transfection with pRcMYOC observable levels of MYOC were present both in intracellular (double band at 57 kDa and 55 kDa) protein extracts and in the cell media (Fig. 16A).

To observe FOXC1 effects on MYOC secretion, FOXC1 was knocked down in HeLa cells, as FOXC1 knockdown was shown to positively regulate RNA and protein levels of all three genes in HeLa cells. HeLa cells were co-transfected with pRcMYOC and either siRNA Control or siRNA FOXC1 (WT). Three days after transfection a media sample was collected and cells were lysed and protein extracts and media samples were used for western blot analysis. Western blots were probed with antibodies against FOXC1, MYOC and TFIID (loading control). Ponceau Red stain was used to control for total protein in

media samples. Images of the western blot were taken with Imagestation4000. Band intensity was normalized to the loading control and then treatment with pRcMYOC+siRNA FOXC1 (WT) was scaled to treatment with pRcMYOC+siRNA Control.

When FOXC1 was significantly knocked down to 0.4 fold, intracellular MYOC levels significantly decreased to 0.8 and 0.7 fold for the MYOC 57kDa (glycosylated form) and 55 kDa (non-glycosylated form) respectively, while extracellular MYOC levels decreased to 0.7 fold (Fig. 16B). The results were unexpected, as I expected that if knocking down FOXC1 lead to decrease in intracellular levels of MYOC, extracellular MYOC levels would increase. Instead my results indicate that decrease in both extracellular and intracellular MYOC levels result from knock down of FOXC1, suggesting that several different processes are occurring. Since MYOC was exogenously expressed, I can rule out transcriptional regulation of MYOC as part of these processes.

To examine if FOXC1's effect on exogenous MYOC is through FOXC1's regulation of RAB3GAP1, RAB3GAP2 and SNAP25, MYOC secretion experiments were repeated with each of the target genes knocked down separately and in combinations when co-transfected with pRcMYOC. As before, HeLa cells were grown for three nights following transfection, following which a sample of cell media was taken, proteins were extracted and Western analysis was performed. Antibodies against RAB3GAP1, RAB3GAP2, SNAP25, MYOC and TFIID (loading control) were used to detect protein bands and Ponceau stain was used for loading control for extracellular proteins. Band intensity for each protein was normalized to TFIID or Ponceau Red then the knockdown treatment was scaled to the control treatment.

When RAB3GAP1 was significantly knocked down to 0.1 fold, MYOC levels significantly decreased to 0.3 fold at 57 kDa and 0.4 fold at 55 kDa and extracellular levels significantly increased 1.4 fold (Fig. 17A), indicating that RAB3GAP1 knockdown increased MYOC secretion.

A similar effect on MYOC was observed when SNAP25 was knocked down. Significant decrease of SNAP25 to 0.1 fold lead to a significant decrease in intercellular MYOC to 0.5 fold at both 57 kDa and 55 kDa, and a significant 1.5 fold increase in extracellular MYOC (Fig.19A). Thus, knockdown of either RAB3GAP1 or SNAP25 promotes secretion of MYOC.

When RAB3GAP2 was significantly knocked down to 0.7 fold intracellular levels of MYOC significantly decreased to 0.7 fold at 57 kDa and 0.5 fold at 55 kDa and extracellular levels significantly decreased to 0.8 fold (Fig. 18A). The effect of RAB3GAP2 knockdown on MYOC secretion was similar to what was observed when FOXC1 was knocked down.

As FOXC1 knockdown was shown to reduce protein levels of all three targets in HeLa cells, in the next set of experiments several of the target genes were knocked down simultaneously to simulate the effect of FOXC1. First, RAB3GAP1 and RAB3GAP2 were knocked down simultaneously, as together they form the complex RAB3GAP. When siRNAs against both genes were used, intracellular levels of MYOC significantly decreased to 0.4 fold at 57 kDa and 0.6 fold at 55 kDa and extracellular levels decreased to 0.6 fold (Fig. 20A). Knocking down all three genes with siRNA resulted in intracellular MYOC significantly decreasing to 0.5 fold at 57 kDa and 0.3 fold at 55 kDa and

extracellular levels significantly decreasing to 0.7 fold (Fig. 21A). Both combination treatments have a similar effect on MYOC secretion as FOXC1 knockdown. A summary of the MYOC secretion experiments is provided in Table.4.

3.7 - FOXC1 knockdown in TM1 cells decreases RNA levels of the additional exocytotic targets SNAP23, SYN2 and STXBP6

I have shown that FOXC1 regulates RAB3GAP1, RAB3GAP2 and SNAP25, three exocytosis related genes. However, in the microarrays performed by Berry et al. (2008) and Paylakhi et al. (2013) additional exocytosis related genes were found, among them *SNAP23*, *SYN2* and *STXBP6* (Amisyn)[69,72]. To see if those targets should be pursued further, I performed a qRT-PCR in TM1 cells following transfection with siRNA FOXC1 to see if FOXC1 knockdown would affect RNA levels of other exoytosis target genes.

When *FOXC1* was significantly knocked down to 0.4 fold, RNA levels of *SNAP23* significantly decreased to 0.7 fold and RNA levels of SYN2 significantly decreased to 0.6 fold (Fig. 22A), indicating positive regulation at the RNA level by FOXC1. Significant knockdown of FOXC1 to 0.4 fold also resulted in *STXBP6* RNA levels significantly decreasing to 0.6 fold in TM1 cells (Fig. 23B), also supporting positive regulation by FOXC1.

3.8 - Potential miRNA's targeting *SNAP25* that might in turn be regulated by FOXC1

SNAP25 was shown to be negatively regulated by FOXC1 in TM1 cells on the RNA and protein level (Fig. 9 and Fig. 12A) while SNAP25 was positively regulated in HeLa cells when FOXC1 was knocked down (Fig. 8 and Fig. 12C). A potential explanation for the differential regulation might be a miRNA that is regulated by FOXC1, expressed in TM1

but not in Hela cells, and in turn also targets SNAP25. To look for potential miRNA candidates, I used two miRNA prediction programs to predict miRNA that could target SNAP25 and other negatively regulated FOXC1 targets from the microarray experiment performed by Berry et al. (2008), including *ABCA8*, *RAB1A*, *SLC12A6*[69].

The miRNA candidates were chosen using three sorting criteria. The first criterion was if they targeted at least one negative FOXC1 target in addition to *SNAP25*, which would increase the likelihood of them being in turn regulated by FOXC1. The second criterion was if they were predicted to target *SNAP25* by both programs, increasing the accuracy of the prediction. To further sort potential candidates, I looked for miRNAs that have been shown to be expressed in trabecular meshwork cells and play a role in pathways associated with glaucoma pathogenesis. Among the miRNAs that were selected for future experiments are miR-15a, miR-15b, which are involved in stress response in the trabecular meshwork and are predicted to regulate *RAB1A* in addition to *SNAP25*[119]. The third and most promising candidate is miR-106a, which is predicted to regulate *ABCA8*, *RAB1A* and *SLC12A6* in addition to SNAP25 and is associated with stress response and apoptosis[119].

4. Tables

Table 1. Glaucoma subtypes.

Glaucoma subtypes	Description
Primary glaucoma	Develops without an underlying disease
Secondary glaucoma	Develops as a complication of another disease
Open angle glaucoma	Open angle between the iris and the cornea
Closed angle glaucoma	Closed angle between the iris and the cornea
Developmental glaucoma	Develops in association with anterior ocular segment dysgenesis disorders
Congenital/infantile glaucoma	Presents at birth or within two years
Juvenile onset glaucoma	Develops between 2 and 40 years of age
Adult onset glaucoma	Develops between after 40 years of age
Hypertensive glaucoma	Glaucoma with abnormally high IOP
Normal tension glaucoma	Glaucoma with normal IOP

Table 2. Primers used for cloning and PCR.

Sense and Antisense Primers		
a. ChIP PCR	**Sense**	**Antisense**
RAB3GAP1	aggggcagagggtagaagtg	aagggaacagaagccaaggt
RAB3GAP2	caggcaaaatctgcatttcat	tcgagaattaaggagggacaaa
SNAP25	aggggtaagtacatgccgtc	catcacacttctgccagctc
b. Transactivation cloning	**Sense**	**Antisense**
RAB3GAP1	gagctcaggggcagagggtagaagtg	agatctaagggaacagaagccaaggt
RAB3GAP2	agatctcaggcaaaatctgcatttcat	gagctctcgagaattaaggagggacaaa
SNAP25	gagctcaggggtaagtacatgccgtc	agatctcatcacacttctgccagctc
c. Mutagenesis	**Sense**	**Antisense**
RAB3GAP1 **.del1 (129-144)**	ctaattggtactaactacaaatatgggtcaacatgctttaggttttttaatacaat	attgtattaaaaaacctaaagcatgttgacccatatttgtagttagtaccaattag
RAB3GAP1 **.del2 (35-50)**	gtagaagtggtattacagcacctatcaataaatagagggtgaatga	tcattcaccctctatttattgataggtgctgtaataccacttctac
RAB3GAP1 **.del3 (67-82)**	tgccttacaatcaataaatagagggcaatagttaaagtgtaagctaattg	caattagcttacactttaactattgccctctatttattgattgtaaggca
RAB3GAP2 **.del (54-70)**	caggagagaggaatagtctgtgcccttgagtcatttg	caaatgactcaagggcacagactattcctctctcctg
SNAP25 **.del (165-180)**	gtcatggtccaaaggacttttcaggttcacctgac	gtcaggtgaacctgaaaagtcctttggaccatgac
d. qRT-PCR	**Sense**	**Antisense**
SNAP25ab	gtgtagtggacgaacgggag	ccatatccagggccatgtgac
SNAP25a	aagggctgaccagttggctgatgagt	ttggttgatatggttcatgccttcttcgacacga
SNAP25b	aagggctgaccagttggctgatgagt	cttattgatttggtccatcccttcctcaatgcgt
RAB3GAP1	aagccaagtttggaactgagaa	ctgcaccggtgactaacactt
RAB3GAP2	ctccacacccagacaaaagaa	gcaattggcacttcagtgttt
FOXC1	tagctgtcaaatggccttccc	cttttcctgctttggggttcg
HPRT1	gccagactttgttggatttga	ggctttgtattttgcttttccag
STXBP6	attaggccgagcagaggagaa	agaagagtcaccaggataggca
SNAP23	tgagtctctggaaagtacgagga	tccaagccttcttctatgcgg
SYN2	acaggtacaaactgtgggtgg	atcagtggcatgctacagtcc

Table 3. Summary of experiments supporting regulation of RAB3GAP1, RAB3GAP2 and SNAP25 by FOXC1.

Experiment	**Results**				
ChIP	**Enrichment of FOXC1 at upstream region compared to control**				
Cell line	***RAB3GAP1***	***RAB3GAP2***	***SNAP25***		
HeLa	strong	strong	strong		
TM1	strong	strong	weak		
Luciferase Transactivation	**Change in Luciferase activation by FOXC1 when upstream region was cloned into reporter compared to empty reporter in HeLa cells**				
Reporter	***RAB3GAP1***	***RAB3GAP2***	***SNAP25***		
pGL3	↑	↓	↓		
pGL3.TK	N/A	↑	↑		
qRT-PCR	**Change in RNA levels following FOXC1 knockdown**				
Cell line	***RAB3GAP1***	***RAB3GAP2***	***SNAP25ab***	***SNAP25a***	***SNAP25b***
HeLa	↓	↓	↓	↓	↓
TM1	↓	↓	↑	↑	N.S.
Western Analysis	**Change in protein levels following FOXC1 knockdown**				
Cell line	**RAB3GAP1**	**RAB3GAP2**	**SNAP25**		
HeLa	↓	↓	↓		
TM1	↓	N.S.	↑		
Western Analysis	**Change in protein levels following FOXC1 over-expression**				
Cell line	**RAB3GAP1**	**RAB3GAP2**	**SNAP25**		
HeLa	↑	positive correlation	↓		

Table 4. Summary of the effects of FOXC1, RAB3GAP1, RAB3GAP2 and SNAP25 knockdown on Myocilin secretion in HeLa cells.

Change in Exogenous Myocilin Protein Levels		
Treatment	**Intracellular Myocilin**	**Extracellular Myocilin**
siRNA FOXC1	↓	↓
siRNA RAB3GAP1	↓	↑
siRNA RAB3GAP2	↓	↓
siRNA SNAP25	↓	↑
siRNA RAB3GAP1 **siRNA RAB3GAP2**	↓	↓
siRNA RAB3GAP1 **siRNA RAB3GAP2** **siRNA SNAP25**	↓	↓

5. Figures

Figure 1. Glaucoma pathogenesis.

(A) Diagram of the eye.

(B) Aqueous humor flow is produced in the ciliary body and circulates through the ciliary epithelium into the anterior chamber. Finally the aqueous humor drains through the trabecular meshwork into Schlemm's canal in the conventional outflow pathway. To lesser degree the aqueous humor also drains through the anterior ciliary body in the unconventional outflow pathway.

(C) During glaucoma pathogenesis both environmental (E) and genetic (G) factors trigger pathogen glaucomatous mechanisms that promote retinal ganglion (RGC) cell death.

Figure 1.

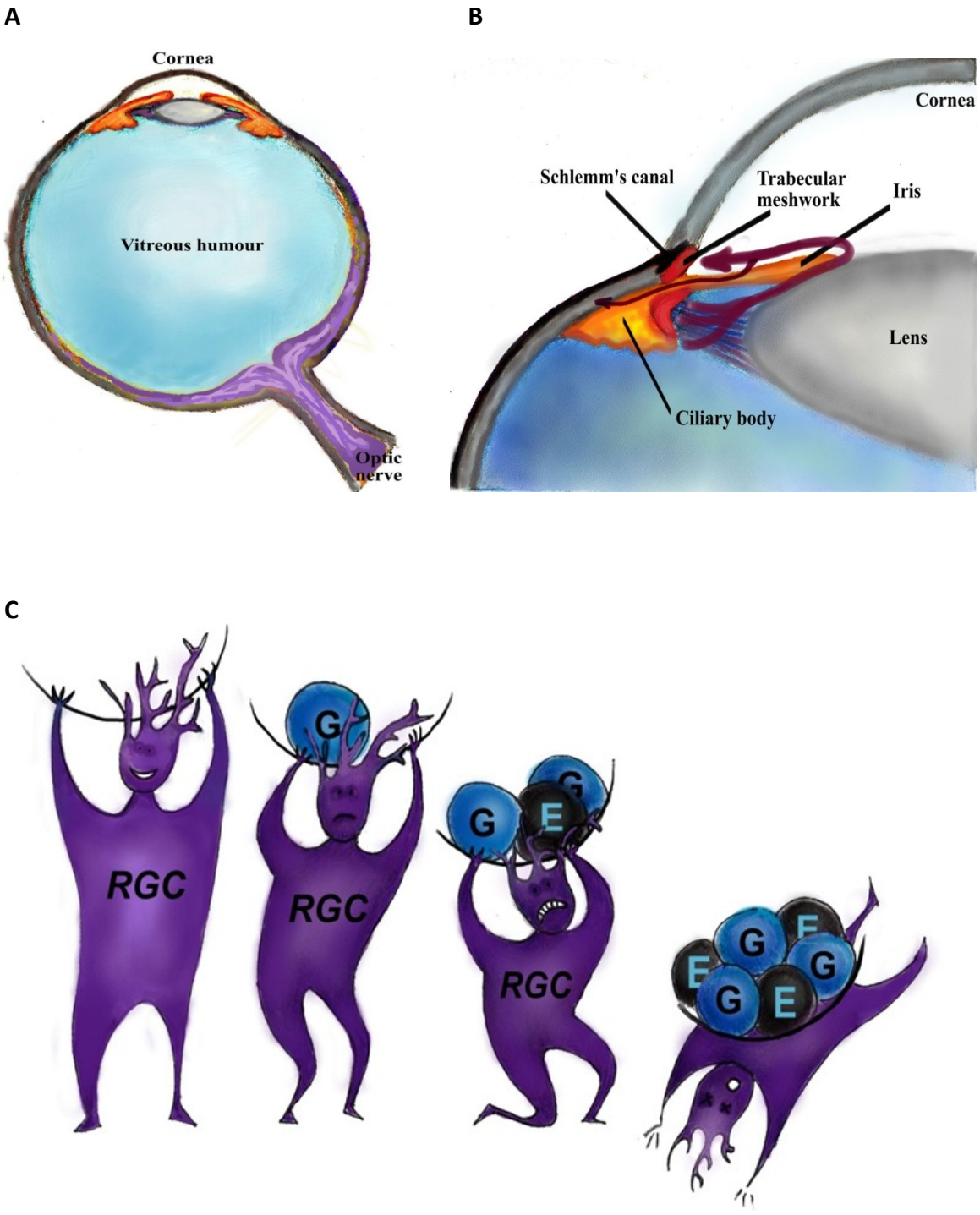
A
Cornea
Vitreous humour
Optic nerve
B
Cornea
Schlemm's canal
Trabecular meshwork
Iris
Lens
Ciliary body
C
RGC
RGC
RGC
G
E

Figure 2. Predicted regulation of MYOC secretion by FOXC1 through its target genes.

FOXC1 is hypothesized to up regulate both subunits of the RAB3GAP complex and down regulate SNAP25. Through regulation of its target genes FOXC1 is predicted to affect MYOC secretion.

Figure 2.

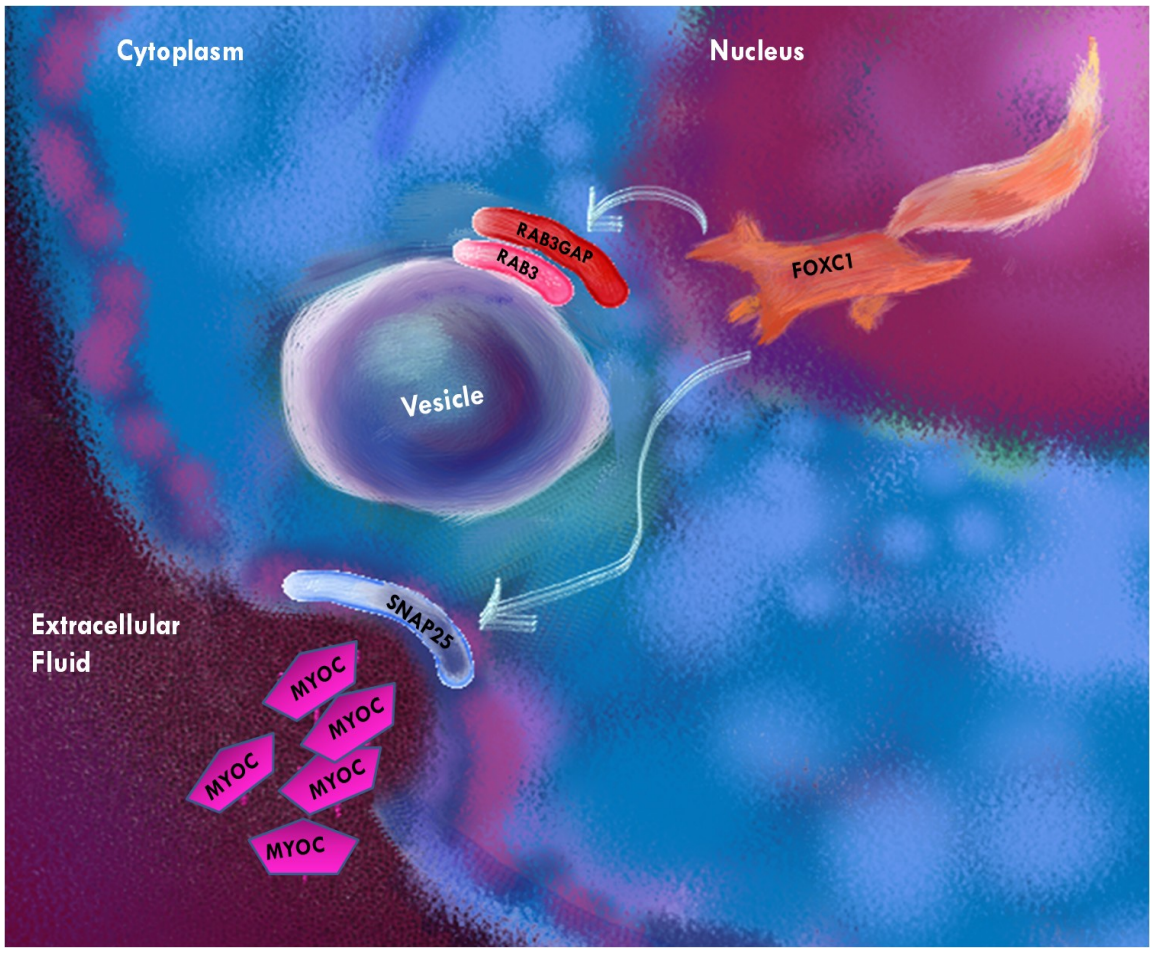
Cytoplasm
Nucleus
RAB3GAP
RAB3
FOXC1
Vesicle
SNAP25
Extracellular
Fluid
MYOC
MYOC
MYOC
MYOC
MYOC

Figure 3. Enrichment of FOXC1 at upstream regions of *RAB3GAP1*, *RAB3GAP2* and *SNAP25*.

(A) Potential FOXC1 binding sites found upstream of *RAB3GAP1*, *RAB3GAP2* and *SNAP25*. The FOXC1 predicted binding site is underlined.

(B) TM1 or HeLa chromatin cross-linked and immunoprecipitated with 3 ng of antibodies against IgG (negative control), H3K4ME3 (active-chromatin marker) and FOXC1. The "Input" sample represents cross-linked but not immunoprecipitated chromatin. The immunoprecipitated chromatin was amplified using PCR with primers surrounding the upstream regions of *RAB3GAP1*, *RAB3GAP2* and *SNAP25* indicated in part (A). Next, DNA was size separated with Agarose gel electrophoresis. Image was taken with Imagestation4000 after 1 minute exposure.

Figure 3.

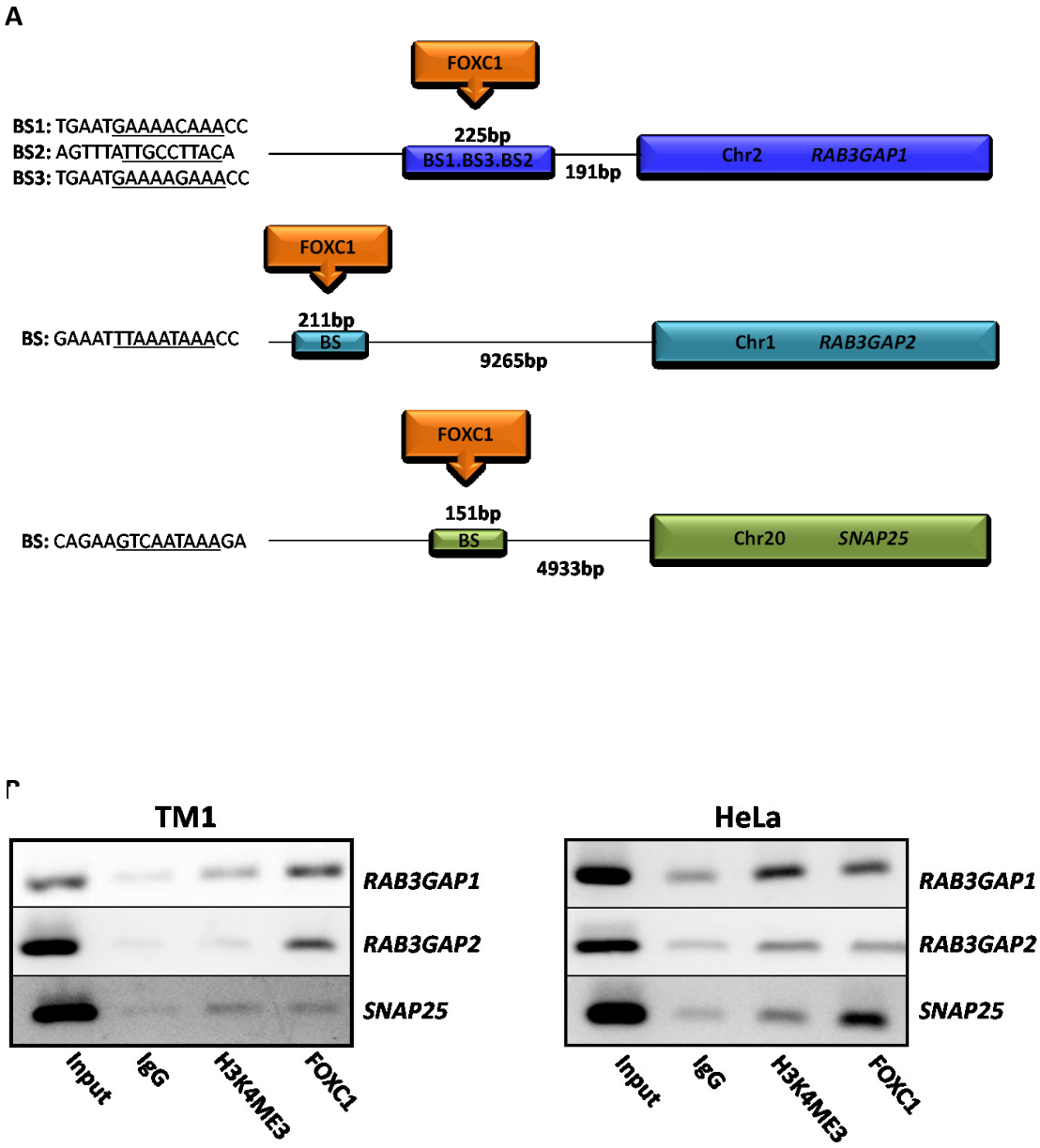
A
FOXC1
BS1: TGAATGAAAACAAACC
BS2: AGTTTATTGCCTTACA
BS3: TGAATGAAAAGAAACC
225bp
BS1.BS3.BS2
191bp
Chr2 RAB3GAP1
FOXC1
BS: GAAATTTAAATAAACC
211bp
BS
9265bp
Chr1 RAB3GAP2
FOXC1
151bp
BS: CAGAAGTCAATAAAGA
BS
4933bp
Chr20 SNAP25
TM1
HeLa
RAB3GAP1
RAB3GAP2
SNAP25
Input
IgG
H3K4ME3
FOXC1

Figure 4. Luciferase transactivation by FOXC1 through upstream region of *RAB3GAP1*.

The 225bp *RAB3GAP1* upstream region (Fig. 3) cloned into a pGL3 luciferase reporter (pGL3.R3G1) and co-transfected with either Xpress-FOXC1(WT) or Xpress-FOXC1(S131L) into HeLa cells, a mutant with reduced activity, and pCMV-β-galactosidase (transfection control). In additional constructs, each of the three predicted FOXC1 binding sites were deleted from the *RAB3GAP1* upstream region and then cloned in to pGL3. In pGL3.R3G1.del1 **(A)**, BS1 (Fig. 3) was deleted. In pGL3.R3G1.del2 and pGL3.R3G1.del3 **(B)**, BS2 and BS3 (Fig. 3) were deleted respectively. pGL3.FOXO1, a construct with a previously tested FOXO1 promoter[69], was used as a positive control. Luciferase activity for each construct was normalized to β-gal values and then scaled to the empty pGL3 reporter co-transfected with Xpress-FOXC1(WT). Experiments were repeated three times in triplicate. Error bars represent standard error. **P*<0.05 versus pGL3 under the Mann-Whitney U-test.

Figure 4.

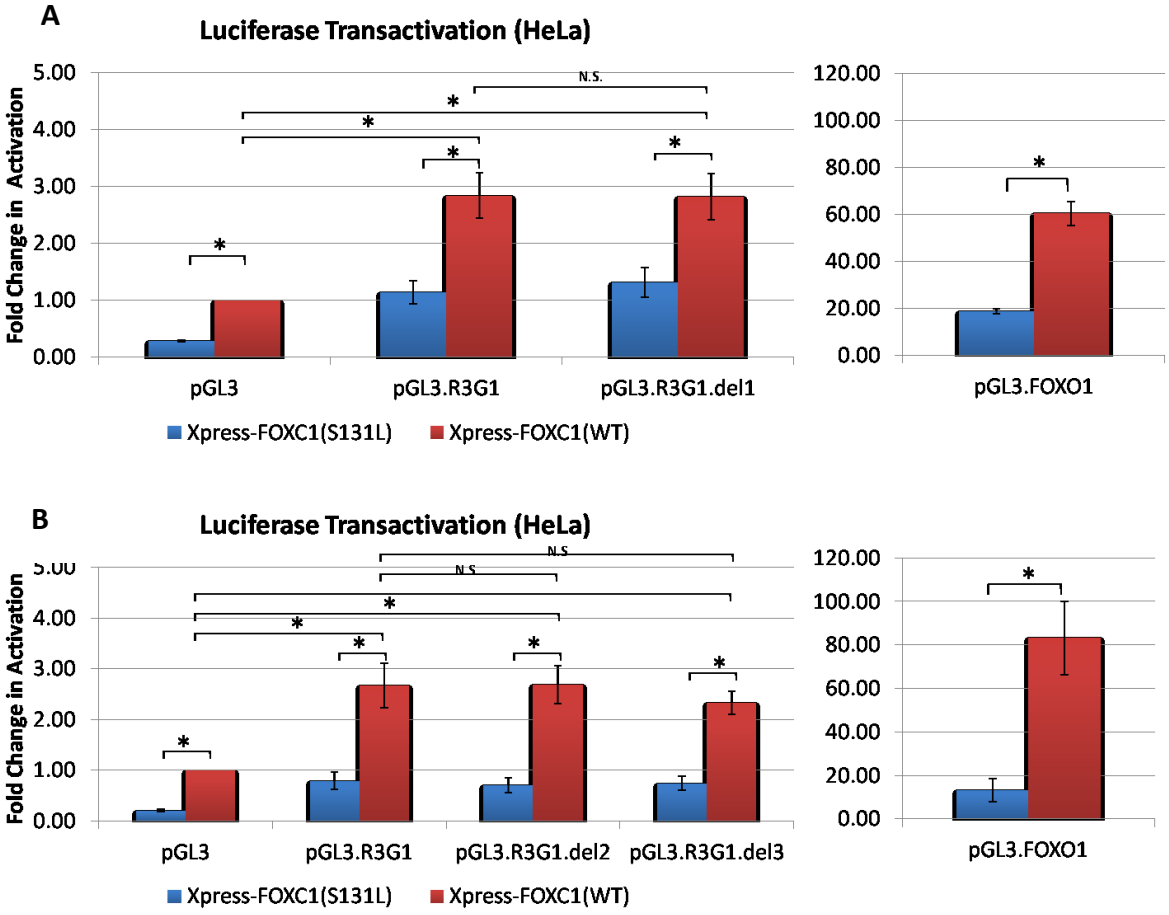
A
Luciferase Transactivation (HeLa)
Fold Change in Activation
5.00
4.00
3.00
2.00
1.00
0.00
N.S.
*
pGL3
pGL3.R3G1
pGL3.R3G1.del1
120.00
100.00
80.00
60.00
40.00
20.00
0.00
pGL3.FOXO1
Xpress-FOXC1(S131L)
Xpress-FOXC1(WT)
B
Luciferase Transactivation (HeLa)
Fold Change in Activation
5.00
4.00
3.00
2.00
1.00
0.00
N.S
N.S
*
pGL3
pGL3.R3G1
pGL3.R3G1.del2
pGL3.R3G1.del3
120.00
100.00
80.00
60.00
40.00
20.00
0.00
pGL3.FOXO1
Xpress-FOXC1(S131L)
Xpress-FOXC1(WT)

Figure 5. Lucifirase transactivation by FOXC1 through upstream region of *RAB3GAP2*.

(A) The 211bp RAB3GAP2 upstream region (Fig. 3) cloned into a pGL3 luciferase reporter (pGL3.R3G2) and co-transfected with either Xpress-FOXC1(WT) or Xpress-FOXC1(S131L) into HeLa cells, a mutant with reduced activity, and pCMV-β-galactosidase (transfection control). In additional construct, the predicted FOXC1 binding site (Fig. 3) was deleted from the *RAB3GAP2* upstream region and then cloned into pGL3 (pGL3.R3G2.del)**.** pGL3.FOXO1, a construct with a previously tested FOXO1 promoter[69], was used as a positive control. Luciferase activity for each construct was normalized to β-galactosidase values and then scaled to the empty pGL3 reporter co-transfected with Xpress-FOXC1(WT). Experiments were repeated three times in triplicate. Error bars represent standard error. **P*<0.05 versus pGL3 under the Mann-Whitney U-test.

(B) The 211bp *RAB3GAP2* upstream region (Fig. 3) cloned into a pGL3.TK luciferase reporter upstream of the TK promoter (pGL3.TK.R3G2) and co-transfected with either Xpress-FOXC1(WT) or Xpress-FOXC1(S131L), a mutant with reduced activity, and pCMV-β-gal (transfection control). In additional construct, the predicted FOXC1 binding site was deleted from the *RAB3GAP2* upstream region and then cloned into pGL3.TK (pGL3.TK.R3G2.del)**.** pGL3.TK.6xFBS, a construct containing the consensus FOXC1 binding site, was used as a positive control. Luciferase activity for each construct was normalized to β- galactosidase values and then scaled to the empty pGL3.TK reporter co-transfected with Xpress-FOXC1(WT). Experiments were repeated three times in triplicate. Error bars represent standard error. **P*<0.05 versus pGL3.TK under the Mann-Whitney U-test.

Figure 5.

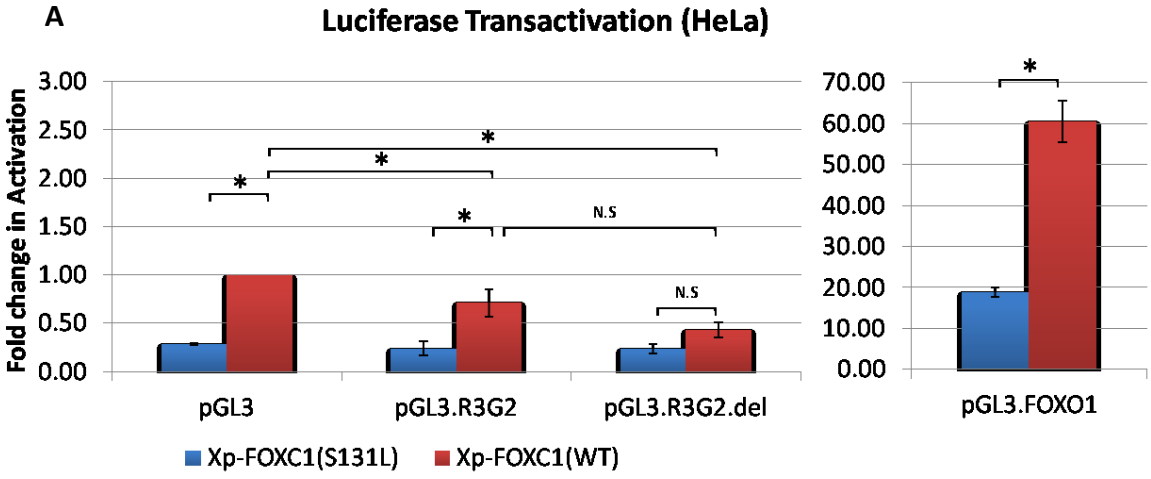
A
Luciferase Transactivation (HeLa)
Fold change in Activation
3.00
2.50
2.00
1.50
1.00
0.50
0.00
70.00
60.00
50.00
40.00
30.00
20.00
10.00
0.00
*
N.S
pGL3
pGL3.R3G2
pGL3.R3G2.del
pGL3.FOXO1
Xp-FOXC1(S131L)
Xp-FOXC1(WT)

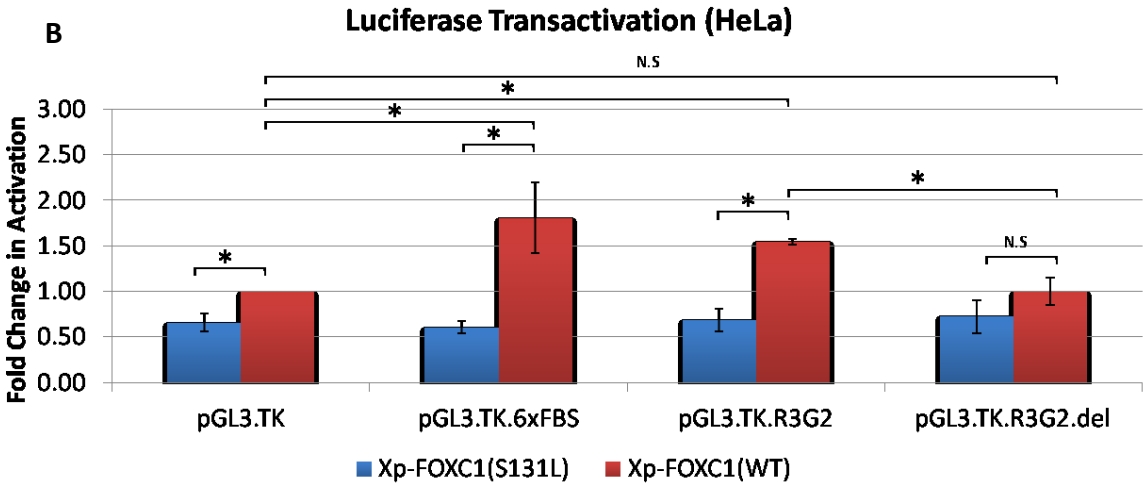
B
Luciferase Transactivation (HeLa)
Fold Change in Activation
3.00
2.50
2.00
1.50
1.00
0.50
0.00
N.S
*
pGL3.TK
pGL3.TK.6xFBS
pGL3.TK.R3G2
pGL3.TK.R3G2.del
Xp-FOXC1(S131L)
Xp-FOXC1(WT)

Figure 6. Luciferase transactivation by FOXC1 through upstream region of *SNAP25*.

(A) The 151bp SNAP25 upstream region (Fig .3) cloned into a pGL3 luciferase reporter (pGL3. SNAP25) and co-transfected with either Xpress-FOXC1(WT) or Xpress-FOXC1(S131L), a mutant with reduced activity, and pCMV-β-gal (transfection control) into HeLa cells. In an additional construct, the predicted FOXC1 binding site (Fig .3) was deleted from the *SNAP25* upstream region and then cloned into pGL3 (pGL3.SNAP25.del)**.** pGL3.FOXO1, a construct with a previously tested FOXO1 promoter[69], was used as a positive control. Luciferase activity for each construct was normalized to β- galactosidase values and then scaled to the empty pGL3 reporter co-transfected with Xpress-FOXC1(WT). Experiments were repeated three times in triplicate. Error bars represent standard error. **P*<0.05 versus pGL3 under the Mann-Whitney U-test.

(B) The 151bp *SNAP25* upstream region (Fig. 3) cloned into a pGL3.TK luciferase reporter upstream of the TK promoter (pGL3.TK. SNAP25) and co-transfected with either Xpress-FOXC1(WT) or Xpress-FOXC1(S131L), a mutant with reduced activity, and pCMV-β-gal (transfection control). In an additional construct, the predicted FOXC1 binding site was deleted from the *SNAP25* upstream region and then cloned into pGL3.TK (pGL3.TK. SNAP25.del)**.** pGL3.TK.6xFBS, a construct containing the consensus FOXC1 binding site, was used as a positive control. Luciferase activity for each construct was normalized to β-gal values and then scaled to the empty pGL3.TK reporter co-transfected with Xpress-FOXC1 (WT). Experiments were repeated four times in triplicate. Error bars represent standard error. **P*<0.05, ***P*<0.01 versus pGL3.TK under the Mann-Whitney U-test.

Figure 6.

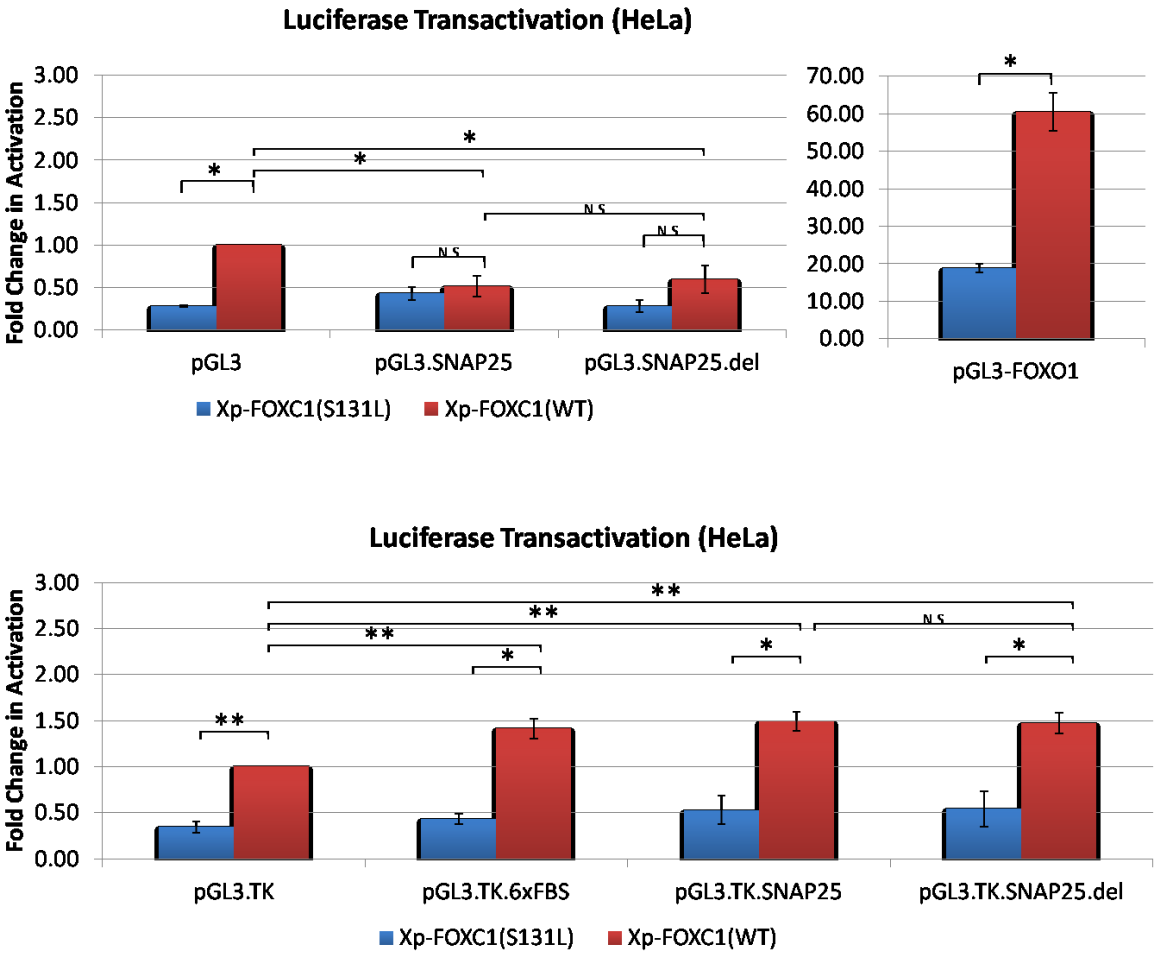
Luciferase Transactivation (HeLa)
Fold Change in Activation
3.00
2.50
2.00
1.50
1.00
0.50
0.00
70.00
60.00
50.00
40.00
30.00
20.00
10.00
0.00
*
NS
pGL3
pGL3.SNAP25
pGL3.SNAP25.del
pGL3-FOXO1
Xp-FOXC1(S131L)
Xp-FOXC1(WT)
Luciferase Transactivation (HeLa)
Fold Change in Activation
**
NS
pGL3.TK
pGL3.TK.6xFBS
pGL3.TK.SNAP25
pGL3.TK.SNAP25.del
Xp-FOXC1(S131L)
Xp-FOXC1(WT)

Figure 7. *FOXC1* knockdown decreases RNA levels of *RAB3GAP1* and *RAB3GAP2*.

HeLa or TM1 cells were transfected with either siRNA Control or siRNA FOXC1 and after three days RNA was isolated and reverse transcribed into cDNA. Quantitative Real-Time PCR (qRT-PCR) was run with the cDNA samples and primers for *FOXC1*, *RAB3GAP1*, *RAB3GAP2* and *HPRT1* (housekeeping control). Relative quantification (RQ) was performed using the ΔΔCt method.

(A) Relative quantification of the change in *FOXC1*, *RAB3GAP1* and *RAN3GAP2* RNA levels following normalization to *HPRT1* and scaling siRNA FOXC1 to siRNA Control in HeLa cells. Experiments were performed three times in triplicate. Error bars represent standard error. **P*<0.05 versus siRNA Control under the Mann-Whitney U-test.

(B) Relative quantification of the change in *FOXC1*, *RAB3GAP1* and *RAB3GAP2* RNA levels following normalization to *HPRT1* and scaling siRNA FOXC1 to siRNA Control in TM1 cells. Experiments were performed four times in triplicate. Error bars represent standard error. ***P*<0.01 versus siRNA Control under the Mann-Whitney U-test.

Figure 7.

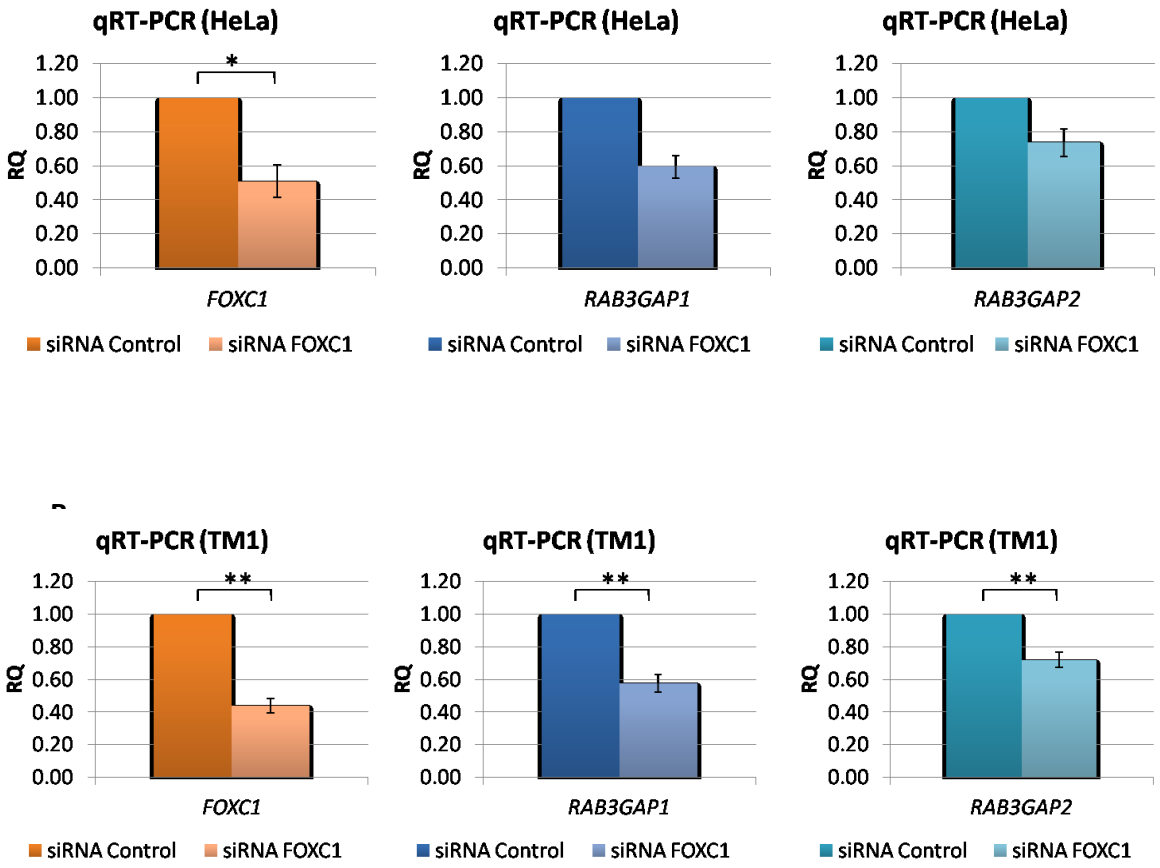
qRT-PCR (HeLa)
RQ
1.20
1.00
0.80
0.60
0.40
0.20
0.00
*
FOXC1
siRNA Control
siRNA FOXC1
qRT-PCR (HeLa)
RAB3GAP1
qRT-PCR (HeLa)
RAB3GAP2
qRT-PCR (TM1)
**
qRT-PCR (TM1)
qRT-PCR (TM1)

Figure 8. *FOXC1* knockdown decreases RNA levels of both *SNAP25* isoforms in HeLa cells.

HeLa cells were transfected with either siRNA Control or siRNA FOXC1 and after three days RNA was isolated and reverse transcribed into cDNA. Quantitative Real-Time PCR (qRT-PCR) was run with the cDNA samples and primers for *FOXC1*, both *SNAP25* isoforms (*SNAP25ab*), *SNAP25* isoform a (*SNAP25a*), *SNAP25* isoform b (*SNAP25b*) and *HPRT1* (housekeeping control). Relative quantification (RQ) was performed using the ΔΔCt method.

(A) Relative quantification of the change in *FOXC1* and *SNAP25ab* levels following normalization to *HPRT1* and scaling siRNA FOXC1 treatment to siRNA Control treatment in HeLa cells. Experiments were performed three times in triplicate. Error bars represent standard error. **P*<0.05 versus siRNA Control under the Mann-Whitney U-test.

(B) Relative quantification of the change in *SNAP25a* and *SNAP25b* RNA levels following normalization to *HPRT1* and scaling siRNA FOXC1 treatment to siRNA Control treatment in HeLa cells. Experiments were performed three times in triplicate. Error bars represent standard error. **P*<0.05 versus siRNA Control under the Mann-Whitney U-test.

Figure 8.

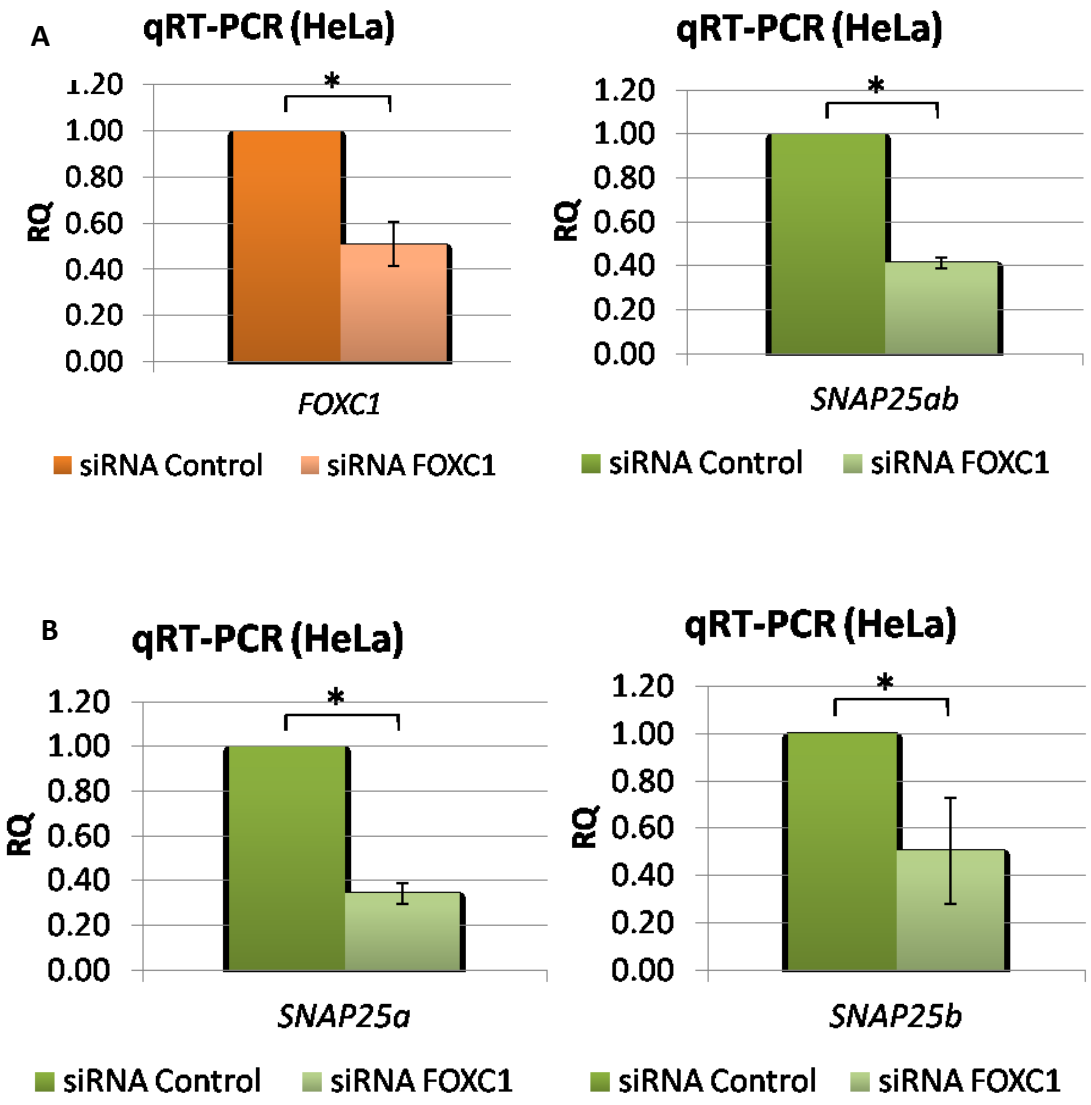
A
qRT-PCR (HeLa)
RQ
1.20
1.00
0.80
0.60
0.40
0.20
0.00
*
FOXC1
siRNA Control
siRNA FOXC1
qRT-PCR (HeLa)
SNAP25ab
siRNA Control
siRNA FOXC1
B
qRT-PCR (HeLa)
SNAP25a
siRNA Control
siRNA FOXC1
qRT-PCR (HeLa)
SNAP25b
siRNA Control
siRNA FOXC1

Figure 9. *FOXC1* knockdown increases RNA levels of *SNAP25a* in TM1 cells but has no effect on *SNAP25b*.

TM1 cells were transfected with either siRNA Control or siRNA FOXC1 and after three days RNA was isolated and reverse transcribed into cDNA. Quantitative Real-Time PCR (qRT-PCR) was run with the cDNA samples and primers for *FOXC1*, both *SNAP25* isoforms (*SNAP25ab*), *SNAP25* isoform a (*SNAP25a*), *SNAP25* isoform b (*SNAP25b*) and *HPRT1* (housekeeping control). Relative quantification (RQ) was performed using the ΔΔCt method.

(A) Relative quantification of the change in *FOXC1* and *SNAP25ab* levels following normalization to *HPRT1* and scaling siRNA FOXC1 to siRNA Control in TM1 cells. Experiments were performed three times in triplicate. Error bars represent standard error. **P*<0.05 versus siRNA Control under the Mann-Whitney U-test.

(B) Relative quantification of the change in *SNAP25a* and *SNAP25b* RNA levels following normalization to *HPRT*1 and scaling siRNA FOXC1 to siRNA Control in TM1 cells. Experiments were performed three times in triplicate. Error bars represent standard error. **P*<0.05 versus siRNA Control under the Mann-Whitney U-test.

Figure 9.

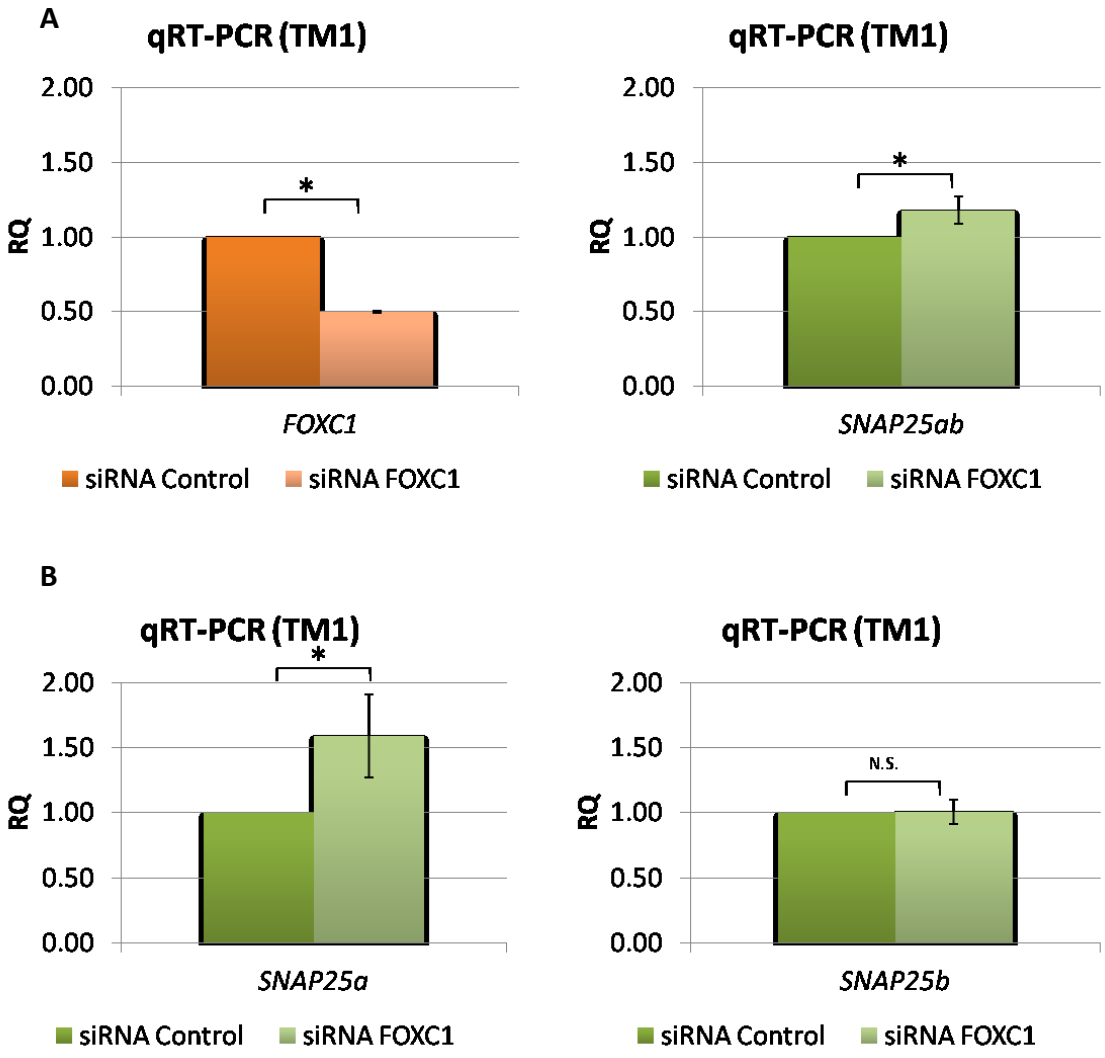
A
qRT-PCR (TM1)
2.00
1.50
1.00
0.50
0.00
RQ
*
FOXC1
siRNA Control
siRNA FOXC1
qRT-PCR (TM1)
2.00
1.50
1.00
0.50
0.00
RQ
*
SNAP25ab
siRNA Control
siRNA FOXC1
B
qRT-PCR (TM1)
2.00
1.50
1.00
0.50
0.00
RQ
*
SNAP25a
siRNA Control
siRNA FOXC1
qRT-PCR (TM1)
2.00
1.50
1.00
0.50
0.00
RQ
N.S.
SNAP25b
siRNA Control
siRNA FOXC1

Figure 10. FOXC1 knockdown decreases protein levels of RAB3GAP1 and RAB3GAP2 in HeLa cells.

HeLa cells were transfected with either siRNA Control or siRNA FOXC1 then lysed after three days. Protein lysates were used for western blot analysis. Antibodies against FOXC1, RAB3GAP1, RAB3GAP2 and α-Tubulin (loading control) were used to detect change in protein levels. Net band intensity for each protein was normalized to α-Tubulin, then siRNA FOXC1treatment was scaled to siRNA control treatment. Experiments were repeated six times.

(A) Relative change in protein levels of FOXC1, RAB3GAP1and RAB3GAP2 following FOXC1 knockdown. Error bars represent standard error. $^{**}P<0.01$, $^{***}P<0.001$ versus siRNA Control under the Mann-Whitney U-test.

(B) Example western blot. Image was taken with Imagestation4000 after a 10 minute exposure.

Figure 10.

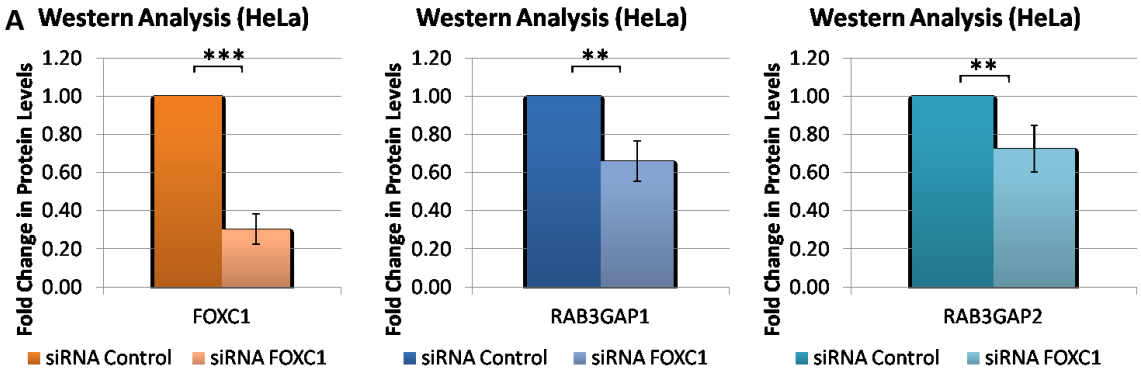
A
Western Analysis (HeLa)
Fold Change in Protein Levels
1.20
1.00
0.80
0.60
0.40
0.20
0.00
***
FOXC1
siRNA Control
siRNA FOXC1
Western Analysis (HeLa)
**
RAB3GAP1
Western Analysis (HeLa)
**
RAB3GAP2

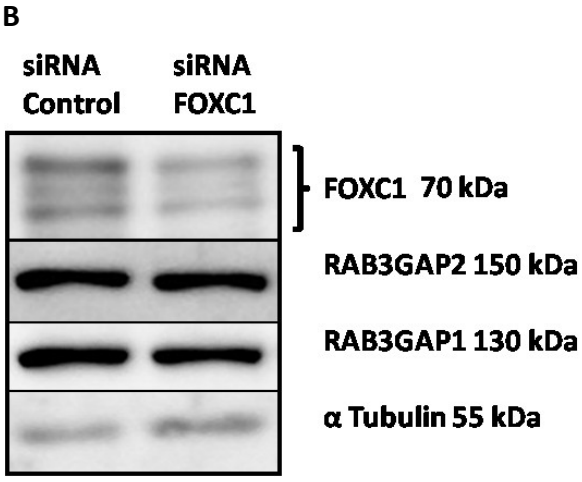
B
siRNA Control
siRNA FOXC1
FOXC1 70 kDa
RAB3GAP2 150 kDa
RAB3GAP1 130 kDa
α Tubulin 55 kDa

Figure 11. FOXC1 knockdown decreases protein levels of RAB3GAP1 in TM1 cells.

TM1 cells were transfected with either siRNA Control or siRNA FOXC1 then lysed after three days. Protein lysates were used for western blot analysis. Antibodies against FOXC1, RAB3GAP1, RAB3GAP2 and α-Tubulin (loading control) were used to detect change in protein levels. Net band intensity for each protein was normalized to α-Tubulin, and then siRNA FOXC1 treatment was scaled to siRNA control treatment. Experiments were repeated four times.

(A) Relative change in protein levels of FOXC1, RAB3GAP1and RAB3GAP2 following FOXC1 knockdown. Error bars represent standard error. $^{**}P<0.01$ versus siRNA Control under the Mann-Whitney U-test.

(B) Example western blot. Image taken with was Imagestation4000 after a 10 minute exposure.

Figure 11.

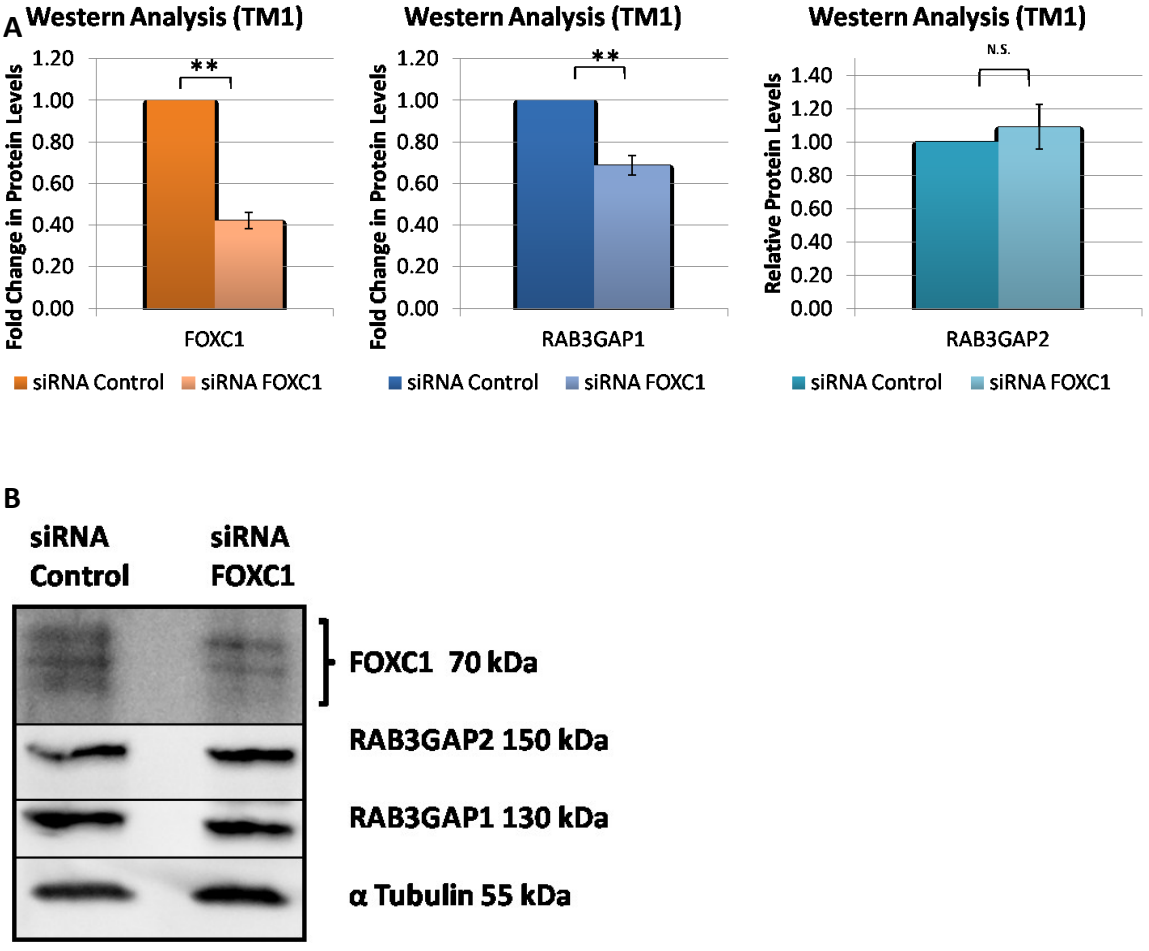
A
Western Analysis (TM1)
Fold Change in Protein Levels
1.20
1.00
0.80
0.60
0.40
0.20
0.00
**
FOXC1
siRNA Control
siRNA FOXC1
Western Analysis (TM1)
Fold Change in Protein Levels
1.20
1.00
0.80
0.60
0.40
0.20
0.00
**
RAB3GAP1
siRNA Control
siRNA FOXC1
Western Analysis (TM1)
Relative Protein Levels
1.40
1.20
1.00
0.80
0.60
0.40
0.20
0.00
N.S.
RAB3GAP2
siRNA Control
siRNA FOXC1
B
siRNA Control
siRNA FOXC1
FOXC1 70 kDa
RAB3GAP2 150 kDa
RAB3GAP1 130 kDa
α Tubulin 55 kDa

Figure 12. FOXC1 knockdown changes protein levels of SNAP25 in HeLa and TM1 cells.

HeLa or TM1 cells were transfected with either siRNA Control or siRNA FOXC1 then lysed after three days. Protein lysates were used for western blot analysis. Antibodies against FOXC1, SNAP25 and α-Tubulin (loading control) were used to detect change in protein levels. Net band intensity for each protein was normalized to α-Tubulin then siRNA FOXC1 treatment was scaled to siRNA control treatment. Experiments were repeated three times.

(A) Relative change in protein levels of FOXC1 and SNAP25 following FOXC1 knockdown in HeLa cells. Error bars represent standard error. *P<0.05 versus siRNA Control under the Mann-Whitney U-test.

(B) Example western blot in HeLa cells. Image taken with Imagestation4000 after a 10 minute exposure.

(C) Relative change in protein levels of FOXC1 and SNAP25 following FOXC1 knockdown in TM1 cells. Error bars represent standard error. *P<0.05 versus siRNA Control under the Mann-Whitney U-test.

(D) Example western blot in TM1 cells. Image was taken with Imagestation4000 after a 10 minute exposure.

Figure 12.

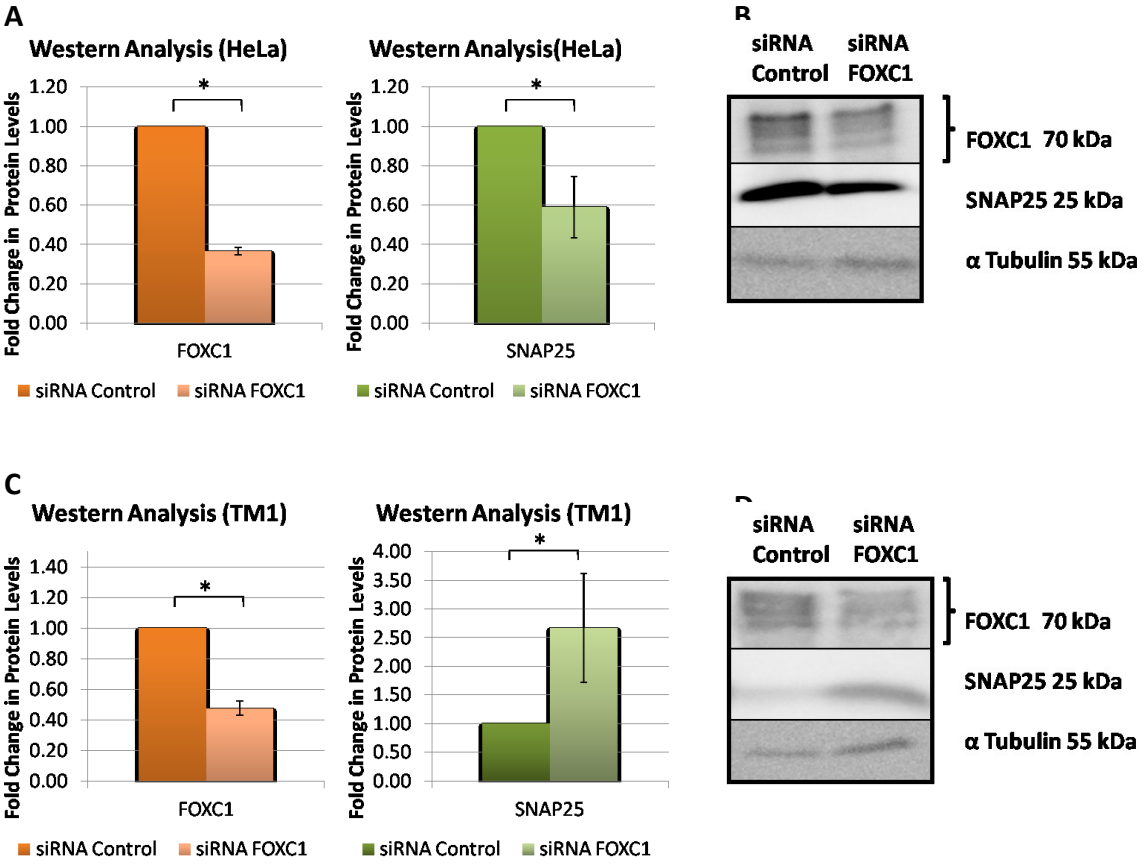
A
Western Analysis (HeLa)
Fold Change in Protein Levels
1.20
1.00
0.80
0.60
0.40
0.20
0.00
*
FOXC1
siRNA Control
siRNA FOXC1
Western Analysis(HeLa)
Fold Change in Protein Levels
1.20
1.00
0.80
0.60
0.40
0.20
0.00
*
SNAP25
siRNA Control
siRNA FOXC1
B
siRNA Control
siRNA FOXC1
FOXC1 70 kDa
SNAP25 25 kDa
α Tubulin 55 kDa
C
Western Analysis (TM1)
Fold Change in Protein Levels
1.40
1.20
1.00
0.80
0.60
0.40
0.20
0.00
*
FOXC1
siRNA Control
siRNA FOXC1
Western Analysis (TM1)
Fold Change in Protein Levels
4.00
3.50
3.00
2.50
2.00
1.50
1.00
0.50
0.00
*
SNAP25
siRNA Control
siRNA FOXC1
siRNA Control
siRNA FOXC1
FOXC1 70 kDa
SNAP25 25 kDa
α Tubulin 55 kDa

Figure 13. FOXC1 over-expression increases protein levels of RAB3GAP1 in HeLa cells.

HeLa cells were transfected with either Xpress-Empty or Xpress-FOXC1(WT) then lysed after three days. Protein lysates were used for western blot analysis. Antibodies against FOXC1, RAB3GAP1 and α-Tubulin (loading control) were used to detect change in protein levels. Net band intensity for each protein was normalized to α-Tubulin then Xpress-FOXC1(WT) treatment was scaled to Xpress-Empty treatment. Experiments were repeated eight times.

(A) Relative change in protein levels of FOXC1 and RAB3GAP1 following FOXC1 over-expression in HeLa cells. Error bars represent standard error. ***$P<0.001$ versus Xpress-Empty under the Mann-Whitney U-test.

(B) Example western blot in HeLa cells. Image was taken with Imagestation4000 after a 10 minute exposure.

Figure 11.

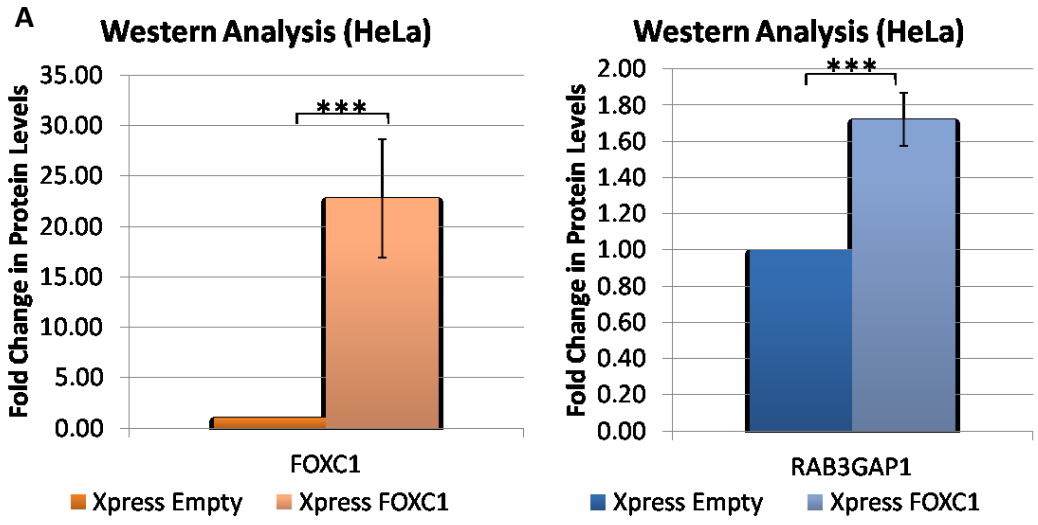
A
Western Analysis (HeLa)
Fold Change in Protein Levels
35.00
30.00
25.00
20.00
15.00
10.00
5.00
0.00
***
FOXC1
Xpress Empty
Xpress FOXC1
Western Analysis (HeLa)
Fold Change in Protein Levels
2.00
1.80
1.60
1.40
1.20
1.00
0.80
0.60
0.40
0.20
0.00
***
RAB3GAP1
Xpress Empty
Xpress FOXC1

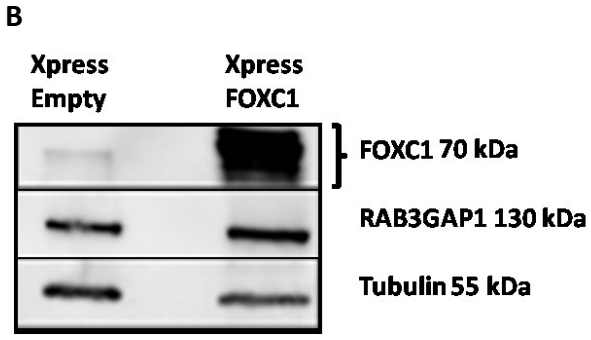
B
Xpress Empty
Xpress FOXC1
FOXC1 70 kDa
RAB3GAP1 130 kDa
Tubulin 55 kDa

Figure 14. RAB3GAP2 protein levels show positive correlation with FOXC1 over-expression in HeLa cells.

HeLa cells were transfected with either Xpress-Empty or Xpress-FOXC1(WT) then lysed after three days. Protein lysates were used for western blot analysis. Antibodies against FOXC1, RAB3GAP2 and α-Tubulin (loading control) were used to detect change in protein levels. Net band intensity for each protein was normalized to α-Tubulin then Xpress-FOXC1(WT) treatment was scaled to Xpress-Empty treatment. Experiments were repeated eight times.

(A) Relative change in protein levels of RAB3GAP2 plotted against relative increase in FOXC1 protein levels in HeLa cells. $P<0.05$ with a Spearman's rank correlation coefficient of 0.72.

(B) Example western blot in HeLa cells. Image was taken with Imagestation4000 after a 10 minute exposure.

Figure 14.

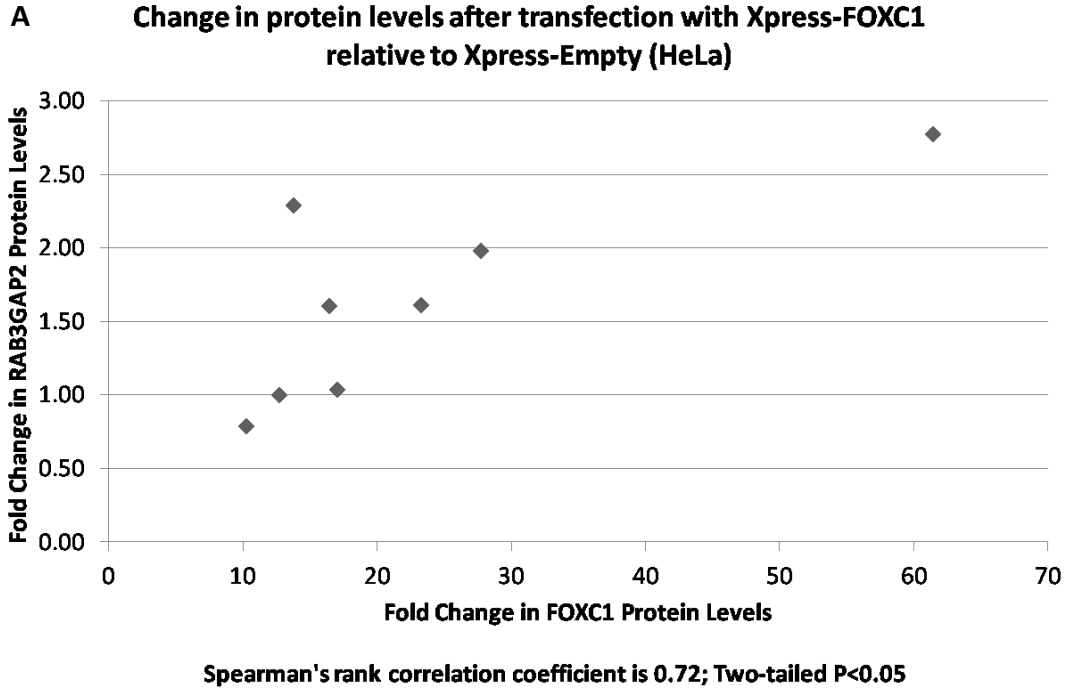
A
Change in protein levels after transfection with Xpress-FOXC1 relative to Xpress-Empty (HeLa)
Fold Change in RAB3GAP2 Protein Levels
3.00
2.50
2.00
1.50
1.00
0.50
0.00
0
10
20
30
40
50
60
70
Fold Change in FOXC1 Protein Levels
Spearman's rank correlation coefficient is 0.72; Two-tailed P<0.05

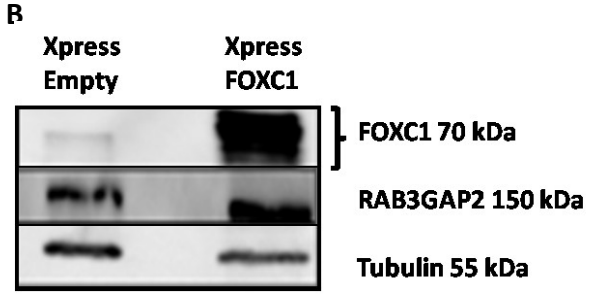
B
Xpress Empty
Xpress FOXC1
FOXC1 70 kDa
RAB3GAP2 150 kDa
Tubulin 55 kDa

Figure 15. FOXC1 over-expression increases protein levels of SNAP25 in HeLa cells.

HeLa cells were transfected with either Xpress-Empty or Xpress-FOXC1 (WT) then lysed after three days. Protein lysates were used for western blot analysis. Antibodies against FOXC1, SNAP25 and α-Tubulin (loading control) were used to detect change in protein levels. Net band intensity for each protein was normalized to α-Tubulin then Xpress-FOXC1(WT) treatment was scaled to Xpress-Empty treatment. Experiments were repeated three times.

(A) Relative change in protein levels of FOXC1 and SNAP25 following FOXC1 over-expression in HeLa cells. Error bars represent standard error. *P<0.05 versus Xpress-Empty under the Mann-Whitney U-test.

(B) Example western blot in HeLa cells. Image was taken with Imagestation4000 after a 10 minute exposure.

Figure 15.

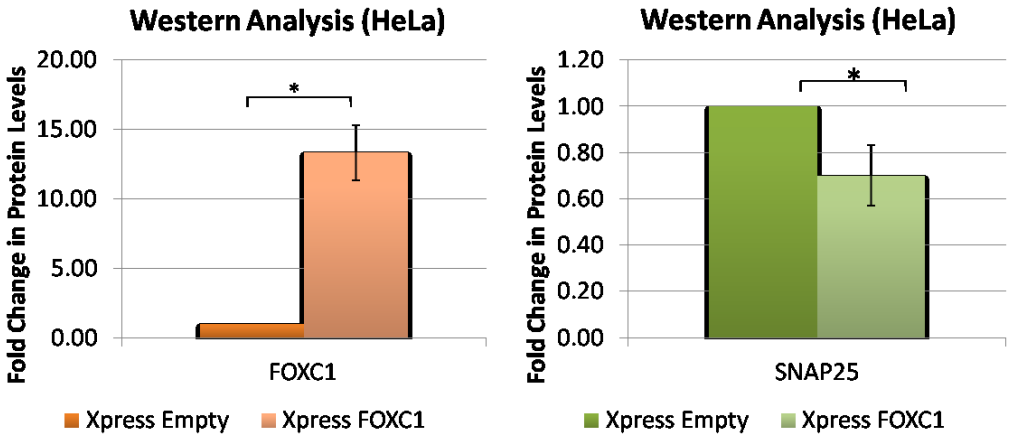
Western Analysis (HeLa)
Fold Change in Protein Levels
20.00
15.00
10.00
5.00
0.00
*
FOXC1
Xpress Empty
Xpress FOXC1
Western Analysis (HeLa)
Fold Change in Protein Levels
1.20
1.00
0.80
0.60
0.40
0.20
0.00
*
SNAP25
Xpress Empty
Xpress FOXC1

B

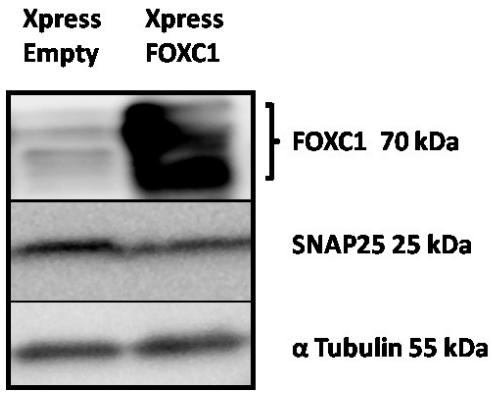
Xpress Empty
Xpress FOXC1
FOXC1 70 kDa
SNAP25 25 kDa
α Tubulin 55 kDa

Figure 16. FOXC1 knockdown decreases intracellular and extracellular levels of exogenous MYOC in HeLa cells.

(A) HeLa cells were either transfected with pRc-MYOC (WT) or left untreated. After three days a sample of cell media was taken and the cells were lysed. Protein lysates or media samples were used for western blot analysis. Antibodies against MYOC and TFIID (loading control) were used to detect proteins. Ponceau Red stain was used for media sample total protein control. Image of Western blot was taken with Imagestation4000 after a 10 minute exposure.

(B) HeLa cells were co-transfected with pRc-MYOC (WT) and either siRNA Control or siRNA FOXC1. After three days a sample of cell media was taken and the cells were lysed. Protein lysates or media samples were used for western blot analysis. Antibodies against MYOC, FOXC1 and TFIID (loading control) were used to detect change in proteins levels. Net band intensity for each protein was normalized to TFIID then siRNA FOXC1 treatment was scaled to siRNA Control treatment. Ponceau stain was used for media sample loading control. Experiments were repeated three times. Error bars represent standard error. *P<0.05 versus siRNA Control under the Mann-Whitney U-test.

(C) Example western blot in HeLa cells. Image was taken with Imagestation4000 after a 10 minute exposure.

Figure 16.

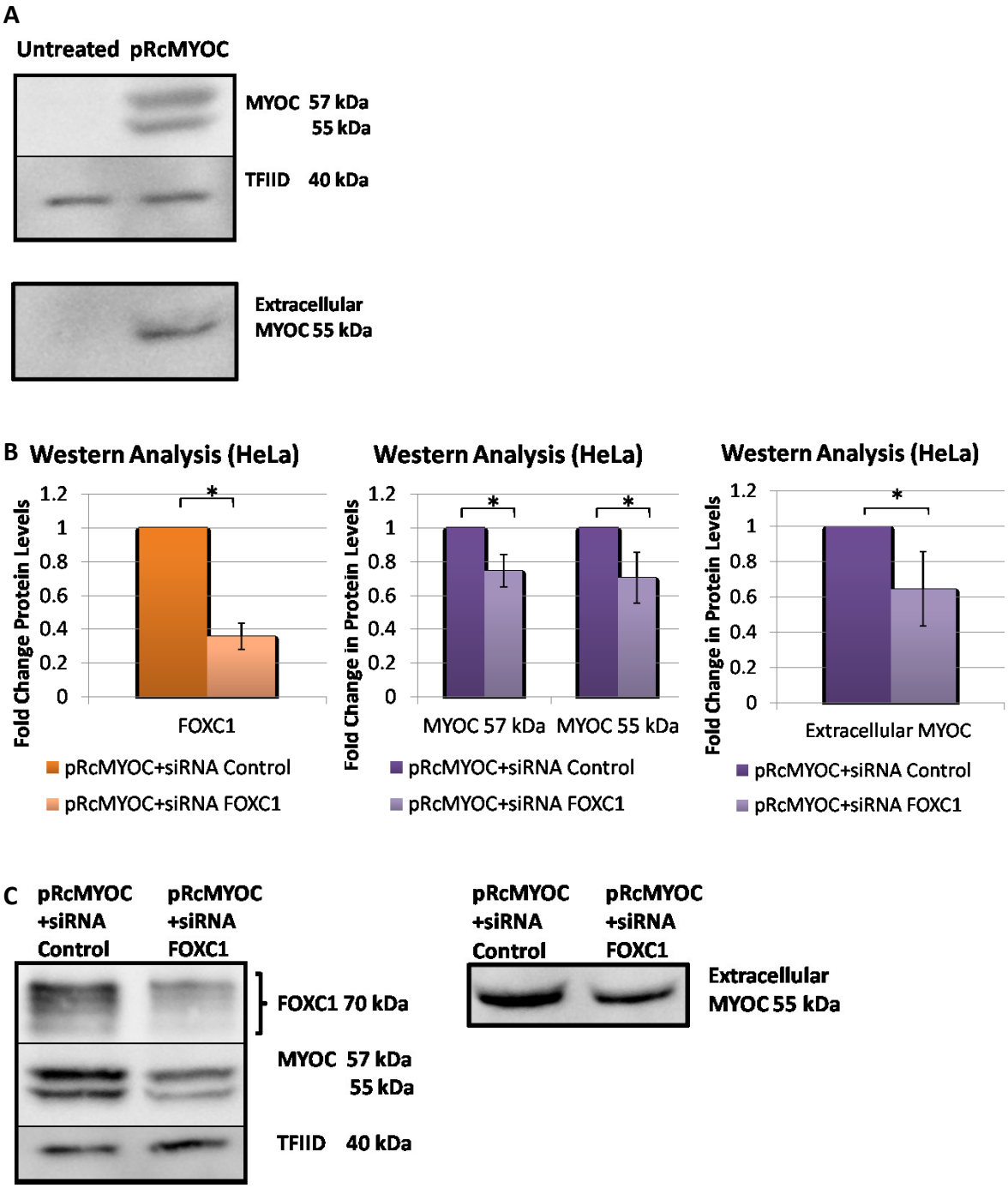
A
Untreated pRcMYOC
MYOC 57 kDa
55 kDa
TFIID 40 kDa
Extracellular
MYOC 55 kDa
B Western Analysis (HeLa)
Fold Change Protein Levels
1.2
1
0.8
0.6
0.4
0.2
0
*
FOXC1
pRcMYOC+siRNA Control
pRcMYOC+siRNA FOXC1
Western Analysis (HeLa)
Fold Change in Protein Levels
MYOC 57 kDa
MYOC 55 kDa
pRcMYOC+siRNA Control
pRcMYOC+siRNA FOXC1
Western Analysis (HeLa)
Fold Change in Protein Levels
Extracellular MYOC
pRcMYOC+siRNA Control
pRcMYOC+siRNA FOXC1
C
pRcMYOC +siRNA Control
pRcMYOC +siRNA FOXC1
FOXC1 70 kDa
MYOC 57 kDa
55 kDa
TFIID 40 kDa
pRcMYOC +siRNA Control
pRcMYOC +siRNA FOXC1
Extracellular
MYOC 55 kDa

Figure 17. RAB3GAP1 knockdown decreases intracellular and increases extracellular levels of exogenous MYOC in HeLa cells.

HeLa cells were co-transfected with pRc- MYOC (WT) and either siRNA control or siRNA RAB3GAP1. After three days a sample of cell media was taken and the cells were lysed. Protein lysates or media samples were used for western blot analysis. Antibodies against MYOC, RAB3GAP1 and TFIID (loading control) were used to detect change in proteins levels. Net band intensity for each protein was normalized to TFIID then siRNA FOXC1 treatment was scaled to siRNA Control treatment. Ponceau Red stain was used for media sample total protein control. Experiments were repeated three times.

(A) Relative change in protein levels of RAB3GAP1 and MYOC following RAB3GAP1 knockdown in HeLa cells. Error bars represent standard error. *P<0.05 versus siRNA Control under the Mann-Whitney U-test.

(B) Example western blot in HeLa cells. Image was taken with Imagestation4000 after a 10 minute exposure.

Figure 17.

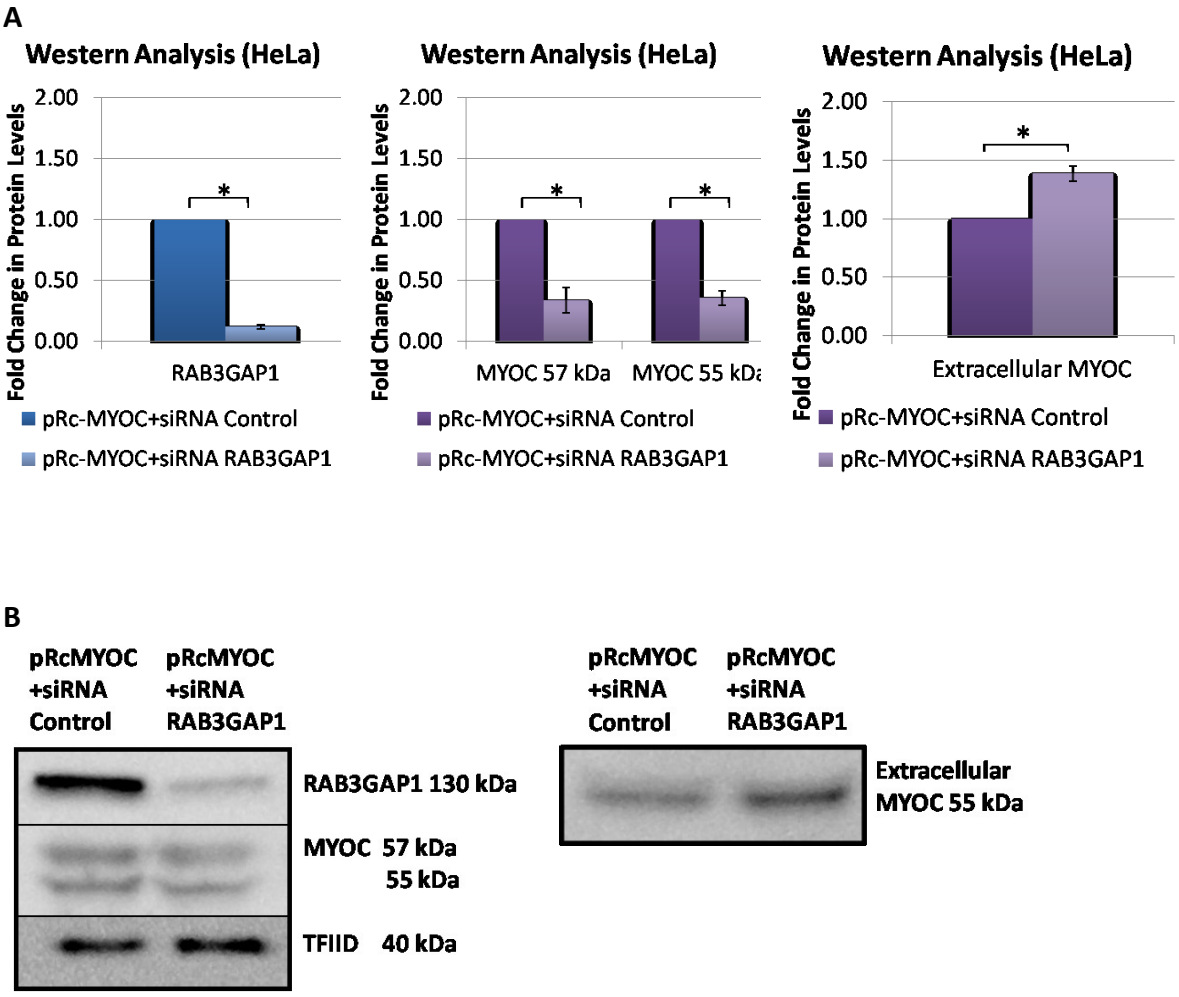
A
Western Analysis (HeLa)
Fold Change in Protein Levels
2.00
1.50
1.00
0.50
0.00
*
RAB3GAP1
pRc-MYOC+siRNA Control
pRc-MYOC+siRNA RAB3GAP1
Western Analysis (HeLa)
Fold Change in Protein Levels
2.00
1.50
1.00
0.50
0.00
*
*
MYOC 57 kDa
MYOC 55 kDa
pRc-MYOC+siRNA Control
pRc-MYOC+siRNA RAB3GAP1
Western Analysis (HeLa)
Fold Change in Protein Levels
2.00
1.50
1.00
0.50
0.00
*
Extracellular MYOC
pRc-MYOC+siRNA Control
pRc-MYOC+siRNA RAB3GAP1
B
pRcMYOC +siRNA Control
pRcMYOC +siRNA RAB3GAP1
RAB3GAP1 130 kDa
MYOC 57 kDa
55 kDa
TFIID 40 kDa
pRcMYOC +siRNA Control
pRcMYOC +siRNA RAB3GAP1
Extracellular MYOC 55 kDa

Figure 18. RAB3GAP2 knockdown decreases intracellular and extracellular levels of exogenous MYOC in HeLa cells.

HeLa cells were co-transfected with pRc-MYOC (WT) and either siRNA control or siRNA RAB3GAP2. After three days a sample of cell media was taken and the cells were lysed. Protein lysates or media sample were used for western blot analysis. Antibodies against MYOC, RAB3GAP2 and TFIID (loading control) were used to detect change in proteins levels. Net band intensity for each protein was normalized to TFIID then siRNA FOXC1 treatment was scaled to siRNA Control treatment. Ponceau Red stain was used for media sample total protein control. Experiments were repeated three times.

(A) Relative change in protein levels of RAB3GAP2 and MYOC following RAB3GAP2 knockdown in HeLa cells. Error bars represent standard error. *P<0.05 versus siRNA Control under the Mann-Whitney U-test.

(B) Example western blot in HeLa cells. Image was taken with Imagestation4000 after a 10 minute exposure.

Figure 18.

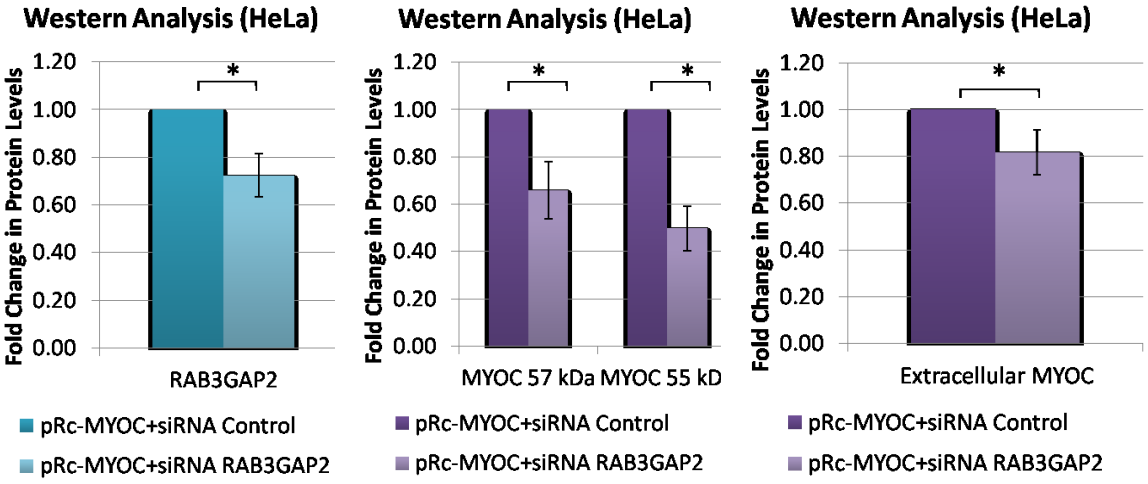
Western Analysis (HeLa)
Fold Change in Protein Levels
1.20
1.00
0.80
0.60
0.40
0.20
0.00
*
RAB3GAP2
pRc-MYOC+siRNA Control
pRc-MYOC+siRNA RAB3GAP2
Western Analysis (HeLa)
Fold Change in Protein Levels
*
*
MYOC 57 kDa
MYOC 55 kD
pRc-MYOC+siRNA Control
pRc-MYOC+siRNA RAB3GAP2
Western Analysis (HeLa)
Fold Change in Protein Levels
*
Extracellular MYOC
pRc-MYOC+siRNA Control
pRc-MYOC+siRNA RAB3GAP2

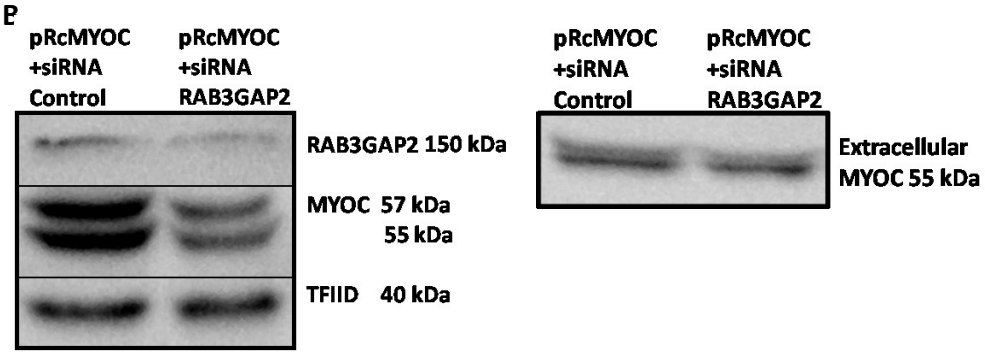
P
pRcMYOC +siRNA Control
pRcMYOC +siRNA RAB3GAP2
RAB3GAP2 150 kDa
MYOC 57 kDa
55 kDa
TFIID 40 kDa
pRcMYOC +siRNA Control
pRcMYOC +siRNA RAB3GAP2
Extracellular MYOC 55 kDa

Figure 19. SNAP25 knockdown decreases intracellular and increases extracellular levels of exogenous MYOC in HeLa cells.

HeLa cells were co-transfected with pRc-MYOC (WT) and either siRNA control or siRNA SNAP25. After three days a sample of cell media was taken and the cells were lysed. Protein lysates or media samples were used for western blot analysis. Antibodies against MYOC, SNAP25 and TFIID (loading control) were used to detect change in proteins levels. Net band intensity for each protein was normalized to TFIID then siRNA FOXC1 treatment was scaled to siRNA Control treatment. Ponceau Red stain was used for media sample total protein control. Experiments were repeated three times.

(A) Relative change in protein levels of SNAP25 and MYOC following SNAP25 knockdown in HeLa cells. Error bars represent standard error. *P<0.05 versus siRNA Control under the Mann-Whitney U-test.

(B) Example western blot in HeLa cells. Image was taken with Imagestation4000 after a 10 minute exposure.

Figure 19.

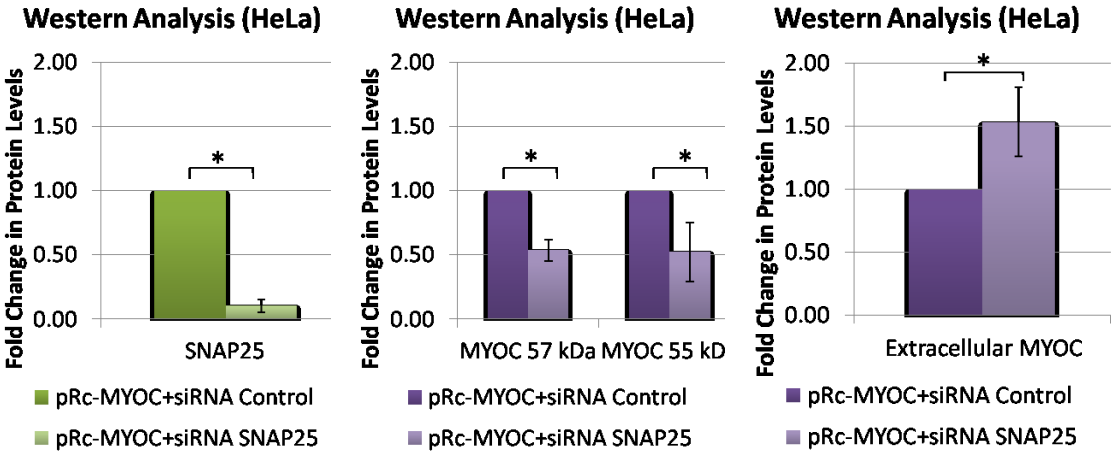
Western Analysis (HeLa)
Fold Change in Protein Levels
2.00
1.50
1.00
0.50
0.00
*
SNAP25
pRc-MYOC+siRNA Control
pRc-MYOC+siRNA SNAP25
Western Analysis (HeLa)
Fold Change in Protein Levels
2.00
1.50
1.00
0.50
0.00
*
*
MYOC 57 kDa
MYOC 55 kD
pRc-MYOC+siRNA Control
pRc-MYOC+siRNA SNAP25
Western Analysis (HeLa)
Fold Change in Protein Levels
2.00
1.50
1.00
0.50
0.00
*
Extracellular MYOC
pRc-MYOC+siRNA Control
pRc-MYOC+siRNA SNAP25

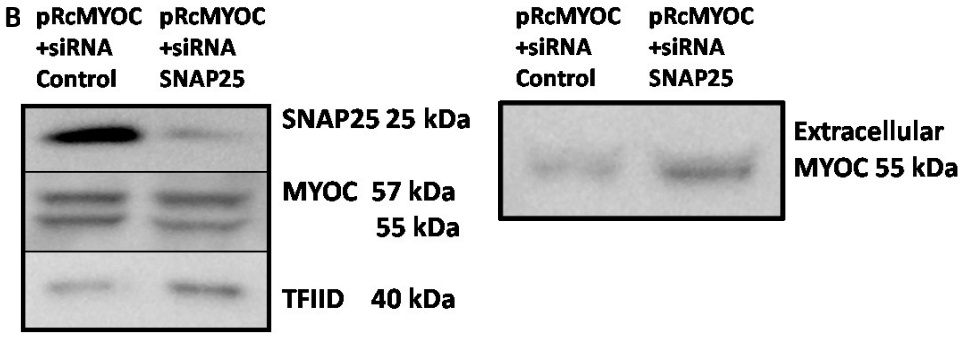
B
pRcMYOC +siRNA Control
pRcMYOC +siRNA SNAP25
SNAP25 25 kDa
MYOC 57 kDa
55 kDa
TFIID 40 kDa
pRcMYOC +siRNA Control
pRcMYOC +siRNA SNAP25
Extracellular MYOC 55 kDa

Figure 20. Combined RAB3GAP1 and RAB3GAP2 knockdown decreases intracellular and extracellular levels of exogenous MYOC in HeLa cells.

HeLa cells were co-transfected with pRc- MYOC (WT) and either siRNA Control or a combination of siRNA RAB3GAP1 and siRNA RAB3GAP2. After three days a sample of cell media was taken and the cells were lysed. Protein lysates or media sample were used for western blot analysis. Antibodies against MYOC and TFIID (loading control) were used to detect change in protein levels. Net band intensity for MYOC was normalized to TFIID then siRNA RAB3GAP1+ siRNA RAB3GAP2 treatment was scaled to siRNA Control treatment. Ponceau Red stain was used for media sample total protein control. Experiments were repeated three times.

(A) Relative change in protein levels of MYOC following RAB3GAP1 and RAB3GAP2 knockdown in HeLa cells. Error bars represent standard error. *P<0.05 versus siRNA Control under the Mann-Whitney U-test.

(B) Example western blot in HeLa cells. Image was taken with Imagestation4000 after a 10 minute exposure.

Figure 20.

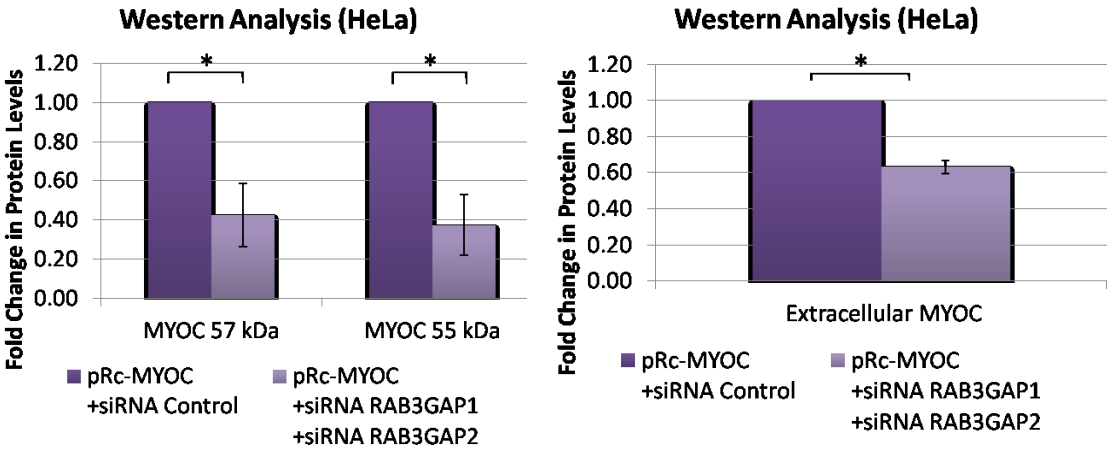
Western Analysis (HeLa)
Fold Change in Protein Levels
1.20
1.00
0.80
0.60
0.40
0.20
0.00
*
*
MYOC 57 kDa
MYOC 55 kDa
pRc-MYOC +siRNA Control
pRc-MYOC +siRNA RAB3GAP1 +siRNA RAB3GAP2
Western Analysis (HeLa)
Fold Change in Protein Levels
1.20
1.00
0.80
0.60
0.40
0.20
0.00
*
Extracellular MYOC
pRc-MYOC +siRNA Control
pRc-MYOC +siRNA RAB3GAP1 +siRNA RAB3GAP2

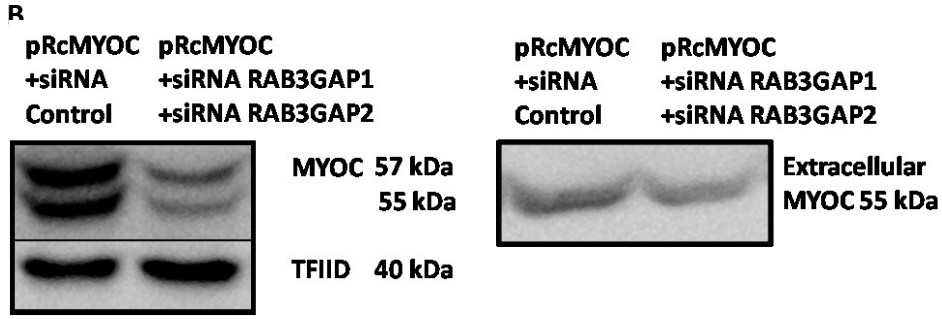
R
pRcMYOC +siRNA Control
pRcMYOC +siRNA RAB3GAP1 +siRNA RAB3GAP2
MYOC 57 kDa
55 kDa
TFIID 40 kDa
pRcMYOC +siRNA Control
pRcMYOC +siRNA RAB3GAP1 +siRNA RAB3GAP2
Extracellular MYOC 55 kDa

Figure 21. Combined SNAP25, RAB3GAP1 and RAB3GAP2 knockdown decreases intracellular and extracellular levels of exogenous MYOC in HeLa cells.

HeLa cells were co-transfected with pRc- MYOC (WT) and either siRNA control or combination of siRNA SNAP25, siRNA RAB3GAP1 and siRNA RAB3GAP2. After three days a sample of cell media was taken and the cells were lysed. Protein lysates or media samples were used for western blot analysis. Antibodies against MYOC and TFIID (loading control) were used to detect change in protein levels. Net band intensity for MYOC was normalized to TFIID then siRNA SNAP25+siRNA RAB3GAP1+ siRNA RAB3GAP2 treatment was scaled to siRNA Control treatment. Ponceau Red stain was used for media sample total protein control. Experiments were repeated three times.

(A) Relative change in protein levels of MYOC following SNAP25, RAB3GAP1 and RAB3GAP2 knockdown in HeLa cells. Error bars represent standard error. *P<0.05 versus siRNA Control under the Mann-Whitney U-test.

(B) Example western blot in HeLa cells. Image was taken with Imagestation4000 after a 10 minute exposure.

Figure 21.

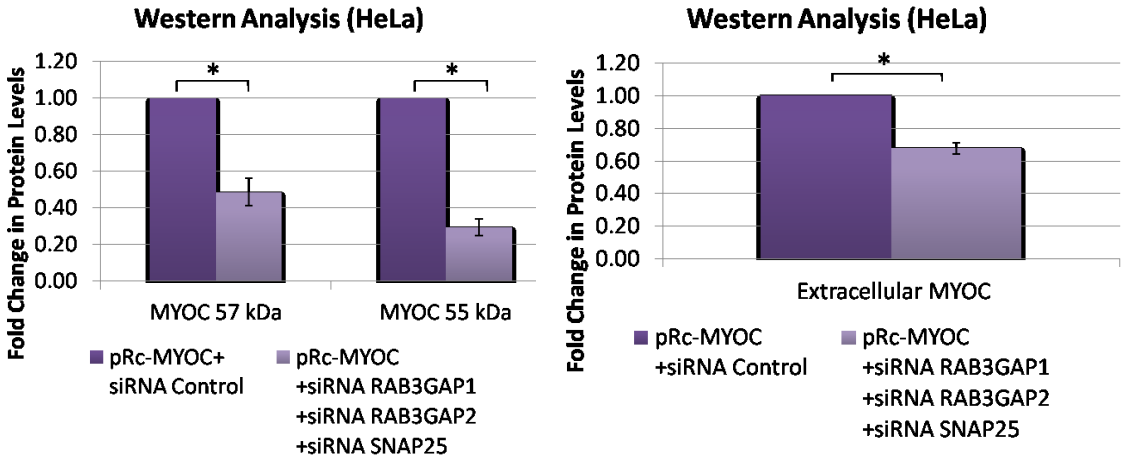
Western Analysis (HeLa)
Fold Change in Protein Levels
1.20
1.00
0.80
0.60
0.40
0.20
0.00
*
*
MYOC 57 kDa
MYOC 55 kDa
pRc-MYOC+ siRNA Control
pRc-MYOC +siRNA RAB3GAP1 +siRNA RAB3GAP2 +siRNA SNAP25
Western Analysis (HeLa)
Fold Change in Protein Levels
1.20
1.00
0.80
0.60
0.40
0.20
0.00
*
Extracellular MYOC
pRc-MYOC +siRNA Control
pRc-MYOC +siRNA RAB3GAP1 +siRNA RAB3GAP2 +siRNA SNAP25

B

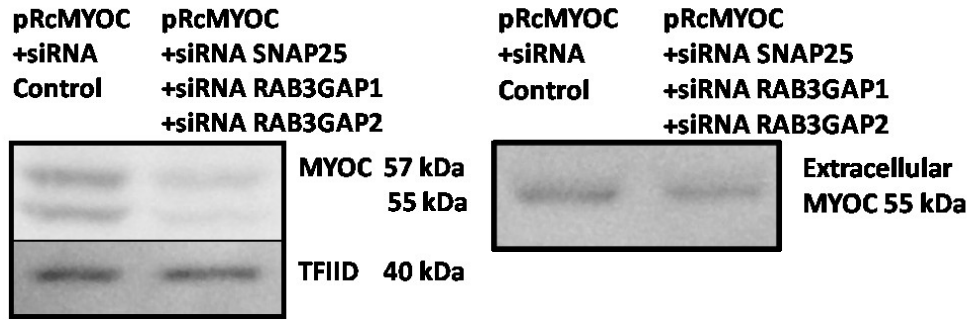
pRcMYOC +siRNA Control
pRcMYOC +siRNA SNAP25 +siRNA RAB3GAP1 +siRNA RAB3GAP2
MYOC 57 kDa
55 kDa
TFIID 40 kDa
pRcMYOC +siRNA Control
pRcMYOC +siRNA SNAP25 +siRNA RAB3GAP1 +siRNA RAB3GAP2
Extracellular MYOC 55 kDa

Figure 22. *FOXC1* knockdown decreases RNA levels of *SNAP23*, *SYN2* and *STXBP6* in TM1 cells.

TM1 cells were transfected with either siRNA Control or siRNA FOXC1 and after 3 days RNA was isolated and reverse transcribed into cDNA. Quantitative Real-Time PCR (qRT-PCR) was run with the cDNA samples and primers for *FOXC1*, *SNAP23*, *SYN2*, *STXBP6* and *HPRT1* (housekeeping control). Relative quantification (RQ) was performed using the ΔΔCt method.

(A) Relative quantification of the change in *FOXC1*, *SNAP23* and *SYN2* RNA levels following normalization to *HPRT1* and scaling siRNA FOXC1 to siRNA Control in TM1 cells. Experiments were performed three times in triplicate. Error bars represent standard error. **P*<0.05 versus siRNA Control under the Mann-Whitney U-test.

(B) Relative quantification (RQ) of the change in *FOXC1* and *STXBP6* RNA levels following normalization to *HPRT1* and scaling siRNA FOXC1 to siRNA Control in TM1 cells. Experiments were performed three times in triplicate. Error bars represent standard error. **P*<0.05 versus siRNA Control under the Mann-Whitney U-test.

Figure 22.

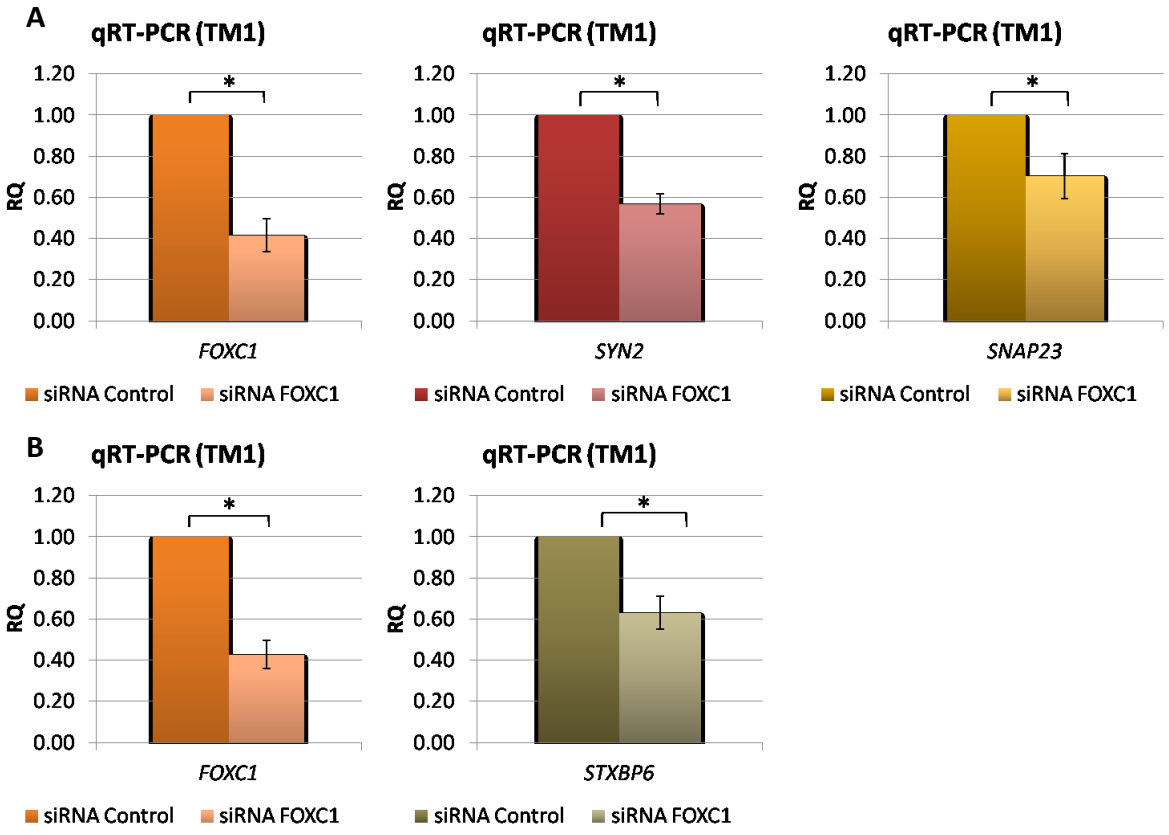
A
qRT-PCR (TM1)
RQ
1.20
1.00
0.80
0.60
0.40
0.20
0.00
*
FOXC1
siRNA Control
siRNA FOXC1
qRT-PCR (TM1)
SYN2
siRNA Control
siRNA FOXC1
qRT-PCR (TM1)
SNAP23
siRNA Control
siRNA FOXC1
B
qRT-PCR (TM1)
FOXC1
siRNA Control
siRNA FOXC1
qRT-PCR (TM1)
STXBP6
siRNA Control
siRNA FOXC1

6. Discussion

Axenfeld-Rieger syndrome (ARS) presents an important model for glaucoma pathogenesis, due the heightened risk of ARS patients to develop early onset glaucoma and their lack of response to glaucoma treatments[51–53]. Mutations leading to abnormal *FOXC1* copy number cause ARS as well as Dandy-Walker syndrome, characterized with abnormal cerebellum development[59,68]. The involvement of FOXC1 in disorders with ocular and neurodevelopmental malformations and in the neurodegenerative disease glaucoma illustrates its importance in neural and ocular development and neuronal health.

FOXC1 was previously found to associate with resistance to oxidative stress through regulation of FOXO1 and HSPA6 and in daily IOP fluctuation through its regulation of the circadian rhythm protein, CLOCK[69,71,74]. In the present work FOXC1 is shown to regulate the exocytotic genes RAB3GAP1, RAB3GAP2 and SNAP25 and modulate MYOC secretion. The new connection to MYOC and exocytosis indicates FOXC1's involvement in additional pathogenic glaucoma mechanisms and further elucidates the mechanisms through which FOXC1 is involved in neurodevelopment.

6.1 - FOXC1 regulation of RAB3GAP1

Previous work, by Berry et al. (2008), detected *RAB3GAP1* and *SNAP25* as potential targets of FOXC1 regulation in NPCE cells[69]. FOXC1 knockdown was also shown to decrease *RAB3GAP1* RNA levels in ocular tissues of zebrafish and NPCE cells[69].

My work further validated RAB3GAP1 as a FOXC1 target. FOXC1 can interact *in vivo* with the upstream region of *RAB3GAP1* in both HeLa and TM1 cells (Fig. 3B). Furthermore, in HeLa cells FOXC1 significantly up regulated Luciferase transactivation

through the upstream *RAB3GAP1* region (Fig. 4A). Luciferase transactivation by the S131L mutant FOXC1, previously shown to have a reduced ability to bind to the FOXC1 consensus binding site, was only 0.3-0.4 fold compared to transactivation by Wild-type FOXC1 (Fig. 4). Taken together, these findings indicate that FOXC1 directly up regulates *RAB3GAP1* transcription through interaction with *RAB3GAP1* upstream promoter elements. FOXC1 likely interacts with any of the three binding sites in the upstream region of *RAB3GAP1* (Fig. 3A), as removal of each one at a time had no effect on transactivation (Fig. 4).

I have also shown that FOXC1 positively regulates *RAB3GAP1* RNA and protein levels in both HeLa and TM1 cells. FOXC1 knockdown significantly decreased *RAB3GAP1* RNA and protein levels in TM1 and HeLa cells (Fig. 7, Fig. 10, Fig. 11), and FOXC1 over-expression significantly increased RAB3GAP1 protein levels in HeLa cells (Fig. 13). Therefore, FOXC1 directly upregulates RAB3GAP1 expression (Table 3).

6.2 - FOXC1 regulation of RAB3GAP2

RAB3GAP1 composes the catalytic subunit of the RAB3GAP complex along with RAB3GAP2, the non-catalytic subunit. While *RAB3GAP2* was not detected in the microarray analysis by Berry et al. (2008) [69] its role in the RAB3GAP complex made it an interesting target to investigate. FOXC1 showed strong interaction with the *RAB3GAP2* upstream region in both HeLa and TM1 cells (Fig. 3B). FOXC1 was not able to transactivate Luciferase through the *RAB3GAP2* upstream region without the presence of an additional promoter (Fig. 5A). However, when the *RAB3GAP2* upstream region was cloned upstream of a TK promoter Wild-Type FOXC1 increased Luciferase transactivation

(Fig. 5B). Furthermore, Luciferase transactivation dropped to 0.4 fold when the mutant S131L FOXC1 was used instead of Wild-Type FOXC1 (Fig. 5B), showing the importance of FOXC1 binding to the upstream *RAB3GAP2* region to induce transactivation. Furthermore, following deletion of the predicted FOXC1 binding site, FOXC1 was no longer able to increase Luciferase transactivation (Fig. 5B), indicating that FOXC1 interacts with the upstream region through the 5'-GAAATTTAAATAAACC-3' sequence. As FOXC1 was able to increase Luciferase transactivation through the upstream *RAB3GAP2* region only in the presence of the TK promoter, this supports that the FOXC1 binding site is not located in a promoter region but rather in an enhancer region. Enhancer regions can be located far from the transcription start site (TSS); however, when they are activated, for example by transcription factor binding, they can undergo chromatin remodeling to become closer to the promoter and boost transcription by helping the general transcription factors to assemble[120]. The FOXC1 binding site is located nearly 10 kb away from the *RAB3GAP2* TSS (Fig. 3A); therefore, FOXC1 likely enhances *RAB3GAP2* transcription by helping other transcription factors interact with the promoter region rather than acting on it directly.

FOXC1 knockdown decreased RNA levels of *RAB3GAP2* in both HeLa and TM1 cells (Fig. 7). However protein levels of RAB3GAP2 decreased in response to FOXC1 knockdown only in HeLa cells (Fig. 10, Fig. 11). Over expression of FOXC1 in HeLa cells increased protein levels of RAB3GAP2 only when FOXC1 protein levels were up regulated at least 13 times (Fig. 14); however, positive correlation was established between FOXC1 over-expression and increase in RAB3GAP2 protein levels. Therefore, FOXC1

regulation of RAB3GAP2 is complex and varies between TM1 and HeLa cell lines (Table 3).

6.3 - Cellular processes and glaucomatous mechanisms which FOXC1 could affect through RAB3GAP regulation

FOXC1 positively regulates both subunits of RAB3GAP in HeLa cells and the catalytic subunit of the complex, RAB3GAP1, in TM1 cells. The RAB3GAP complex is important in inactivating RAB3 by promoting its GTP hydrolysis[121]. In its activated form, RAB3 forms complexes with various effectors to direct progress of both exocytosis and endocytosis, responsible for extracellular traficking[122,123]. However, RAB3 inactivation is necessary for it to dissociate from its effectors and repeat its action in the exocytosis-endocytosis cycle of cell trafficking[124]. I therefore predict that FOXC1 regulates RAB3 indirectly through its regulation of RAB3GAP.

RAB3 is the most abundant RAB protein in the brain and is mainly associated with synaptic vesicle exocytosis[125]. RAB3 is involved in synaptic vesicle and granule secretion as well as regulated secretion[77]. Among its effectors are rabphilin-3, responsible for initiating vesicle fusion, RIM1 and RIM2 involved in membrane fusion and Calmodulin, important for Ca^{2+} sensitivity[77].

Therefore, through regulation of RAB3GAP, FOXC1 is predicted to influence the balance of active versus inactive RAB3 important for exocytosis progression. Exocytosis in glaucoma is involved in glutamate excitotoxicity, ATP secretion, important for prostaglandin production, and potentially MYOC secretion, indicating novel pathogenic mechanisms through which FOXC1 might promote glaucoma[82,83,126].

RAB3 was also shown to be involved in endocytosis, as its effecter Rabfilin-3 needs to be released following RAB3 inactivation to interact with Rabaptin-5 and promote receptor mediated Transferrin endocytosis[123]. Endocytosis abnormalities in glaucoma are associated with *OPTN* mutations, causing adult onset glaucoma[15]. The glaucomatous *OPTN* E50K mutation increases inhibition of RAB8 by TBC1D17, a RAB-GTPase activating protein, thereby interrupting Transferrin receptor recycling[85]. In addition, in RGC-5 cells both WT and M98K mutant variant of OPTN co-localized with RAB12, and M98K-OPTN promoted RAB12 mediated Transferrin receptor degradation leading to autophagic death[86]. Therefore, FOXC1 mutations, through misregulation of RAB3GAP, are predicted to affect RAB3 involvement in endocytosis and potentially act in similar pathogenic mechanisms as *OPTN* mutations and promote autophagic death.

The RAB3GAP complex was also shown to act independently of RAB3 in protein aggregation and autophagy initiation[127]. Autophagy is responsible for breakdown and transport of cytosolic components, in autophagosomes, to lysosomes where they are degraded[127]. The RAB3GAP complex is hypothesized to be promote autophagosome biogenesis through lipid transfer[127]. RAB3GAP exhibited interaction with FEZ1, an autophagy suppressor, and likely interferes with its action to promote autophagy[127]. FOXC1 is therefore likely to modulate authophagy both through the role of RAB3GAP in Transferrin endocytosis and autophagosome biogenesis. Therefore, FOXC1 regulation of RAB3GAP opens new directions for FOXC1 involvement in glaucoma pathogenesis through regulations of exocytosis, endocytosis and autophagy.

6.4 - FOXC1 regulation of SNAP25

Another exocytotic target detected in the microarray by Berry et al. (2008) was *SNAP25*[69]. SNAP25 plays a central role in secretory vesicle fusion with the plasma membrane through formation of the SNARE complex. SNAP25 was predicted to be negatively regulated in NPCE cells by FOXC1, in contrast to previous FOXC1 targets which FOXC1 was shown to activate[69]. FOXC1 showed far stronger interaction with the upstream region of SNAP25 in HeLa cells compared to TM1 cells, indicating differential regulation of SNAP25 between cell lines (Fig. 3B).

FOXC1 was not able to transactivate Luciferase through the SNAP25 upstream region without the presence of an additional promoter (Fig.6A). However when the SNAP25 upstream region was cloned upstream of a TK promoter, Wild Type FOXC1 increased Luciferase transactivation (Fig. 6B). Furthermore Luciferase transactivation dropped to 0.4 fold when the mutant S131L FOXC1 was used instead of Wild-Type FOXC1 (Fig. 6B), showing the importance of functional FOXC1 binding to the upstream SNAP25 region to increase transactivation. Following deletion of the predicted FOXC1 binding site, no change in FOXC1 ability to transactivate Luciferase was observed (Fig.4B). Additional binding sites were found when the SNAP25 upstream region was re-examined, indicating that, as was observed with RAB3GAP1, FOXC1 interaction with the region is not dependent on a single binding site. As FOXC1 was able to increase Luciferase transactivation through the upstream SNAP25 region only in the presence of the TK promoter, this supports that the FOXC1 binding site is not located in a promoter region but rather in an enhancer region located around 5 kb away from the TSS (Fig. 3A), similarly to RAB3GAP2. FOXC1 ability to enhance transactivation through the SNAP25 upstream

region indicates a potentially positive regulation of SNAP25 by FOXC1 in HeLa cells, contradicting the negative regulatory relationship predicted by the microarray performed by Berry et al. (2008) in NPCE cells[69]. However, as the microarray was performed in NPCE cells, differential regulation might occur due to different cell environments, and TM1 cells, an ocular cell line similar to NPCE is more likely to exhibit negative regulation of SNAP25 by FOXC1 as was predicted in the microarray experiment.

Differential regulation of SNAP25 by FOXC1 between HeLa and TM1 cells was further illustrated following FOXC1 knockdown. In HeLa cells FOXC1 decrease resulted in decreased RNA levels of both *SNAP25a* and *SNAP25b* decreasing (Fig. 8). Protein levels of SNAP25 decreased as well in HeLa cells following FOXC1 knockdown (Fig. 12A) further confirming positive regulation of SNAP25 by FOXC1 in HeLa cells.

Interestingly, FOXC1 over-expression in HeLa cells decreased protein levels of SNAP25. Two explanations present themselves to explain why FOXC1 knockdown and over expression have a similar effect on SNAP25 protein levels. First, it is possible that there is a positive correlation between FOXC1 over-expression and SNAP25 up regulation, similarly to RAB3GAP2; however, FOXC1 was not over-expressed sufficiently to reach the threshold above which it would up regulate SNAP25. This hypothesis is supported by the Luciferase transactivation experiment which showed that FOXC1 is able to enhance transactivation through the upstream region of SNAP25 (Fig. 6B). A second possible explanation is that SNAP25 is subjected to bimodular regulation by FOXC1, where deviations from a certain FOXC1 range of activity, whether above or below a specific threshold, leads to decrease in SNAP25 expression. This hypothesis is interesting in the context of FOXC1 mutations in ARS patients where missense and frame shift mutations in

patients, leading to reduced FOXC1 function, have similar phenotype to patients with FOXC1 duplications. FOXC1 dosage is crucial since ARS mutations that decrease FOXC1 activity below 80%, and ARS FOXC1 duplications that increase FOXC1 copies to 150% both lead to elevated IOP and glaucoma pathogenesis[128].

When SNAP25 regulation by FOXC1 was examined in TM1 cells, a negative regulatory relationship was observed. Following FOXC1 knockdown, *SNAP25a* increased significantly while *SNAP25b* showed no change (Fig. 9). Protein levels of SNAP25 also increased following FOXC1 knockdown in TM1 cells (Fig. 12D).

FOXC1 differentially regulates SNAP25 in HeLa versus TM1 cell lines. FOXC1 knockdown down-regulated both SNAP25 isoforms in HeLa cells and FOXC1 was also shown to increase transactivation through an enhancer region upstream of SNAP25. However, in TM1 cells FOXC1 knockdown up regulates *SNAP25a* but has no effect on *SNAP25b*, at least not at the RNA level (Table 3).

The difference in FOXC1 regulation of SNAP25 isoforms is interesting, as in rat brains mRNA levels of *SNAP25a* have higher expression during development until few weeks after birth when *SNAP25b* expression sharply increases[129]. While *SNAP25b* mRNA is highly expressed in post-natal brain regions in rats, *SNAP25a* is the dominant isoform in adrenal and pituitary glands[130]. As FOXC1 is associated with neurodevelopmental disorders it will be interesting to look at the regulatory relationship between FOXC1 and SNAP25 isoforms in model organisms such as rats or mice with FOXC1 mutations, to see if SNAP25 misregulation by FOXC1 might contribute to neurodevelopment defects observed in patients with FOXC1 mutations.

The negative regulation of SNAP25 by FOXC1 observed in TM1 cells is not likely to be mediated by a protein, as the microarray by Berry et al. (2008) degraded all other protein prior to FOXC1 induction[69]. Therefore, the likeliest mediator between FOXC1 and SNAP25 is a microRNA. MicroRNAs (miRNA) are small non-coding RNA's, transcribed as pri-miRNAs that in turn are converted to precursor microRNA in the nucleus and transported to the cytoplasm where they are cleaved by Dicer into mature miRNAs[131]. miRNA bind to the RNA-induced silencing complex (RISC) and target mRNA for degradation, thereby inhibiting translation of their target genes[131,132].

FOXC1 could inhibit SNAP25 expression by activating a miRNA which in turn binds to *SNAP25* mRNA and promotes its degradation. miRNA prediction programs detected multiple miRNA predicted to target *SNAP25*. They were further sorted by their ability to target additional negative FOXC1 targets. The microarray by Berry et al. (2008) also detected *ABCA8*, *RAB1A*, *SLC12A6* as potential targets of negative regulation by FOXC1[69]. If a miRNA is predicted to target several FOXC1 target genes, I hypothesize that there is a greater likelihood that it is in turn activated by FOXC1. Another criterion for sorting was previously described roles for miRNA in the trabecular meshwork. An interesting candidate miRNA that I detected is miR-106a. miR-106a is predicted to target *SNAP25* as well as three additional negative FOXC1 target genes, *ABCA8*, *RAB1A*, *SLC12A6*. Furthermore, miR-106a was shown to associate with stress-induced premature senescence in human trabecular meshwork cells and increased expression of the cyclin-dependent kinase inhibitor, $p21^{CDKN1A}$, thereby promoting stress-induced cell death[119]. It will be interesting to see if FOXC1 knockdown alters miR-106a levels, as it would present an additional role for FOXC1 in the stress response. If FOXC1 is shown to activate miR-106a,

a follow up experiment with transfection of TM1 cells with miR-106a and observing its effect on RNA levels of *SNAP25a* could further validate a FOXC1- miR-106a-*SNAP25* regulatory network. Additional miRNAs that are worth exploring as possible links in negative regulation of SNAP25 by FOXC1 in TM1 cells are miR-15a and miR-15b, which are predicted to target *RAB1A* in addition to *SNAP25* and were shown to be down-regulated in human trabecular meshwork cells with stress-induced premature senescence[119].

6.5 - Cellular processes and glaucomatous mechanisms which FOXC1 could affect through SNAP25 regulation

SNAP25 regulation by FOXC1 is complex (Table 3), with a negative regulatory relationship in TM1 cells and a bimodular regulation in HeLa cells. By modulating SNAP25, FOXC1 can potentially regulate both exocytosis and endocytosis. SNAP25 plays a central role in exocytosis by forming the SNARE complex necessary for vesicle fusion[133]. SNAP25 was shown to be essential in glutamatergic and GABAergic neurons for fast neurotransmission in both excitatory and inhibitory circuits[133]. SNAP25 inhibition was also shown to interfere with the formation of the SNARE complex and decreased evoked glutamate release rat cerebellar neurons[134]. Therefore, FOXC1 is likely to play a role in glutamate excitotoxicity through its regulation of SNAP25.

SNAP25 is also essential for endocytosis as SNAP25 cleavage with BoNT inhibited endocytosis[99]. FOXC1 is therefore associated with endocytosis through regulation of RAB3GAP and SNAP25, and potentially acts through a similar pathogenic mechanisms as *OPTN* mutations promoting Transferrin degradation[86].

6.6 - FOXC1 regulation of MYOC secretion through its target genes RAB3GAP1, RAB3GAP2 and SNAP25

FOXC1 was shown to regulate the RAB3GAP complex and SNAP25, both of which have central roles in exocytosis and endocytosis. To determine if the regulation has physiological consequences, I looked at exogenous MYOC secretion in HeLa cells. HeLa cells were chosen as in these cells RAB3GAP1, RAB3GAP2 and SNAP25 are all positively regulated by FOXC1, allowing examination of their combined impact on exocytosis. I decided to look at MYOC secretion as it is a protein associated with early onset glaucoma, similarly to FOXC1, and is also involved in steroid induced glaucoma[114,135]. Looking at MYOC secretion would examine the effect of FOXC1 on exocytosis and also provide a potential link to another central gene in glaucoma pathogenesis. As FOXC1 is a transcription factor I also wanted to rule out potential involvement of FOXC1 in transcriptional regulation of MYOC. Therefore, I looked at secretion of exogenous MYOC, by inducing MYOC expression with the pRcMYOC plasmid (Fig. 16A).

Decrease in RAB3GAP and SNAP25 activity has been previously linked to inhibition of exocytosis, and I have shown FOXC1 knockdown decreases levels of the RAB3GAP subunits, RAB3GAP1 and RAB3GAP2, as well as SNAP25 (Table 3). FOXC1 knockdown would therefore be predicted to inhibit secretion of MYOC. However FOXC1 knockdown had an unexpected effect on MYOC secretion.

Knockdown of FOXC1 or either of its targets RAB3GAP1, RAB3GAP2 and SNAP25, separately or in combination lead to a decrease in intracellular MYOC levels (Fig. 17-21,

Table 4). As knocking down RAB3GAP1 or SNAP25 also resulted in increased extracellular MYOC levels, it is likely that knockdown of FOXC1 or its target genes leads to initial increase in MYOC secretion; however when RAB3GAP2 is knocked down as well there is a reduction in extracellular MYOC (Fig. 17-21, Table 4), potentially through a process of degradation triggered by RAB3GAP2 outside the cell. MYOC secretion when all three targets are knocked down simultaneously paralleled the condition in which FOXC1 is knocked down (Fig. 17, Fig. 21, Table 4). These results support the idea that FOXC1's effect on MYOC is through its regulation of RAB3GAP1, RAB3GAP2 and SNAP25, though other unknown exocytotic FOXC1 targets might also contribute to its affect on MYOC secretion.

The effect of SNAP25 knockdown on MYOC secretion is especially interesting as SNAP25 is considered to act mainly in neuronal cells and in non-neuronal cells is thought to be replaced by its non-neuronal homolog, SNAP23[136]. My results show that SNAP25 is involved in secretion in HeLa cells and might potentially play an important role in other non-neuronal cell lines.

The unexpected effect of FOXC1 and its targets RAB3GAP1, RAB3GAP2 and SNAP25 have on MYOC secretion has two potential explanations. First, it's possible that roles of exocytic proteins are not conserved in HeLa's as it has been previously shown that SNAP23, considered essential for SNARE complex formation in non-neuronal cells, was not required for exocytosis in HeLa cells[136]. Both RAB3GAP and SNAP25 could therefore have unusual roles in exocytosis in HeLa cells. To test this hypothesis, an alkaline phosphatase secretion assay could be performed in HeLa cells, to see if knocking down FOXC1 and its targets would have a similar effect as was observed with MYOC.

A second possibility is that MYOC secretion is more complex than the traditional exocytosis route. Extracellular trafficking of MYOC is not well understood but suggested to associate with exosome-like vesicles[82]. In addition, MYOC was found to localize both in the membrane and in the cytosol and it interact with other intracellular membrane proteins through coiled-coil structures, similarly to SNAREs [137]. MYOC is also hypothesized to affect vesicle movement through its olfactomedin domain during vesicle secretion[137]. It is therefore possible that MYOC secretion would not be impacted by inhibition of SNAP25 and RAB3GAP as for other extracellular cargo.

Another experiment that could address the unexpected effect of FOXC1 on MYOC secretion in HeLa cells would be looking at the effect of FOXC1 and its targets on MYOC secretion in TM1 cells, and to see how results differ from observations in HeLa's. However, only FOXC1 regulation of RAB3GAP1 is similar between cell lines, with FOXC1 positively regulating both RNA and protein levels of RAB3GAP1. SNAP25 was shown to be negatively regulated by FOXC1 in TM1 cells and only RNA levels of RAB3GAP2 were regulated by FOXC1. Therefore, looking at the effect of RAB3GAP1 knockdown on MYOC secretion in TM1 cells could address whether RAB3GAP1 has a similar role in exocytosis between HeLa and TM1 cell lines and partially mimic the effect of FOXC1 knockdown. As SNAP25 is negatively regulated by FOXC1 in TM1 cells, the isoform SNAP25a would need to be over-expressed to mimic the effects of FOXC1 knockdown. While FOXC1 regulation of RAB3GAP2 is not likely to contribute to FOXC1 regulation of MYOC secretion in TM1 cells, and FOXC1 regulation of SNAP25 and RAB3GAP1 might have contradictory effects on MYOC secretion, it is important to look at the effect of FOXC1 on MYOC exocytosis in TM1 cells. TM1 are an ocular cell line and

likely to reflect the effect of FOXC1 in the trabecular meshwork of ARS patients as well as potentially show differential regulation of MYOC secretion by FOXC1 between different cells which would be important consideration for the role of FOXC1 in different human tissues. While the mechanism through which SNAP25 and RAB3GAP regulate MYOC secretion needs to be investigated further, I have shown that FOXC1 modulates MYOC secretion and that it acts through regulation of both RAB3GAP subunits and SNAP25.

The new connection between MYOC and FOXC1 can improve our understanding of the role of FOXC1 in glaucoma pathogenesis. Pathogenic MYOC mutations found in glaucoma patients were shown to affect MYOC secretion and result in intracellular accumulation of MYOC [116,138]. MYOC is also linked to ER stress and inflammatory stress responses in trabecular meshwork cells[41,81,139]. There is also increasing evidence pointing to MYOC as an inhibitor of neuronal regeneration. Increased levels of MYOC mRNA and protein were found in glial scars of astrocytes isolated from injured cerebral cortexes compared to uninjured controls[140]. Furthermore, in an assay measuring neurite outgrowth ganglia stopped neurite outgrowth upon reaching areas with immobilized MYOC protein[140]. When soluble-recombinant MYOC was added to media, neurite growth was also inhibited, in a dose dependent manner, despite the presence of NGF, known to stimulate neurite outgrowth[140]. Moreover, over-expression of wild type MYOC along with P370L mutant reduced the length and quantity of neurites in PC12 and RGC5 cells[141]. These findings indicate a pathogenic mechanism where MYOC acts to prevent regeneration of retinal astrocytes following injury further accelerating their death[141]. Therefore, FOXC1 mutations would likely disrupt normal MYOC secretion and affect both stress response in the trabecular meshwork and RGC regeneration.

6.7 – Conclusions

I have shown that FOXC1 regulates the protein components of the RAB3GAP complex and SNAP25. Both proteins have central roles in exocytosis; RAB3GAP is important for secratory vesicle docking and tethering, while SNAP25 is required for fusion of the vesicle with the plasma membrane. I have also shown that FOXC1 is able to modulate extracellular trafficking of MYOC by controlling levels of the RAB3GAP complex and SNAP25. My results indicate that FOXC1 is an important regulator of exocytosis and that ARS patients might be affected by similar pathogenic pathways as JOAG patients with MYOC mutations.

Through regulation of its target genes FOXC1 was previously shown to be involved both in IOP modulation and stress response in glaucoma pathogenesis in addition to ocular developmental defects. The present work also links FOXC1 to exocytosis, indicating a potential role in glutamate excitotoxicity and prostaglandin production. I have also shown a new connection between FOXC1 and MYOC through FOXC1 modulation of MYOC secretion. Those findings further establish ARS as an important model of glaucoma, as FOXC1 mutations are involved in multiple pathways in glaucoma pathogenesis.

6.8 - Future directions

FOXC1 regulation of exocytosis could be further explored by looking at ATP release. ATP release in trabecular meshwork cells is important for mobilization of arachidonic acid which in turn is necessary for prostaglandin production[83]. FOXC1 mutations can affect ATP release at the trabecular meshwork and interrupt prostaglandin secretion, which could underlie the lack of response of ARS patients to IOP lowering prostaglandin medication[53].

FOXC1 involvement in endocytosis should also be investigated further, as both RAB3GAP and SNAP25 were shown to affect endocytosis, which is linked to glaucoma through *OPTN* mutations which disrupt Transferrin endocytosis[86]. As *OPTN* mutations are linked to normal tension glaucoma, FOXC1 acting through a similar mechanism to OPTN might further explain the poor response of ARS patient to treatments, which aim to lower IOP[15,53].

An additional pathogenic mechanism which FOXC1 is likely to affect through its regulation of RAB3GAP is autophagy. RAB3GAP is associated with autophagsome biogenesis and through its regulation of RAB3 with Transferrin receptor degradation leading to autophagic death[86,142]. Through its regulation of RAB3GAP FOXC1 might potentially be involved in RGC autophagy induced apoptosis[143].

I have also shown that FOXC1 knockdown down regulates RNA levels of the additional exocytic targets *SNAP23*, *SYN2* and *STXBP6* (Fig.20). It would be interesting to validate FOXC1 regulation of these targets further to better understand the effect FOXC1 has on exocytosis. FOXC1 regulation of SNAP23 is especially interesting as it is considered a non-neuronal isoform of SNAP25, and has a similar role in the SNARE complex formation[144].

References

1. Tham YC, Li X, Wong TY, Quigley HA, Aung T, Cheng CY. Global prevalence of glaucoma and projections of glaucoma burden through 2040: A systematic review and meta-analysis. *Ophthalmology*. 2014;121(11):2081-2090. doi:10.1016/j.ophtha.2014.05.013.

2. Broman AT, Quigley HA, West SK, et al. Estimating the rate of progressive visual field damage in those with open-angle glaucoma, from cross-sectional data. *Invest Ophthalmol Vis Sci*. 2008;49(1):66-76. doi:10.1167/iovs.07-0866.

3. Quigley HA. Glaucoma. *Lancet*. 2011;377(9774):1367-1377. doi:10.1016/S0140-6736(10)61423-7.

4. Sigal IA, Ethier CR. Biomechanics of the optic nerve head. *Exp Eye Res*. 2009;88(4):799-807. doi:10.1016/j.exer.2009.02.003.

5. ANDERSON DR, HENDRICKSON A. Effect of Intraocular Pressure on Rapid Axoplasmic Transport in Monkey Optic Nerve. *Invest Ophthalmol Vis Sci*. 1974;13(10):771-783. http://iovs.arvojournals.org.login.ezproxy.library.ualberta.ca/article.aspx?articleid=2122520&resultClick=1. Accessed February 24, 2016.

6. Buckingham BP, Inman DM, Lambert W, et al. Progressive ganglion cell degeneration precedes neuronal loss in a mouse model of glaucoma. *J Neurosci*. 2008;28(11):2735-2744. doi:10.1523/JNEUROSCI.4443-07.2008.

7. Voykov B, Dimopoulos S, Leitritz MA, Doycheva D, William A. Long-term results

of ab externo trabeculotomy for glaucoma secondary to chronic uveitis. *Graefe's Arch Clin Exp Ophthalmol = Albr von Graefes Arch für Klin und Exp Ophthalmol*. 2016;254(2):355-360. doi:10.1007/s00417-015-3204-y.

8. Khan AO. Genetics of primary glaucoma. *Curr Opin Ophthalmol*. 2011;22:347-355. doi:10.1097/ICU.0b013e32834922d2.

9. Walton DS, Katsavounidou G. Newborn primary congenital glaucoma: 2005 update. *J Pediatr Ophthalmol Strabismus*. 42(6):333-341; quiz 365-366. http://www.ncbi.nlm.nih.gov/pubmed/16382557. Accessed March 1, 2016.

10. Bejjani BA, Lewis RA, Tomey KF, et al. Mutations in CYP1B1, the gene for cytochrome P4501B1, are the predominant cause of primary congenital glaucoma in Saudi Arabia. *Am J Hum Genet*. 1998;62(2):325-333. doi:10.1086/301725.

11. Mashima Y, Suzuki Y, Sergeev Y, et al. Novel cytochrome P4501B1 (CYP1B1) gene mutations in Japanese patients with primary congenital glaucoma. *Invest Ophthalmol Vis Sci*. 2001;42(10):2211-2216. http://www.ncbi.nlm.nih.gov/pubmed/11527932. Accessed March 1, 2016.

12. Raymond V. Molecular genetics of the glaucomas: mapping of the first five "GLC" loci. *Am J Hum Genet*. 1997;60(2):272-277. http://www.pubmedcentral.nih.gov/articlerender.fcgi?artid=1712410&tool=pmcentrez&rendertype=abstract. Accessed March 1, 2016.

13. Shimizu S, Lichter PR, Johnson AT, et al. Age-dependent prevalence of mutations at the GLC1A locus in primary open-angle glaucoma. *Am J Ophthalmol*.

2000;130(2):165-177. http://www.ncbi.nlm.nih.gov/pubmed/11004290. Accessed March 7, 2016.

14. Kapetanakis V V, Chan MPY, Foster PJ, Cook DG, Owen CG, Rudnicka AR. Global variations and time trends in the prevalence of primary open angle glaucoma (POAG): a systematic review and meta-analysis. *Br J Ophthalmol*. 2015;100(1):86-93. doi:10.1136/bjophthalmol-2015-307223.

15. Rezaie T, Child A, Hitchings R, et al. Adult-onset primary open-angle glaucoma caused by mutations in optineurin. *Science*. 2002;295(5557):1077-1079. doi:10.1126/science.1066901.

16. Alward WLM, Kwon YH, Khanna CL, et al. Variations in the myocilin gene in patients with open-angle glaucoma. *Arch Ophthalmol (Chicago, Ill 1960)*. 2002;120(9):1189-1197. http://www.ncbi.nlm.nih.gov/pubmed/12215093. Accessed March 1, 2016.

17. Reis LM, Semina E V. Genetics of anterior segment dysgenesis disorders. *Curr Opin Ophthalmol*. 2011;22(5):314-324. doi:10.1097/ICU.0b013e328349412b.

18. Libby RT, Gould DB, Anderson MG, John SWM. Complex genetics of glaucoma susceptibility. *Annu Rev Genomics Hum Genet*. 2005;6:15-44. doi:10.1146/annurev.genom.6.080604.162209.

19. Cairns JE. Trabeculectomy. *Am J Ophthalmol*. 1968;66(4):673-679. doi:10.1016/0002-9394(68)91288-9.

20. Digiuni M, Fogagnolo P, Rossetti L. A review of the use of latanoprost for glaucoma

since its launch. *Expert Opin Pharmacother*. 2012;13(5):723-745. doi:10.1517/14656566.2012.662219.

21. Foster PJ. The definition and classification of glaucoma in prevalence surveys. *Br J Ophthalmol*. 2002;86(2):238-242. doi:10.1136/bjo.86.2.238.

22. Wallace DM, Pokrovskaya O, O'Brien CJ. The Function of Matricellular Proteins in the Lamina Cribrosa and Trabecular Meshwork in Glaucoma. *J Ocul Pharmacol Ther*. 2015;31(7):386-395. doi:10.1089/jop.2014.0163.

23. Tamm ER. The trabecular meshwork outflow pathways: structural and functional aspects. *Exp Eye Res*. 2009;88(4):648-655. doi:10.1016/j.exer.2009.02.007.

24. Friedman DS, Wilson MR, Liebmann JM, Fechtner RD, Weinreb RN. An evidence-based assessment of risk factors for the progression of ocular hypertension and glaucoma. *Am J Ophthalmol*. 2004;138(3 Suppl):S19-S31. doi:10.1016/j.ajo.2004.04.058.

25. Saccà SC, Pulliero A, Izzotti A. The dysfunction of the trabecular meshwork during glaucoma course. *J Cell Physiol*. 2015;230(3):510-525. doi:10.1002/jcp.24826.

26. Wiggs JL. The cell and molecular biology of complex forms of glaucoma: Updates on genetic, environmental, and epigenetic risk factors. *Investig Ophthalmol Vis Sci*. 2012;53:2467-2469. doi:10.1167/iovs.12-9483e.

27. Mehra KS, Roy PN, Khare BB. Tobacco smoking and glaucoma. *Ann Ophthalmol*. 1976;8(4):462-464. http://www.ncbi.nlm.nih.gov/pubmed/1267318. Accessed February 26, 2016.

28. Wang D, Huang Y, Huang C, et al. Association analysis of cigarette smoking with onset of primary open-angle glaucoma and glaucoma-related biometric parameters. *BMC Ophthalmol*. 2012;12(1):59. doi:10.1186/1471-2415-12-59.

29. Yoshida M, Take S, Ishikawa M, et al. Association of smoking with intraocular pressure in middle-aged and older Japanese residents. *Environ Health Prev Med*. 2014;19(2):100-107. doi:10.1007/s12199-013-0359-1.

30. ARMALY MF. Effect of Corticosteroids on Intraocular Pressure and Fluid Dynamics. *Arch Ophthalmol*. 1963;70(4):482. doi:10.1001/archopht.1963.00960050484010.

31. François J, Heintz-De Bree C, Tripathi RC. The Cortisone Test and the Heredity of Primary Open-Angle Glaucoma. *Am J Ophthalmol*. 1966;62(5):844-852. doi:10.1016/0002-9394(66)91908-8.

32. BECKER B. Intraocular Pressure Response to Topical Corticosteroids. *Invest Ophthalmol Vis Sci*. 1965;4(2):198-205. http://iovs.arvojournals.org/article.aspx?articleid=2203651. Accessed March 6, 2016.

33. Tripathi RC, Parapuram SK, Tripathi BJ, Zhong Y, Chalam K V. Corticosteroids and glaucoma risk. *Drugs Aging*. 1999;15(6):439-450. http://www.ncbi.nlm.nih.gov/pubmed/10641955. Accessed March 4, 2016.

34. Armaly MF. Inheritance of Dexamethasone Hypertension and Glaucoma. *Arch Ophthalmol*. 1967;77(6):747-751. doi:10.1001/archopht.1967.00980020749006.

35. Armaly MF. The heritable nature of dexamethasone-induced ocular hypertension. *Arch Ophthalmol (Chicago, Ill 1960)*. 1966;75(1):32-35. http://www.ncbi.nlm.nih.gov/pubmed/5900502. Accessed March 6, 2016.

36. ARMALY MF. EFFECT OF CORTICOSTEROIDS ON INTRAOCULAR PRESSURE AND FLUID DYNAMICS. I. THE EFFECT OF DEXAMETHASONE IN THE NORMAL EYE. *Arch Ophthalmol (Chicago, Ill 1960)*. 1963;70:482-491. http://www.ncbi.nlm.nih.gov/pubmed/14078870. Accessed March 6, 2016.

37. ARMALY MF. EFFECT OF CORTICOSTEROIDS ON INTRAOCULAR PRESSURE AND FLUID DYNAMICS. II. THE EFFECT OF DEXAMETHASONE IN THE GLAUCOMATOUS EYE. *Arch Ophthalmol (Chicago, Ill 1960)*. 1963;70:492-499. http://www.ncbi.nlm.nih.gov/pubmed/14078871. Accessed March 6, 2016.

38. Becker B. Elevated Intraocular Pressure Following Corticosteroid Eye Drops. *JAMA J Am Med Assoc*. 1963;185(11):884. doi:10.1001/jama.1963.03060110088027.

39. Nguyen TD, Chen P, Huang WD, Chen H, Johnson D, Polansky JR. Gene structure and properties of TIGR, an olfactomedin-related glycoprotein cloned from glucocorticoid-induced trabecular meshwork cells. *J Biol Chem*. 1998;273(11):6341-6350. http://www.ncbi.nlm.nih.gov/pubmed/9497363. Accessed March 6, 2016.

40. Polansky JR, Fauss DJ, Chen P, et al. Cellular pharmacology and molecular biology of the trabecular meshwork inducible glucocorticoid response gene product. *Ophthalmol J Int d'ophtalmologie Int J Ophthalmol Zeitschrift für Augenheilkd*. 1997;211(3):126-139. http://www.ncbi.nlm.nih.gov/pubmed/9176893. Accessed

February 27, 2016.

41. Joe MK, Sohn S, Hur W, Moon Y, Choi YR, Kee C. Accumulation of mutant myocilins in ER leads to ER stress and potential cytotoxicity in human trabecular meshwork cells. *Biochem Biophys Res Commun*. 2003;312(3):592-600. doi:10.1016/j.bbrc.2003.10.162.

42. Almasieh M, Wilson AM, Morquette B, Cueva Vargas JL, Di Polo A. The molecular basis of retinal ganglion cell death in glaucoma. *Prog Retin Eye Res*. 2012;31(2):152-181. doi:10.1016/j.preteyeres.2011.11.002.

43. Li S, Mallory M, Alford M, Tanaka S, Masliah E. Glutamate transporter alterations in Alzheimer disease are possibly associated with abnormal APP expression. *J Neuropathol Exp Neurol*. 1997;56(8):901-911. http://www.ncbi.nlm.nih.gov/pubmed/9258260. Accessed February 29, 2016.

44. Siliprandi R, Canella R, Carmignoto G, et al. N-methyl-D-aspartate-induced neurotoxicity in the adult rat retina. *Vis Neurosci*. 1992;8(6):567-573. http://www.ncbi.nlm.nih.gov/pubmed/1586655. Accessed March 1, 2016.

45. Dreyer EB, Zurakowski D, Schumer RA, Podos SM, Lipton SA. Elevated glutamate levels in the vitreous body of humans and monkeys with glaucoma. *Arch Ophthalmol (Chicago, Ill 1960)*. 1996;114(3):299-305. http://www.ncbi.nlm.nih.gov/pubmed/8600890. Accessed March 1, 2016.

46. Jones DP. Radical-free biology of oxidative stress. *Am J Physiol Cell Physiol*. 2008;295(4):C849-C868. doi:10.1152/ajpcell.00283.2008.

47. Tang Y, Scheef EA, Wang S, et al. CYP1B1 expression promotes the proangiogenic phenotype of endothelium through decreased intracellular oxidative stress and thrombospondin-2 expression. *Blood*. 2009;113(3):744-754. doi:10.1182/blood-2008-03-145219.

48. Tang Y, Scheef E a, Gurel Z, Sorenson CM, Jefcoate CR, Sheibani N. CYP1B1 and endothelial nitric oxide synthase combine to sustain proangiogenic functions of endothelial cells under hyperoxic stress. *Am J Physiol Cell Physiol*. 2010;298(44):C665-C678. doi:10.1152/ajpcell.00153.2009.

49. Gould DB. Anterior segment dysgenesis and the developmental glaucomas are complex traits. *Hum Mol Genet*. 2002;11(10):1185-1193. doi:10.1093/hmg/11.10.1185.

50. Tümer Z, Bach-Holm D. Axenfeld-Rieger syndrome and spectrum of PITX2 and FOXC1 mutations. *Eur J Hum Genet*. 2009;17(June):1527-1539. doi:10.1038/ejhg.2009.93.

51. Shields MB. Axenfeld-Rieger syndrome: a theory of mechanism and distinctions from the iridocorneal endothelial syndrome. *Trans Am Ophthalmol Soc*. 1983;81:736-784. http://www.pubmedcentral.nih.gov/articlerender.fcgi?artid=1312467&tool=pmcentrez&rendertype=abstract. Accessed March 5, 2016.

52. Alward WL. Axenfeld-Rieger syndrome in the age of molecular genetics. *Am J Ophthalmol*. 2000;130(1):107-115. http://www.ncbi.nlm.nih.gov/pubmed/11004268. Accessed March 1, 2016.

53. Strungaru MH, Dinu I, Walter MA. Genotype-phenotype correlations in Axenfeld-Rieger malformation and glaucoma patients with FOXC1 and PITX2 mutations. *Invest Ophthalmol Vis Sci*. 2007;48(1):228-237. doi:10.1167/iovs.06-0472.

54. Gripp KW, Hopkins E, Jenny K, Thacker D, Salvin J. Cardiac anomalies in Axenfeld-Rieger syndrome due to a novel FOXC1 mutation. *Am J Med Genet A*. 2013;161A(1):114-119. doi:10.1002/ajmg.a.35697.

55. Tsai JC, Grajewski AL. Cardiac valvular disease and Axenfeld-Rieger syndrome. *Am J Ophthalmol*. 1994;118(2):255-256. http://www.ncbi.nlm.nih.gov/pubmed/8053476. Accessed March 5, 2016.

56. Swiderski RE, Reiter RS, Nishimura DY, et al. Expression of the Mf1 gene in developing mouse hearts: implication in the development of human congenital heart defects. *Dev Dyn*. 1999;216(1):16-27. doi:10.1002/(SICI)1097-0177(199909)216:1<16::AID-DVDY4>3.0.CO;2-1.

57. Fuse N, Takahashi K, Yokokura S, Nishida K. Novel mutations in the FOXC1 gene in Japanese patients with Axenfeld-Rieger syndrome. *Mol Vis*. 2007;13:1005-1009. http://www.pubmedcentral.nih.gov/articlerender.fcgi?artid=2776537&tool=pmcentrez&rendertype=abstract. Accessed March 5, 2016.

58. Semina E V, Reiter R, Leysens NJ, et al. Cloning and characterization of a novel bicoid-related homeobox transcription factor gene, RIEG, involved in Rieger syndrome. *Nat Genet*. 1996;14(4):392-399. doi:10.1038/ng1296-392.

59. Mears AJ, Jordan T, Mirzayans F, et al. Mutations of the forkhead/winged-helix

gene, FKHL7, in patients with Axenfeld-Rieger anomaly. *Am J Hum Genet*. 1998;63(5):1316-1328. doi:10.1086/302109.

60. Berry FB, Lines MA, Oas JM, et al. Functional interactions between FOXC1 and PITX2 underlie the sensitivity to FOXC1 gene dose in Axenfeld-Rieger syndrome and anterior segment dysgenesis. *Hum Mol Genet*. 2006;15(6):905-919. doi:10.1093/hmg/ddl008.

61. Benayoun B a., Caburet S, Veitia R a. Forkhead transcription factors: Key players in health and disease. *Trends Genet*. 2011;27(6):224-232. doi:10.1016/j.tig.2011.03.003.

62. Clark KL, Halay ED, Lai E, Burley SK. Co-crystal structure of the HNF-3/fork head DNA-recognition motif resembles histone H5. *Nature*. 1993;364(6436):412-420. doi:10.1038/364412a0.

63. Nishimura DY, Searby CC, Alward WL, et al. A spectrum of FOXC1 mutations suggests gene dosage as a mechanism for developmental defects of the anterior chamber of the eye. *Am J Hum Genet*. 2001;68(2):364-372. doi:10.1086/318183.

64. Saleem RA, Banerjee-Basu S, Berry FB, Baxevanis AD, Walter MA. Analyses of the effects that disease-causing missense mutations have on the structure and function of the winged-helix protein FOXC1. *Am J Hum Genet*. 2001;68(3):627-641. doi:10.1086/318792.

65. Lehmann OJ, Ebenezer ND, Jordan T, et al. Chromosomal duplication involving the forkhead transcription factor gene FOXC1 causes iris hypoplasia and glaucoma. *Am*

J Hum Genet. 2000;67(5):1129-1135. doi:10.1016/S0002-9297(07)62943-7.

66. Lehmann OJ, Ebenezer ND, Ekong R, et al. Ocular Developmental Abnormalities and Glaucoma Associated with Interstitial 6p25 Duplications and Deletions. *Invest Ophthalmol Vis Sci*. 2002;43(6):1843-1849. http://iovs.arvojournals.org/article.aspx?articleid=2123464. Accessed March 5, 2016.

67. Pierrou S, Enerbäck S, Carlsson P. Selection of high-affinity binding sites for sequence-specific, DNA binding proteins from random sequence oligonucleotides. *Anal Biochem*. 1995;229(1):99-105. doi:10.1006/abio.1995.1384.

68. Aldinger KA, Lehmann OJ, Hudgins L, et al. FOXC1 is required for normal cerebellar development and is a major contributor to chromosome 6p25.3 Dandy-Walker malformation. *Nat Genet*. 2009;41(9):1037-1042. doi:10.1038/ng.422.

69. Berry FB, Skarie JM, Mirzayans F, et al. FOXC1 is required for cell viability and resistance to oxidative stress in the eye through the transcriptional regulation of FOXO1A. *Hum Mol Genet*. 2008;17(4):490-505. doi:10.1093/hmg/ddm326.

70. Ponugoti B, Xu F, Zhang C, Tian C, Pacios S, Graves DT. FOXO1 promotes wound healing through the up-regulation of TGF-??1 and prevention of oxidative stress. *J Cell Biol*. 2013;203(2):327-343. doi:10.1083/jcb.201305074.

71. Ito YA, Goping IS, Berry F, Walter MA. Dysfunction of the stress-responsive FOXC1 transcription factor contributes to the earlier-onset glaucoma observed in Axenfeld-Rieger syndrome patients. *Cell Death Dis*. 2014;5(2):e1069.

doi:10.1038/cddis.2014.8.

72. Paylakhi SH, Moazzeni H, Yazdani S, et al. FOXC1 in human trabecular meshwork cells is involved in regulatory pathway that includes miR-204, MEIS2, and ITGβ1. *Exp Eye Res*. 2013;111:112-121. doi:10.1016/j.exer.2013.03.009.

73. Conte I, Carrella S, Avellino R, et al. miR-204 is required for lens and retinal development via Meis2 targeting. *Proc Natl Acad Sci U S A*. 2010;107(35):15491-15496. doi:10.1073/pnas.0914785107.

74. Paylakhi SH, Moazzeni H, Yazdani S, et al. FOXC1 in human trabecular meshwork cells is involved in regulatory pathway that includes miR-204, MEIS2, and ITGβ1. *Exp Eye Res*. 2013;111:112-121. doi:10.1016/j.exer.2013.03.009.

75. Gundelfinger ED, Kessels MM, Qualmann B. Temporal and spatial coordination of exocytosis and endocytosis. *Nat Rev Mol Cell Biol*. 2003;4(2):127-139. doi:10.1038/nrm1016.

76. Söllner TH. Regulated exocytosis and SNARE function (Review). *Mol Membr Biol*. 20(3):209-220. doi:10.1080/0968768031000104953.

77. Zerial M, McBride H. Rab proteins as membrane organizers. *Nat Rev Mol Cell Biol*. 2001;2(February):107-117. doi:10.1038/35052055.

78. Touchot N, Chardin P, Tavitian A. Four additional members of the ras gene superfamily isolated by an oligonucleotide strategy: molecular cloning of YPT-related cDNAs from a rat brain library. *Proc Natl Acad Sci U S A*. 1987;84(23):8210-8214.

http://www.pubmedcentral.nih.gov/articlerender.fcgi?artid=299511&tool=pmcentrez&rendertype=abstract. Accessed March 26, 2016.

79. Pfeffer SR. Rab GTPases: specifying and deciphering organelle identity and function. *Trends Cell Biol*. 2001;11(12):487-491. http://www.ncbi.nlm.nih.gov/pubmed/11719054. Accessed March 6, 2016.

80. Zerial M, McBride H. Rab proteins as membrane organizers. *Nat Rev Mol Cell Biol*. 2001;2(2):107-117. doi:10.1038/35052055.

81. Itakura T, Peters DM, Fini ME. Glaucomatous MYOC mutations activate the IL-1/NF-κB inflammatory stress response and the glaucoma marker SELE in trabecular meshwork cells. *Mol Vis*. 2015;21:1071-1084. /pmc/articles/PMC4575906/?report=abstract. Accessed March 6, 2016.

82. Hardy KM, Hoffman E a., Gonzalez P, McKay BS, Stamer WD. Extracellular trafficking of myocilin in human trabecular meshwork cells. *J Biol Chem*. 2005;280:28917-28926. doi:10.1074/jbc.M504803200.

83. Luna C, Li G, Qiu J, Challa P, Epstein DL, Gonzalez P. Extracellular release of ATP mediated by cyclic mechanical stress leads to mobilization of AA in trabecular meshwork cells. *Invest Ophthalmol Vis Sci*. 2009;50(12):5805-5810. doi:10.1167/iovs.09-3796.

84. Malarkey EB, Parpura V. Mechanisms of glutamate release from astrocytes. *Neurochem Int*. 2008;52(1-2):142-154. doi:10.1016/j.neuint.2007.06.005.

85. Vaibhava V, Nagabhushana a., Chalasani MLS, Sudhakar C, Kumari a., Swarup G.

Optineurin mediates negative regulation of Rab8 function by TBC1D17, a GTPase activating protein. *J Cell Sci*. 2012;8:5026-5039. doi:10.1242/jcs.102327.

86. Sirohi K, Chalasani MLS, Sudhakar C, Kumari A, Radha V, Swarup G. M98K-OPTN induces transferrin receptor degradation and RAB12-mediated autophagic death in retinal ganglion cells. *Autophagy*. 2013;9(4):510-527. doi:10.4161/auto.23458.

87. Clabecq a., Henry JP, Darchen F. Biochemical characterization of Rab3-GTPase-activating protein reveals a mechanism similar to that of Ras-GAP. *J Biol Chem*. 2000;275(41):31786-31791. doi:10.1074/jbc.M003705200.

88. Fukui K, Sasaki T, Imazumi K, Matsuura Y, Nakanishi H, Takai Y. Isolation and characterization of a GTPase activating protein specific for the Rab3 subfamily of small G proteins. *J Biol Chem*. 1997;272(8):4655-4658. http://www.ncbi.nlm.nih.gov/pubmed/9030515. Accessed March 7, 2016.

89. Aligianis I a, Johnson C a, Gissen P, et al. Mutations of the catalytic subunit of RAB3GAP cause Warburg Micro syndrome. *Nat Genet*. 2005;37(3):221-223. doi:10.1038/ng1517.

90. Warburg M, Sjö O, Fledelius HC, Pedersen SA. Autosomal recessive microcephaly, microcornea, congenital cataract, mental retardation, optic atrophy, and hypogenitalism. Micro syndrome. *Am J Dis Child*. 1993;147(12):1309-1312. http://www.ncbi.nlm.nih.gov/pubmed/8249951. Accessed March 7, 2016.

91. Mégarbané A, Choueiri R, Bleik J, Mezzina M, Caillaud C. Microcephaly,

microphthalmia, congenital cataract, optic atrophy, short stature, hypotonia, severe psychomotor retardation, and cerebral malformations: a second family with micro syndrome or a new syndrome? *J Med Genet*. 1999;36(8):637-640. http://www.pubmedcentral.nih.gov/articlerender.fcgi?artid=1762968&tool=pmcentrez&rendertype=abstract. Accessed March 7, 2016.

92. Derbent M, Agras PI, Gedik S, Oto S, Alehan F, Saatçi U. Congenital cataract, microphthalmia, hypoplasia of corpus callosum and hypogenitalism: report and review of Micro syndrome. *Am J Med Genet A*. 2004;128A(3):232-234. doi:10.1002/ajmg.a.30109.

93. Graham JM, Hennekam R, Dobyns WB, Roeder E, Busch D. MICRO syndrome: an entity distinct from COFS syndrome. *Am J Med Genet A*. 2004;128A(3):235-245. doi:10.1002/ajmg.a.30060.

94. Nassogne MC, Henrot B, Saint-Martin C, Kadhim H, Dobyns WB, Sébire G. Polymicrogyria and motor neuropathy in Micro syndrome. *Neuropediatrics*. 2000;31(4):218-221. doi:10.1055/s-2000-7463.

95. Li X, Bykhovskaya Y, Haritunians T, et al. A genome-wide association study identifies a potential novel gene locus for keratoconus, one of the commonest causes for corneal transplantation in developed countries. *Hum Mol Genet*. 2012;21(2):421-429. doi:10.1093/hmg/ddr460.

96. Aligianis I a, Morgan N V, Mione M, et al. Mutation in Rab3 GTPase-activating protein (RAB3GAP) noncatalytic subunit in a kindred with Martsolf syndrome. *Am J Hum Genet*. 2006;78(April):702-707. doi:10.1086/502681.

97. Söllner T, Whiteheart SW, Brunner M, et al. SNAP receptors implicated in vesicle targeting and fusion. *Nature*. 1993;362(6418):318-324. doi:10.1038/362318a0.

98. Verderio C, Coco S, Bacci A, et al. Tetanus toxin blocks the exocytosis of synaptic vesicles clustered at synapses but not of synaptic vesicles in isolated axons. *J Neurosci*. 1999;19(16):6723-6732. http://europepmc.org/abstract/MED/10436029. Accessed March 8, 2016.

99. Xu J, Luo F, Zhang Z, et al. SNARE Proteins Synaptobrevin, SNAP-25, and Syntaxin Are Involved in Rapid and Slow Endocytosis at Synapses. *Cell Rep*. 2013;3(5):1414-1421. doi:10.1016/j.celrep.2013.03.010.

100. Bark IC, Wilson MC. Human cDNA clones encoding two different isoforms of the nerve terminal protein SNAP-25. *Gene*. 1994;139(2):291-292. http://www.ncbi.nlm.nih.gov/pubmed/8112622. Accessed February 23, 2016.

101. Prescott GR, Chamberlain LH. Regional and developmental brain expression patterns of SNAP25 splice variants. *BMC Neurosci*. 2011;12:35. doi:10.1186/1471-2202-12-35.

102. Faraone S V, Perlis RH, Doyle AE, et al. Molecular genetics of attention-deficit/hyperactivity disorder. *Biol Psychiatry*. 2005;57(11):1313-1323. doi:10.1016/j.biopsych.2004.11.024.

103. Ayalew M, Le-Niculescu H, Levey DF, et al. Convergent functional genomics of schizophrenia: from comprehensive understanding to genetic risk prediction. 2012;(February). doi:10.1038/mp.2012.37.

104. Basoglu C, Oner O, Ates A, et al. Synaptosomal-associated protein 25 gene polymorphisms and antisocial personality disorder: Association with temperament and psychopathy. *Can J Psychiatry*. 2011;56(6):341-347.

105. Wei C, Thatcher EJ, Olena AF, et al. miR-153 Regulates SNAP-25, Synaptic Transmission, and Neuronal Development. *PLoS One*. 2013;8(2). doi:10.1371/journal.pone.0057080.

106. Corradini I, Verderio C, Sala M, Wilson MC, Matteoli M. SNAP-25 in neuropsychiatric disorders. *Ann N Y Acad Sci*. 2009;1152:93-99. doi:10.1111/j.1749-6632.2008.03995.x.

107. Ravichandran V, Chawla A, Roche PA. Identification of a novel syntaxin- and synaptobrevin/VAMP-binding protein, SNAP-23, expressed in non-neuronal tissues. *J Biol Chem*. 1996;271(23):13300-13303. http://www.ncbi.nlm.nih.gov/pubmed/8663154. Accessed February 23, 2016.

108. Cesca F, Baldelli P, Valtorta F, Benfenati F. The synapsins: key actors of synapse function and plasticity. *Prog Neurobiol*. 2010;91(4):313-348. doi:10.1016/j.pneurobio.2010.04.006.

109. Lohmann SM, Ueda T, Greengard P. Ontogeny of synaptic phosphoproteins in brain. *Proc Natl Acad Sci U S A*. 1978;75(8):4037-4041. http://www.pubmedcentral.nih.gov/articlerender.fcgi?artid=392926&tool=pmcentrez&rendertype=abstract. Accessed March 8, 2016.

110. Bogen IL, Jensen V, Hvalby O, Walaas SI. Synapsin-dependent development of

glutamatergic synaptic vesicles and presynaptic plasticity in postnatal mouse brain. *Neuroscience*. 2009;158(1):231-241. doi:10.1016/j.neuroscience.2008.05.055.

111. Constable JRL, Graham ME, Morgan A, Burgoyne RD. Amisyn regulates exocytosis and fusion pore stability by both syntaxin-dependent and syntaxin-independent mechanisms. *J Biol Chem*. 2005;280:31615-31623. doi:10.1074/jbc.M505858200.

112. Chang TC, Summers CG, Schimmenti L a., Grajewski a. L. Axenfeld-Rieger syndrome: new perspectives. *Br J Ophthalmol*. 2012;96:318-322. doi:10.1136/bjophthalmol-2011-300801.

113. Casson RJ. Possible role of excitotoxicity in the pathogenesis of glaucoma. *Clin Exp Ophthalmol*. 2006;34(October 2005):54-63. doi:10.1111/j.1442-9071.2006.01146.x.

114. Partridge CA, Weinstein BI, Southren AL, Gerritsen ME. Dexamethasone induces specific proteins in human trabecular meshwork cells. *Invest Ophthalmol Vis Sci*. 1989;30(8):1843-1847. http://www.ncbi.nlm.nih.gov/pubmed/2759798. Accessed March 6, 2016.

115. Héraud C, Chevrier L, Meunier AC, Muller J-M, Chadéneau C. Vasoactive intestinal peptide-induced neuritogenesis in neuroblastoma SH-SY5Y cells involves SNAP-25. *Neuropeptides*. 2008;42(5-6):611-621. doi:10.1016/j.npep.2008.05.005.

116. Gobeil S, Rodrigue M-A, Moisan S, et al. Intracellular sequestration of hetero-oligomers formed by wild-type and glaucoma-causing myocilin mutants. *Invest Ophthalmol Vis Sci*. 2004;45(10):3560-3567. doi:10.1167/iovs.04-0300.

117. Spang N, Feldmann A, Huesmann H, et al. RAB3GAP1 and RAB3GAP2 modulate basal and rapamycin-induced autophagy. *Autophagy*. 2014;10(12):2297-2309. doi:10.4161/15548627.2014.994359.

118. Saleem RA, Banerjee-Basu S, Berry FB, Baxevanis AD, Walter MA. Analyses of the effects that disease-causing missense mutations have on the structure and function of the winged-helix protein FOXC1. *Am J Hum Genet*. 2001;68(3):627-641. doi:10.1086/318792.

119. Li G, Luna C, Qiu J, Epstein DL, Gonzalez P. Alterations in microRNA expression in stress-induced cellular senescence. *Mech Ageing Dev*. 2009;130(11-12):731-741. doi:10.1016/j.mad.2009.09.002.

120. Daniel B, Nagy G, Nagy L. The intriguing complexities of mammalian gene regulation: how to link enhancers to regulated genes. Are we there yet? *FEBS Lett*. 2014;588(15):2379-2391. doi:10.1016/j.febslet.2014.05.041.

121. Barr F, Lambright DG. Rab GEFs and GAPs. *Curr Opin Cell Biol*. 2010;22(4):461-470. doi:10.1016/j.ceb.2010.04.007.

122. Huang CC, Yang DM, Lin CC, Kao L Sen. Involvement of Rab3A in vesicle priming during exocytosis: Interaction with Munc13-1 and Munc18-1. *Traffic*. 2011;12:1356-1370. doi:10.1111/j.1600-0854.2011.01237.x.

123. Ohya T, Sasaki T, Kato M, Takai Y. Involvement of Rabphilin3 in endocytosis through interaction with Rabaptin5. *J Biol Chem*. 1998;273(1):613-617. http://www.ncbi.nlm.nih.gov/pubmed/9417123. Accessed March 6, 2016.

124. Chavrier P, Goud B. The role of ARF and Rab GTPases in membrane transport. *Curr Opin Cell Biol*. 1999;11(Figure 1):466-475. doi:10.1016/S0955-0674(99)80067-2.

125. Collins RN. Rab and ARF GTPase regulation of exocytosis. *Mol Membr Biol*. 2009;20(2):105-115. doi:10.1080/0968768031000085892.

126. Dhami GK, Ferguson SSG. Regulation of metabotropic glutamate receptor signaling, desensitization and endocytosis. *Pharmacol Ther*. 2006;111:260-271. doi:10.1016/j.pharmthera.2005.01.008.

127. Spang N, Feldmann A, Huesmann H, et al. RAB3GAP1 and RAB3GAP2 modulate basal and rapamycin-induced autophagy. *Autophagy*. 2014;10(12):2297-2309. doi:10.4161/15548627.2014.994359.

128. Walter MA. PITs and FOXes in Ocular Genetics The Cogan Lecture. *Investig Opthalmology Vis Sci*. 2003;44(4):1402. doi:10.1167/iovs.02-0618.

129. Boschert U, O'Shaughnessy C, Dickinson R, et al. Developmental and plasticity-related differential expression of two SNAP-25 isoforms in the rat brain. *J Comp Neurol*. 1996;367(2):177-193. doi:10.1002/(SICI)1096-9861(19960401)367:2<177::AID-CNE2>3.0.CO;2-2.

130. Grant NJ, Hepp R, Krause W, Aunis D, Oehme P, Langley K. Differential expression of SNAP-25 isoforms and SNAP-23 in the adrenal gland. *J Neurochem*. 1999;72:363-372. doi:10.1046/j.1471-4159.1999.0720363.x.

131. Gonzalez P, Li G, Qiu J, Wu J, Luna C. Role of microRNAs in the trabecular

meshwork. *J Ocul Pharmacol Ther*. 30(2-3):128-137. doi:10.1089/jop.2013.0191.

132. Chen PY, Meister G. microRNA-guided posttranscriptional gene regulation. *Biol Chem*. 2005;386(12):1205-1218. doi:10.1515/BC.2005.139.

133. Tafoya LCR, Shuttleworth CW, Yanagawa Y, Obata K, Wilson MC. The role of the t-SNARE SNAP-25 in action potential-dependent calcium signaling and expression in GABAergic and glutamatergic neurons. *BMC Neurosci*. 2008;9:105. doi:10.1186/1471-2202-9-105.

134. Yang Y, Xia Z, Liu Y. SNAP-25 functional domains in SNARE core complex assembly and glutamate release of cerebellar granule cells. *J Biol Chem*. 2000;275(38):29482-29487. doi:10.1074/jbc.M003237200.

135. Kaur K, Reddy a. BM, Mukhopadhyay a., et al. Myocilin gene implicated in primary congenital glaucoma. *Clin Genet*. 2005;67(12):335-340. doi:10.1111/j.1399-0004.2005.00411.x.

136. Okayama M, Arakawa T, Mizoguchi I, Tajima Y, Takuma T. SNAP-23 is not essential for constitutive exocytosis in HeLa cells. *FEBS Lett*. 2007;581(24):4583-4588. doi:10.1016/j.febslet.2007.08.046.

137. Stamer WD, Perkumas KM, Hoffman E a., Roberts BC, Epstein DL, McKay BS. Coiled-coil targeting of myocilin to intracellular membranes. *Exp Eye Res*. 2006;83:1386-1395. doi:10.1016/j.exer.2006.07.018.

138. Caballero M, Borrás T. Inefficient Processing of an Olfactomedin-Deficient Myocilin Mutant: Potential Physiological Relevance to Glaucoma. *Biochem Biophys*

Res Commun. 2001;282(3):662-670. doi:10.1006/bbrc.2001.4624.

139. Gobeil S, Letartre L, Raymond V. Functional analysis of the glaucoma-causing TIGR/myocilin protein: integrity of amino-terminal coiled-coil regions and olfactomedin homology domain is essential for extracellular adhesion and secretion. *Exp Eye Res*. 2006;82(6):1017-1029. doi:10.1016/j.exer.2005.11.002.

140. Jurynec MJ, Riley CP, Gupta DK, Nguyen TD, McKeon RJ, Buck CR. TIGR is upregulated in the chronic glial scar in response to central nervous system injury and inhibits neurite outgrowth. *Mol Cell Neurosci*. 2003;23:69-80. doi:10.1016/S1044-7431(03)00019-8.

141. Koga T, Shen X, Park J-S, et al. Differential effects of myocilin and optineurin, two glaucoma genes, on neurite outgrowth. *Am J Pathol*. 2010;176(1):343-352. doi:10.2353/ajpath.2010.090194.

142. Taylor P, Spang N, Feldmann A, et al. RAB3GAP1 and RAB3GAP2 modulate basal and rapamycin-induced autophagy. 2015;(February):37-41. doi:10.4161/15548627.2014.994359.

143. Park HYL, Kim JH, Park CK. Activation of autophagy induces retinal ganglion cell death in a chronic hypertensive glaucoma model. *Cell Death Dis*. 2012;3:e290. doi:10.1038/cddis.2012.26.

144. Mandolesi G, Vanni V, Cesa R, et al. Distribution of the SNAP25 and SNAP23 synaptosomal-associated protein isoforms in rat cerebellar cortex. *Neuroscience*. 2009;164(3):1084-1096. doi:10.1016/j.neuroscience.2009.08.067.